Open access • Posted Content • DOI:10.21203/RS.3.RS-596219/V1

Chaotic dynamics of a tri-topic food chain model with Beddington–DeAngelis functional response in presence of fear effect — Source link

Surajit Debnath, Prahlad Majumdar, Susmita Sarkar, Uttam Ghosh

Institutions: University of Calcutta

Published on: 21 Sep 2021 - Nonlinear Dynamics (Springer Netherlands)

Chaotic Dynamics of a Tri-Topic Food Chain Model with Beddington-DeAngelis Functional Response in Presence of Fear Effect

Surajit Debnath
University of Calcutta
Prahlad Majumdar
University of Calcutta
Susmita Sarkar
University of Calcutta
Uttam Ghosh (uttam_math@yahoo.co.in)
University of Calcutta https://orcid.org/0000-0001-7274-7793

Research Article

Keywords: Fear effect, Beddington-DeAngelis functional response, Global stability, Bifurcations, Direction of Hopf bifurcation, Chaos

Posted Date: June 10th, 2021

DOI: https://doi.org/10.21203/rs.3.rs-596219/v1

Version of Record: A version of this preprint was published at Nonlinear Dynamics on September 21st, 2021. See the published version at https://doi.org/10.1007/s11071-021-06896-0.

Nonlinear Dynamics manuscript No.
(will be inserted by the editor)

Chaotic dynamics of a tri-topic food chain model with Beddington-DeAngelis functional response in presence of fear effect

Surajit Debnath · Prahlad Majumdar · Susmita Sarkar · Uttam Ghosh

Received: date / Accepted: date

Abstract The most important fact in the field of theoretical ecology and evolutionary biology is the strategy of predation for predators and the avoidance of prey from predator attack. A lot of experimental works suggest that the reduction of prey depends on both direct predation and fear of predation. We explore the impact of fear effect and mutual interference into a three-species food chain model. In this manuscript, we have considered a tri-topic food web model with Beddington-DeAngelis functional response between interacting species, incorporating the reduction of prey and intermediate predator growth because of the fear of intermediate and top predator respectively. We have provided parametric conditions on the existence of biologically feasible equilibria as well as their local and global stability also. We have established conditions of transcritical, saddle-node and Hopf bifurcation in vicinity of different equilibria. Finally, we performed some numerical investigations to justify analytical findings.

Mathematics Subject Classification : 39A30, 92D25, 92D50.

Keywords : Fear effect; Beddington-DeAngelis functional response; Global stability; Bifurcations; Direction of Hopf bifurcation; Chaos.

1 Introduction

Analysis of dynamical activities of prey-predator interaction is one of the momentous themes for researchers in mathematical biology and theoretical ecology. Uniform existence and universal importance make the prey-predator interplay an attractive field of investigation. Prey-predator interplay becomes the focus of theoretical ecologist and experimental biologist from the last few decades [1,2]. Many mathematical models of prey-predator interactions have been formulated and considered to investigate the consumption and survival dynamics of species [3,4]. Prey-predator interactions may be governed by ordinary differential equations [3,5], fractional differential equations [6,7], partial differential equations [4,8] and stochastic differential equations [9], delay differential equations [10] and difference equations also. These mathematical models are constructed and studied to identify different environmental effects such as the interaction between species, Allee effect, refuge of species, harvesting, pattern formation, environmental fluctuations etc. In the early nineteenth century Malthus first formulated prey-predator interaction through mathematical models [11,12]. The celebrated Lotka-Volterra model was eventually enhanced by introducing logistic growth function for prey species [13,14], incorporating various functional response and environmental effects and these developments makes prey-predator interplay more and more realistic [15,16,17]. The dynamics of prey-predator interaction can significantly be affected in presence of fear effect in the field of environmental biology and ecology [18].

The presence of predator populations has the most impact on a prey-predator system through direct predation as well as fear of predation. A large number of mathematical models have been concerned about considering the direct predation only [19,20,21,22,23] and reference therein. Those models are constructed with only prey dependent, both monotone and non-monotone functional responses [15,16,20,24,

Uttam Ghosh
Department of Applied Mathematics, University of Calcutta, Kolkata-700054, India
E-mail: uttam_math@yahoo.co.in

25], both prey and predator dependent functional response like Cowley-Martin type functional response [17], Beddington-DeAngelis type functional response [26,27], Monod-Haldane type functional response [28] and ratio-dependent functional response [20,29]. In 2009, Takeuchi *et al.* studied the dissension along with investing time on taking care of juvenile and searching for food/nutrients of mature prey in absence of direct predation, while they assumed that matures accommodate their parental care time via learning [30]. Krivan (2007) investigated that exchange among foraging and predation based on classical Lotka-Volterra prey-predator system where either prey or predator or both species were adaptive to maximize their independent sturdiness [31].

The second one is that in presence of predator species, prey species may gently modify their behaviour because of the fear of predation threat. Appearance of predator may influence prey species more effectively than direct predation [32,33,34,35,36]. The birth rate of prey species has been subjected to modification through the introduction of fear effect [18,37]. A lot of field observation suggests including the cost of fear in a prey-predator system, not only direct predation [33,34,35,36]. It also may be the cause of anti-predator behaviour for prey species which plays a significant responsibility on demography of prey species [38]. For example, the reproduction physiology of elks (*Cervus elaphus*) influenced by wolves (*Canis lupus*) in Greate Yellowstone Ecosystem [39].

Prey species may transform their habitat from higher-risk zone to lower risk zone, to reduce the predation rate [35]. In 2011, Zanette *et al.* [36] observed during a whole breeding season that song sparrows (Melospiza melodia) reduces their reproduction due to fear of predators in their offspring season. This reduction is being occurred because of their anti-predator behaviour which persuades growth rate, in addition to their offspring endurance rates since female song sparrows laid a few eggs. Only some of those eggs can survive while most of the nestlings perished in a nest. They also observed that a variety of anti-predator behaviour is responsible for this effect. For example, frightened parents suckled their nestlings less, their nestlings were lighter and much more likely to perish. Correlational affirmation for birds [33,40,41,42], Elk [39], Snowshoe hares [43] and dugongs [44] also display some indication that fear can interrupt prey-predator interactions. Very recently Elliott *et al.*, [45] studied some field experiments on Drosophila melanogaster as prey and mantid as their predator species, to observe the effect of fear on populations robustness in relation to species density. They explored that in presence of mantid, the reproductive rate of drasophila reduces in both their breeding in addition to non-breeding seasons.

Depending on field experimental data, Wang *et al.*, Zanette *et al.* [18,36] developed mathematical formulation for prey-predator interaction by introducing the cost of fear for prey because of predator species, where fear shows a crucial function on prey birth rate. They also observed that strong anti-predator behaviour or correspondingly most important cost of fear may reduce the risk of the existence of oscillatory behaviours and thus eliminate the scenarios "paradox of enrichment". They also displayed that cost of fear can stabilize the system by eliminating periodic behaviour as observed in prey-predator interactions. Also, periodic oscillations may arise, emerging from either sub-critical or supercritical Hopf bifurcation under comparatively lower cost for fear [18]. Thus, the effect of fear can produce multi-stability in prey-predator interplays. In 2017, Wang and Zou formulate a stage-structured prey-predator interaction with adaptive avoidance for predator species by including fear of predator for prey species [37]. They divided the prey population into juvenile and mature stage and constitute a system of delay differential system with maturation delay. Das and Samanta [46] analysed a stochastic prey-predator system with the effect of fear due to predator on prey species and additional food is provided for a predator. Recently, Panday *et al.* [47] analysed a tri-topic food web system considering the effect of fear of top predator and intermediate predator on reproduction of intermediate predator and prey species respectively. Here, they study the cost of fear on the stability dynamics of the model system.

In this paper, the Hastings–Powell model [48] has been modified incorporating fear of intermediate and top predator to prey and intermediate predator respectively with Beddington–DeAngelis functional response for both species. The organization of the manuscript is as follows: in the next segment, we have formulated the model system. The basic dynamical results such as positivity, boundedness property and persistence of model are provided in section 3. Biologically feasible equilibria of the model system and parametric conditions of local and global stability are determined in section 4. Section 5 is dedicated to studying transcritical bifurcation at an axial equilibrium point and conditions for the occurrence of saddle-node and Hopf bifurcation around coexistence equilibrium point along with stability direction of Hopf bifurcation. In Section 6, we perform some numerical simulations to justify our analytical findings, which also shows the roles of fear effect on the dynamics of prey-predator interactions. Finally, in section 7, we summarize some biological indications from our analytical observation and possible future scope for upcoming research works.

2 Model formulation

In this research article, our main objective is to investigate the change of basic dynamical behaviour of a tri-topic food chain model in presence of fear due to the appearance of higher species. For this purpose, we start by considering the Hestings-Powell model [48]. In 1991 Hestings and Powell proposed a continuous tri-topic food chain model by considering more naturalist logistic growth function for prey species and Holling type-II functional response in the form,

$$\frac{dX}{dT} = R_0X(1 - \frac{X}{K_0}) - \frac{R_1XY}{A_1X + C_1} \tag{1a}$$

$$\frac{dY}{dT} = \frac{E_1R_1XY}{A_1X + C_1} - D_1Y - \frac{R_2YZ}{A_2Y + C_2} \tag{1b}$$

$$\frac{dZ}{dT} = \frac{E_2R_2YZ}{A_2Y + C_2} - D_2Z \tag{1c}$$

with initial condition $X(0) \geq 0, Y(0) \geq 0, Z(0) \geq 0$. $X(T)$, $Y(T)$ and $Z(T)$ are population densities of prey, middle/intermediate predator and top predator population at any instant of time T respectively and description of model parameters are given in Table 1. In 2018, Pandey *et al.* [47], incorporated effect of fear in above considered tri-topic food chain model. They assumed that intrinsic growth rate of prey population reduces due to appearance of intermediate predator and modified intrinsic growth rate of prey population becomes $\phi_1(K_1, Y) = \frac{R_1}{1 + K_1Y}$, which is a monotonically decreasing function of both K_1 and Y. Similarly modified growth rate of intermediate predator population is $\phi_2(K_2, Z) = \frac{R_2}{1 + K_2Z}$, which is also a monotonically decreasing function of both K_2 and Z. K_1, K_2 are level of fear parameters of prey and middle predator population respectively. On behalf of above consideration they investigate the dynamics of following modified tri-topic food chain model

$$\frac{dX}{dT} = \frac{R_0X}{1 + K_1Y}(1 - \frac{X}{K_0}) - \frac{R_1XY}{A_1X + C_1} \tag{2a}$$

$$\frac{dY}{dT} = \frac{E_1R_1XY}{(1 + K_2Z)(A_1X + C_1)} - D_1Y - \frac{R_2YZ}{A_2Y + C_2} \tag{2b}$$

$$\frac{dZ}{dT} = \frac{E_2R_2YZ}{A_2Y + C_2} - D_2Z \tag{2c}$$

Fear functions $\phi_1(K_1, Y)$ and $\phi_2(K_2, z)$ satisfies following ecological hypothesis :
1. $\phi_1(0, Y) = 1$ and $\phi_2(0, Z) = 1$; i.e., if there is no anti-predator behaviours of prey and middle predator species, then there will be no reduction in the birth rate of prey and middle predator species.
2. $\phi_1(K_1, 0) = 1$ and $\phi_2(K_2, 0) = 1$; i.e., if middle or top predator species becomes zero, then there is no reduction in the birth rate of prey and middle predator species.
3. $\lim_{K_1\to\infty} \phi_1(K_1, Y) = 0$ and $\lim_{K_2\to\infty} \phi_2(K_2, Z) = 0$; i.e., if anti-predator behaviour is very large, then prey an middle predator reproduction ultimately becomes zero.
4. $\lim_{Y\to\infty} \phi_1(K_1, Y) = 0$ and $\lim_{Z\to\infty} \phi_2(K_2, Z) = 0$; i.e., if middle predator and top predator species is very large, then respectively prey and middle predator reproduction reduces and ultimately goes to zero, due to large anti-predator behaviours.
5. $\frac{\partial\phi_1}{\partial K_1} < 0$ and $\frac{\partial\phi_2}{\partial K_2} < 0$; i.e., reproduction of prey and middle predator species decreases with increase of anti-predator behaviours.
6. $\frac{\partial\phi_1}{\partial Y} < 0$ and $\frac{\partial\phi_2}{\partial Z} < 0$; i.e., reproduction of prey and middle species decreases with an increase of middle predator and top predator species density respectively.
They discuss boundedness, positivity of system solutions and persistence of the considered model system. Parametric conditions of local and global stability of different feasible equilibria are investigated by them also. However, in the study by Pandey *et al.*[47], it was assumed that prey-predator interplay depends only on prey density alone and it is of type-II functional response. A huge number of detailed critical inspection on ecology and physiological evidence suggests that competition within predator species might be good for predator population under certain conditions in a deterministic environment [49].
To take account of the above observation, we have modified the model of Pandey *et al.* [47] by considering the Beddington-DeAngelis type function response, depending on both interacting species. Thus the modified

Symbol	Definition	Dimension	Non-dimensional representation
T	Time	*time*	$t = R_0T$
X	Prey density	*biomass*	$x = \frac{X}{K_0}$
Y	Intermediate predator density	*biomass*	$y = \frac{Y}{K_0E_1}$
Z	Top predator density	*biomass*	$z = \frac{Z}{K_0E_1E_2}$
R_0	Prey intrinsic growth rate	$time^{-1}$	...
R_1	Maximum predation rate of intermediate predator	$time^{-1}$	...
R_2	Maximum predation rate of top predator	$time^{-1}$	...
K_0	Prey carrying capacity	*biomass*	...
K_1	Fear level of prey	*biomass*	$k_1 = K_0K_1E_1$
K_2	Fear level of prey	*biomass*	$k_1 = K_0K_2E_1E_2$
A_1	Handling time of middle predator	$biomass^{-1}$	$a_1 = \frac{R_0A_1}{R_1E_1}$
A_2	Handling time of top predator	$biomass^{-1}$	$a_2 = \frac{R_0A_2}{R_2E_2}$
B_1	Mutual interference among middle predators	$biomass^{-1}$	$b_1 = \frac{R_0B_1}{R_1}$
B_2	Mutual interference among top predators	$biomass^{-1}$	$b_2 = \frac{R_0B_2}{R_2}$
C_1	Environmental protection for prey	*dimensionless*	$c_1 = \frac{R_0C_1}{K_0E_1R_1}$
C_2	Environmental protection for middle predator	*dimensionless*	$c_2 = \frac{R_0C_2}{K_0E_1E_2R_2}$
D_1	Intermediate predator mortality rate	$time^{-1}$	$d_1 = \frac{D_1}{r_0}$
D_2	Top predator mortality rate	$time^{-1}$	$d_2 = \frac{D_2}{r_0}$
E_1	Conversion efficiency of intermediate predator	*dimensionless*	...
E_2	Conversion efficiency of top predator	*dimensionless*	...

Table 1: Description of system variables and system parameters with their dimensions and non-dimensional representation.

shape of above-considered model with Beddington-DeAngelis type function response is as follows:

$$\frac{dX}{dT} = \frac{R_0X}{1+K_1Y}(1-\frac{X}{K_0}) - \frac{R_1XY}{A_1X+B_1Y+C_1} \tag{3a}$$

$$\frac{dY}{dT} = \frac{E_1R_1XY}{(1+K_2Z)(A_1X+B_1Y+C_1)} - D_1Y - \frac{R_2YZ}{A_2Y+B_2Z+C_2} \tag{3b}$$

$$\frac{dZ}{dT} = \frac{E_2R_2YZ}{A_2Y+B_2Z+C_2} - D_2Z \tag{3c}$$

where B_1, B_2 represents mutual interference among middle predators and top predators respectively. To reduce number of system parameters, we introduce following dimensionless variables $x = \frac{X}{K_0}$, $y = \frac{Y}{K_0E_1}$, $z = \frac{Z}{K_0E_1E_2}$ and $t = R_0T$. Then the above system reduces to following form:

$$\frac{dx}{dt} = \frac{x}{1+k_1y}(1-x) - \frac{xy}{a_1x+b_1y+c_1} := F_1(x,y,z), \tag{4a}$$

$$\frac{dy}{dt} = \frac{xy}{(1+k_2z)(a_1x+b_1y+c_1)} - d_1y - \frac{yz}{a_2y+b_2z+c_2} := F_2(x,y,z), \tag{4b}$$

$$\frac{dz}{dt} = \frac{yz}{a_2y+b_2z+c_2} - d_2z := F_3(x,y,z) \tag{4c}$$

with the initial condition $x(0) \geq 0$, $y(0) \geq 0$ and $z(0) \geq 0$ and we introduce dimensionless parameters as $k_1 = K_0K_1E_1$, $a_1 = \frac{A_1R_0}{E_1R_1}$, $b_1 = \frac{B_1R_0}{R_1}$, $c_1 = \frac{C_1R_0}{R_1K_0E_1}$, $d_1 = \frac{D_1}{R_0}$, $k_2 = K_0K_2E_1E_2$, $a_2 = \frac{A_2R_0}{E_2R_2}$, $b_2 = \frac{B_2R_0}{R_2}$, $c_2 = \frac{C_2R_0}{R_2K_0E_1E_2}$ and $d_2 = \frac{D_2}{R_0}$.

In next segment of the manuscript, we shall establish boundedness, positivity of system solutions and persistence of the system which will refer to that system is feasible, well-posed and exist for a long time.

3 Positivity, boundedness and persistence of system solutions

In Theorem 1-3, we shall establish respectively positivity, boundedness and permanence of the model system (4).

Theorem 1 *All system solutions of the model system (4) are positively invariant.*

Proof Right hand side of model system (4) are continuous functions of dependent variables x, y and z. After integration of equations of system (4), we get

$$x(t) = x(0)exp\left[\int_0^t \left\{\frac{y(s)}{1+k_1y(s)} - \frac{y(s)}{a_1x(s)+b_1y(s)+c_1}\right\}ds\right]$$
$$y(t) = y(0)exp\left[\int_0^t \left\{\frac{x(s)}{(1+k_2z(s))(a_1x(s)+b_1y(s)+c_1)} - d_1 - \frac{z(s)}{a_2y(s)+b_2z(s)+c_2}\right\}ds\right]$$
$$z(t) = z(0)exp\left[\int_0^t \left\{\frac{z(s)}{a_2y(s)+b_2z(s)+c_2} - d_2\right\}ds\right].$$

It is apparent from above expressions that $x(t)$, $y(t)$ and $z(t)$ remain non-negative for future infinite time if solution curve initiate from any interior point of $\mathbb{R}^3_+ = \left\{(x(t), y(t), z(t)) \in \mathbb{R}^3 : x(t) \geq 0, y(t) \geq 0, z(t) \geq 0\right\}$. Hence $\mathbb{R}^3_+$ is positively invariant set for the system (4).

Theorem 2 *All solutions $(x(t), y(t), z(t))$ of model system (4) with positive initial conditions i.e., initiate from $\mathbb{R}^3_+ - \{0\}$ are uniformly bounded.*

Proof We consider the function $L(t)$ as

$$L(t) = x(t) + y(t) + z(t).$$

Differentiating the above relation with respect to t and using system (4)

$$\begin{aligned}\frac{dL}{dt} =& \frac{dx}{dt} + \frac{dy}{dt} + \frac{dz}{dt}\\ =& \frac{x}{1+k_1y}(1-x) - \frac{xy}{a_1x+b_1y+c_1}\left(1 - \frac{1}{1+k_2z}\right) - d_1y - d_2z\end{aligned}$$

Therefore, for any arbitrary constant γ we have

$$\frac{dL}{dt} + \gamma L = \frac{x}{1+k_1y}(1-x) + \gamma x - (d_1-\gamma)y - (d_2-\gamma)z - \frac{xy}{a_1x+b_1y+c_1}\left(1 - \frac{1}{1+k_2z}\right)$$
$$\text{or, } \frac{dL}{dt} \leq x(1-x+\gamma) - (d_1-\gamma)y - (d_2-\gamma)z \leq \frac{(1+\gamma)^2}{4} = M(\text{say})$$

where $\gamma \leq min\{d_1, d_2\}$. Using theory of differential inequality, we have following inequality

$$0 \leq L \leq \frac{M(1-e^{-dt})}{d} + L(x(0), y(0), z(0))e^{-dt}$$

Hence, as $t \to \infty$, above relation reduces to $0 \leq L \leq \frac{M}{d}$. Therefore, all system solutions $(x(t), y(t), z(t))$ of model system (4) with positive initial conditions i.e., initiate from $\mathbb{R}^3_+ - \{0\}$ are uniformly bounded in the region:

$$\left\{(x, y, z) \in \mathbb{R}^3 : 0 < L \leq \frac{M}{d} + \epsilon, \text{for any } \epsilon > 0\right\}$$

.

On the other hand persistence of a system mathematically implies that minimum population densities of all three population are away from zero and bounded. Also, all populations can survive for a long time range.

Dissipativeness: Biologically the dissipativeness refers upper boundedness of all population.

Theorem 3 *The model system (4) is dissipative if* $\frac{b_2}{1+d_1b_2} < c_1 < \frac{1}{d_1}$.

Proof From the system of equations (4), we have

$$\begin{aligned}
\frac{dx}{dt} &\leq x(1-x),\\
\frac{dy}{dt} &\leq y\left(\frac{x}{c_1} - d_1 - \frac{z}{a_2y + b_2z + c_2}\right),\\
\frac{dz}{dt} &\leq z\left(\frac{y}{c_2} - d_2\right)
\end{aligned}$$

Applying standard comparison theorem [20], we can write from above inequality that $\lim_{t-\infty} supx(t) \leq S_1$, $\lim_{t-\infty} supy(t) \leq S_2$ and $\lim_{t-\infty} supz(t) \leq S_3$ where S_1, S_2, S_3 are positive real solutions of the system of equations $1-x=0$, $\frac{x}{c_1} - d_1 - \frac{z}{a_2y + b_2z + c_2} = 0$, $\frac{y}{c_2} - d_2 = 0$ for x, y, z respectively. Solving, we get $S_1 = 1$, $S_2 = c_2d_2$ and $S_3 = \frac{c_2(1-c_1d_1)(1+a_2d_2)}{c_1 - b_2(1-c_1d_1)}$.
Here, S_1, S_2 are positive real numbers and S_3 will be positive if conditions declared in the statement of the theorem is satisfied.
Hence the system is dissipative if $\frac{b_2}{1+d_1b_2} < c_1 < \frac{1}{d_1}$.

Uniform Permanence : Biologically permanence means all three populations survive in future time. Mathematically it says that system solutions are always away from zero.

Theorem 4 *The model system (4) is permanent if* $c_1 > s_2(1+k_1s_2)$ *and* $d_1(a_1s_1 + b_1s_2 + c_1) < s_1$ *holds.*

Proof From the system of equations (4), we have

$$\begin{aligned}
\frac{dx}{dt} &\geq x\left[\frac{1-x}{1+k_1y} - \frac{y}{c_1}\right],\\
\frac{dy}{dt} &\geq y\left[\frac{x}{(1+k_2z)(a_1x + b_1y + c_1)} - d_1 - \frac{z}{c_2}\right],\\
\frac{dz}{dt} &\geq z\left[\frac{y}{a_2S_2 + b_2S_3 + c_2} - d_2\right]
\end{aligned}$$

Applying standard comparison theorem [20], we can write from above inequality that $\lim_{t-\infty} infx(t) \geq s_1$, $\lim_{t-\infty} infy(t) \geq s_2$ and $\lim_{t-\infty} infz(t) \geq s_3$ where (s_1, s_2, s_3) are positive real solution for (x, y, z) of the system of equations: $\frac{1-x}{1+k_1y} - \frac{y}{c_1} = 0$, $\frac{x}{(1+k_2z)(a_1x + b_1y + c_1)} - d_1 - \frac{z}{c_2} = 0$, $\frac{y}{a_2S_2 + b_2S_3 + c_2} - d_2 = 0$.
Solving, we obtain $s_1 = 1 - \frac{s_2(1+k_1s_2)}{c_1}$, $s_2 = d_2(a_2S_2 + b_2S_3 + c_2)$ and s_3 is positive real root of the equation $k_2z^2 + (c_2d_1k_2 + 1)z + c_2d_1 - \frac{c_2s_1}{a_1s_1 + b_1s_2 + c_1} = 0$. Here, s_2 is positive real number and s_1, s_3 will be positive real if $c_1 > s_2(1+k_1s_2)$ and $d_1(a_1s_1 + b_1s_2 + c_1) < s_1$. Hence the system is permanent if conditions stated in the statement of the theorem are satisfied.

4 Equilibria and their stability analysis

Here, we find equilibria of the model system (4) with their existence criterion and studied their local and global stability.

4.1 Equilibria of the model system

As we are studying an ecological system, we are mainly interested to feasible equilibrium points only. Feasible equilibria of the system (4) are summarized below:
(1) The trivial equilibria $E_0(0,0,0)$ and it is always exists.
(2) Predators-free axial equilibria $E_1(1,0,0)$, which also always exists.
(3) The top predator-free planer equilibria $E_2(x_2, y_2, 0)$, where $y_2 = \frac{(1-a_1d_1)x_2 - c_1d_1}{b_1d_1}$ and x_2 satisfies the equation

$$C_2x^2 + C_1x + C_0 = 0 \tag{5}$$

k_1	k_2	a_1	a_2	b_1	b_2	c_1	c_2	d_1	d_2
0.2	1.2	0.66	0.8	0.1	0.91	0.12	1.02	0.1	0.12

Table 2: Emperical values of system parameters of the model (4)

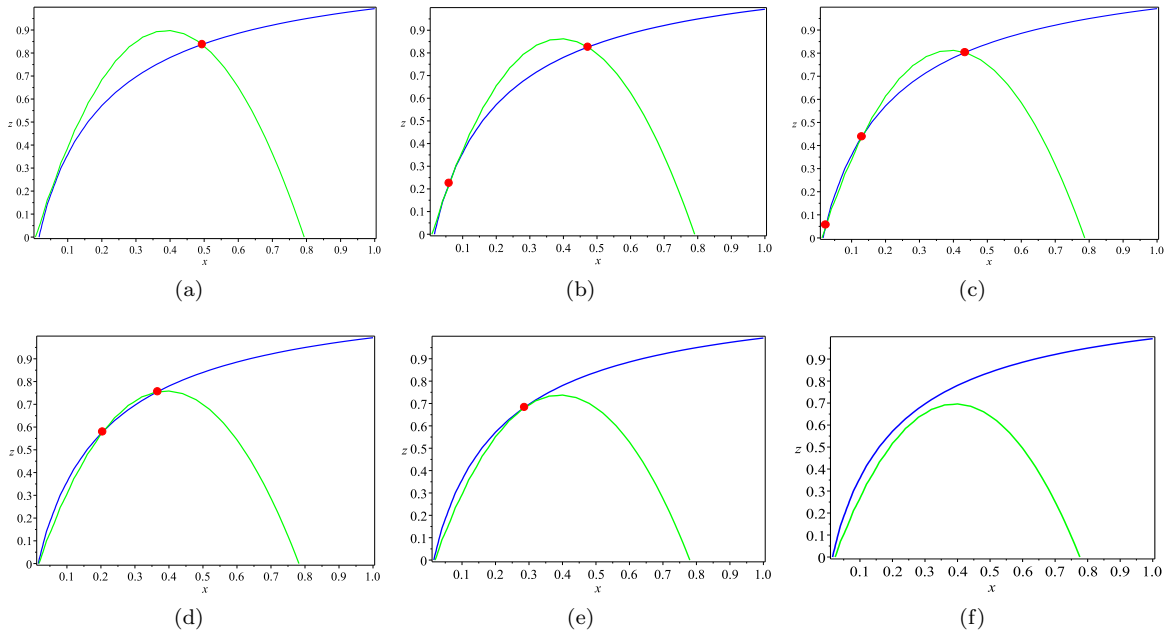

Fig. 1: Projection of interior equilibrium points in the $x-z$ plane for different values of parameter k_1 of the system (4) as : (a) $k_1 = 0.02$, (b) $k_1 = 0.09078075523$, (c) $k_1 = 0.2$, (d) $k_1 = 0.33$, (e) $k_1 = 0.3840366382$, (f) $k_1 = 0.5$ and other system parameters are fixed in Table 2.

with, $C_2 = a_1^2 d_1^2 k_1 - 2a_1 d_1 k_1 + b_1^2 d_1 + k_1, C_1 = 2a_1 c_1 d_1 k_1 - a_1 b_1 d_1 - b_1^2 - 2c_1 k_1 + b_1, C_0 = c_1^2 k_1 - c_1 b_1$. The above equation can have at most two positive real roots, hence the system may have at most two planer equilibria.
(4) The interior equilibria $E_3(x^*, y^*, z^*)$, where (x^*, y^*, z^*) is positive real solution of the system of equations

$$\begin{aligned}
&\frac{1-x}{1+k_1 y} - \frac{y}{a_1 x + b_1 y + c_1} = 0\\
&\frac{x}{(1+k_2 z)(a_1 x + b_1 y + c_1)} - d_1 - \frac{z}{a_2 y + b_2 z + c_2} = 0\\
&\frac{y}{a_2 y + b_2 z + c_2} - d_2 = 0
\end{aligned}$$

Eliminating x, y from above equations we have verified z satisfies a polynomial equation of degree five. If z^* be a root of that polynomial then one can write
$x^* = \dfrac{(a_1 - b_1 y^* - c_1) + \sqrt{(a_1 - b_1 y^* - c_1)^2 - 4a_1\left(k_1 y^{*2} + (1-b_1)y^* - c_1\right)}}{2a_1}$ and $y^* = \dfrac{d_2(b_2 z^* + c_2)}{1 - a_2 d_2}$.
It is obvious that if $a_2 d_2 < 1$ then for positive value of z^*, y^* will be positive.

In Fig. 1, we have presented the projection of various interior equilibria of model system (4) in $x-z$ plane with parametric restriction $a_2 d_2 < 1$ for different values of parameter fear level of prey (k_1) with other parameters are taken from Table 2. Here trivial, axial and planer equilibrium points are always exist. The system have one coexistence equilibrium point for the value of $k_1 = 0.02$ (see Fig. 1(a)) and we represent it by E_{31}. For $k_1 = 0.09078075523$ the system has two interior equilibria, namely E_{31} and coincident equilibria point E_3'' (see Fig. 1(b)). Increasing the fear level to $k_1 = 0.2$, three interior equilibria arise (see Fig. 1(c)). Equilibrium point with higher, moderate and lower population density of top predator are represented by E_{31}, E_{32} and E_{33} respectively. Then the interior equilibrium point E_{33} vanishes (see Fig. 1(d)) for $k_1 = 0.33$ and remaining two interior equilibrium points exists. For $k_1 = 0.3840366382$ remaining two interior equilibrium points E_{31}, E_{32} coincide to interior equilibria E_3' (see Fig. 1(e)). Fig. 1(f) represents

the existence of no interior equilibrium point for value of $k_1 = 0.5$. It is clear that the coincident interior equilibria of E_{31}, E_{32} and E_{32}, E_{33} are $E_3{}'$ and $E_3{}''$ respectively.

4.2 **Local stability analysis of equilibria**

The local stability of equilibria will be discussed by determining eigenvalues of the Jacobian matrix at corresponding equilibrium points. We set up stability-instability conditions of equilibria in the following theorems.

Theorem 5 *The trivial equilibria $E_0(0,0,0)$ is always a saddle point.*

Proof The Jacobian matrix of model system (4) at trivial equilibria E_0 is

$$J(E_0) = \begin{bmatrix} 1 & 0 & 0 \\ 0 & -d_1 & 0 \\ 0 & 0 & -d_2 \end{bmatrix}$$

Eigenvalues of $J(E_0)$ are $1, -d_1$ and $-d_2$. Since, one eigenvalue is positive and other two are negative, hence the equilibria E_0 is always saddle. Solutions in the vicinity of this equilibrium point are unstable in nature.

Biologically this result is an evidence of the long survival of the system i.e. all three species will not go to extinction concurrently.

Theorem 6 *The axial equilibria $E_1(1,0,0)$ is locally asymptotically stable if $d_1 > \dfrac{1}{(a_1+c_1)}$.*

Proof The Jacobian matrix of model system (4) at axial equilibrium point E_1 is

$$J(E_1) = \begin{bmatrix} -1 & -\dfrac{1}{a_1+c_1} & 0 \\ 0 & \dfrac{1}{a_1+c_1} - d_1 & 0 \\ 0 & 0 & -d_2 \end{bmatrix}$$

Eigenvalues of $J(E_1)$ are -1, $\dfrac{1}{a_1+c_1} - d_1$ and $-d_2$. It is clear from expressions of eigenvalues that the system will be locally asymptotically stable if $d_1 > \dfrac{1}{(a_1+c_1)}$ and unstable if $d_1 < \dfrac{1}{(a_1+c_1)}$.

Biologically the above result is most important because if the mortality rate of the intermediate predator crosses the critical value $\dfrac{1}{(a_1+c_1)} = d_1^{[TC]}$ (say), then the middle predator will go to extinction and as a result top predator will also go to extinction and only prey population will survive in the system.

Theorem 7 *The top predator-free planer equilibria $E_2(x_2, y_2, 0)$ is locally asymptotically stable if $y_2 < \dfrac{c_2 d_2}{1 - a_2 d_2}$, $\xi_1 > 0$ and $\xi_2 > 0$, where ξ_1, ξ_2 are defined in the proof.*

Proof The Jacobian matrix of model system (4) at the planer equilibria $E_2(x_2, y_2, 0)$ is

$$J(E_2) = \begin{bmatrix} a_{11} & a_{12} & 0 \\ a_{21} & a_{22} & a_{23} \\ 0 & 0 & a_{33} \end{bmatrix}$$

where $a_{11} = -\dfrac{x_2}{1+k_1 y_2} + \dfrac{a_1 x_2 y_2}{(a_1 x_2 + b_2 y_2 + c_1)^2}$, $a_{12} = -\dfrac{k_1 x_2 (1-x_2)}{(1+k_1 y_2)^2} - \dfrac{x_2(a_1 x_2 + c_1)}{(a_1 x_2 + b_2 y_2 + c_1)^2}$, $a_{21} = \dfrac{y_2(b_1 y_2 + c_1)}{(a_1 x_2 + b_1 y_2 + c_1)^2}$, $a_{22} = -\dfrac{b_1 x_2 y_2}{(a_1 x_2 + b_1 y_2 + c_1)^2}$, $a_{23} = -\dfrac{y_2(a_2 y_2 + c_2)}{(a_2 y_2 + c_2)^2}$ and $a_{33} = \dfrac{y_2}{a_2 y_2 + c_2} - d_2$.

The characteristic equation of above Jacobian matrix is

$$(\lambda - a_{33})(\lambda^2 + \xi_1 \lambda + \xi_2) = 0$$

with $\xi_1 = -(a_{11} + a_{22})$ and $\xi_2 = a_{11}a_{22} - a_{21}a_{12}$.

One eigenvalue of the Jacobian matrix $J(E_2)$ is $\dfrac{y_2}{a_2 y_2 + c_2} - d_2$ and this will be negative if $y_2 < \frac{c_2 d_2}{1 - a_2 d_2}$.

Other two eigenvalues are negative or having negative real parts if $\xi_1 > 0$ and $\xi_2 > 0$.

Hence the planer equilibria $E_2(x_2, y_2, 0)$ is locally asymptotically stable if $y_2 < \dfrac{c_2 d_2}{1 - a_2 d_2}$, $\xi_1 > 0$ and $\xi_2 > 0$ holds.

Theorem 8 *The interior equilibria $E^*(x^*, y^*, z^*)$ is locally asymptotically stable if $C_1 > 0$, $C_3 > 0$ and $C_1C_2 > C_3$ where C_1, C_2 and C_3 are defined in the proof.*

Proof The Jacobian matrix of model system (4) at interior equilibria $E^*(x^*, y^*, z^*)$ is

$$J(E^*) = \begin{bmatrix} b_{11} & b_{12} & 0 \\ b_{21} & b_{22} & b_{23} \\ 0 & b_{32} & b_{33} \end{bmatrix}$$

where $b_{11} = -\frac{x^*}{1+k_1y^*} + \frac{a_1x^*y^*}{(a_1x^*+b_2y^*+c_1)^2}$, $b_{12} = -\frac{k_1x^*(1-x^*)}{(1+k_1y^*)^2} - \frac{x^*(a_1x^*+c_1)}{(a_1x^*+b_2y^*+c_1)^2}$, $b_{21} = \frac{y^*(b_1y^*+c_1)}{(1+k_2z^*)(a_1x^*+b_1y^*+c_1)^2}$, $b_{22} = -\frac{b_1x^*y^*}{(1+k_2z^*)(a_1x^*+b_1y^*+c_1)^2} + \frac{b_2y^*z^*}{(a_2y^*+b_2z^*+c_2)^2}$, $b_{23} = -\frac{k_2x^*y^*}{(1+k_2z^*)^2(a_1x^*+b_1y^*+c_1)} - \frac{y_2(a_2y^*+c_2)}{(a_2y^*+b_2z^*+c_2)^2}$, $b_{32} = \frac{z^*(b_2z^*+c_2)}{(a_2y^*+b_2z^*+c_2)^2}$ and $b_{33} = -\frac{b_2y^*z^*}{(a_2y^*+b_2z^*+c_2)^2}$.
The characteristic equation of above Jacobian matrix is

$$\lambda^3 + C_1\lambda^2 + C_2\lambda + C_3 = 0 \tag{6}$$

with $C_1 = -(b_{11}+b_{22}+b_{33})$, $C_2 = b_{11}b_{22} + b_{22}b_{33} + b_{33}b_{11} - b_{12}b_{21} - b_{23}b_{32}$, and $C_3 = -(b_{11}b_{22}b_{33} - b_{11}b_{23}b_{32} - b_{12}b_{21}b_{33})$.
According to the Routh-Hurwitz criterion [50], interior equilibria E^* is locally asymptotically stable if conditions stated in the statement of the theorem are satisfied.

If $C_1C_2 = C_3$ then the system losses its stability at interior equilibria $E^*(x^*, y^*, z^*)$ through Hopf bifurcation if the tranversility condition is satisfied.

4.3 **Global stability analysis of equilibria**

Here, we shall establish conditions and domain of global stability of different equilibria. The global stability of an equilibria implies the corresponding equilibria will follow the same nature irrespective of the initial population size ever.

Theorem 9 *The predator-free axial equilibria $E_1(1, 0, 0)$ is globally asymptotically stable if $d_1 > \frac{2}{a_1}$ and $d_2 > \frac{1}{a_2}$ hold.*

Proof To established the global stability of axial equilibria E_1, we introduced the Lyapunov function V_1 as follows :

$$V_1 = \frac{1}{2}(x-1)^2 + \frac{1}{2}y^2 + \frac{1}{2}z^2 + y$$

Then, time derivative of above expression is

$$\begin{aligned}
\frac{dV_1}{dt} &= (x-1)\frac{dx}{dt} + y\frac{dy}{dt} + z\frac{dz}{dt} + \frac{dy}{dt} \\
&= -\frac{x(1-x)^2}{1+k_1y} - \frac{x^2y}{a_1x+b_2y+c_1} + \frac{xy}{a_1x+b_2y+c_1} + \frac{xy^2}{(1+k_2z)(a_1x+b_1y+c_1)} - d_1y^2 \\
&- \frac{y^2z}{a_2y+b_2z+c_2} + \frac{yz^2}{a_2y+b_2z+c_2} - d_2z^2 + \frac{xy}{(1+k_2z)(a_1x+b_1y+c_1)} - d_1y - \frac{yz}{a_2y+b_2z+c_2} \\
&\leq -\frac{x(1-x)^2}{1+k_1y} - \frac{x^2y}{a_1x+b_2y+c_1} + \frac{2y}{a_1} + \frac{y^2}{a_1} - d_1y^2 - \frac{y^2z}{a_2y+b_2z+c_2} + \frac{z^2}{a_2} - d_2z^2 - d_1y - \frac{yz}{a_2y+b_2z+c_2} \\
&\leq -\frac{x(1-x)^2}{1+k_1y} - \frac{x^2y}{a_1x+b_2y+c_1} + \left(\frac{2}{a_1} - d_1\right)y + \left(\frac{1}{a_1} - d_1\right)y^2 - \frac{y^2z}{a_2y+b_2z+c_2} + \left(\frac{1}{a_2} - d_2\right)z^2 \\
&- \frac{yz}{a_2y+b_2z+c_2}
\end{aligned}$$

Therefore, $\frac{dV_1}{dt} \leq 0$ if $d_1 > \frac{2}{a_1}$, $d_2 > \frac{1}{a_2}$ and the equality sign occurs when $(x, y, z) = (1, 0, 0)$.
Hence by using Lyapunov-Lasalle's invariance principle [51] we can say that the axial equilibria $E_1(1, 0, 0)$ is globally asymptotically stable.

Theorem 10 *The top predator-free planer equilibria $E_2(x_2, y_2, 0)$ is globally asymptotically stable if $a_1y_2(k_1y_2+1) < c_1(a_1x_2 + b_1y_2 + c_1)$ holds.*

Proof To established the global stability of planer equilibrium point $E_2(x_2, y_2, 0)$, we construct the Lyapunov function L^* as follows :

$$V_2 = (x - x_2 - x_2 \log \frac{x}{x_2}) + \mu(y - y_2 - y_2 \log \frac{y}{y_2})$$

Then, time derivative of above expression along solution curve of system (4) is

$$\begin{aligned}\frac{dV_2}{dt} =& \frac{x - x_2}{x}\frac{dx}{dt} + \mu\frac{y - y_2}{y}\frac{dy}{dt}\\ =&(x - x_2)\left(\frac{1 - x}{1 + k_1y} - \frac{y}{a_1x + b_1y + c_1}\right) + \mu(y - y_2)\left(\frac{x}{a_1x + b_1y + c_1} - d_1\right)\end{aligned}$$

Also we have, $1 = x_2 + \dfrac{y_2(1 + k_1y_2)}{a_1x_2 + b_1y_2 + c_1}$ and $d_1 = \dfrac{x_2}{a_1x_2 + b_1y_2 + c_1}$ at the planer equilibrium point $E_2(x_2, y_2, 0)$.
Then, using these relations the above equation reduces to

$$\begin{aligned}\frac{dV_2}{dt} =&(x - x_2)\left(-\frac{x - x_2}{1 + k_1y} + \frac{y_2(1 + k_1y_2)}{(1 + k_1y)(a_1x_2 + b_1y_2 + c_1)} - \frac{y}{a_1x + b_1y + c_1}\right)\\ &+ \mu(y - y_2)\left(\frac{x}{a_1x + b_1y + c_1} - \frac{x_2}{a_1x_2 + b_1y_2 + c_1}\right)\\ \leq& -\frac{(x - x_2)^2}{1 + k_1y} + \frac{a_1k_1y_2^2(x - x_2)^2}{(1 + k_1y)(a_1x + b_1y + c_1)(a_1x_2 + b_1y_2 + c_1)} + \frac{a_1y_2(x - x_2)^2}{(1 + k_1y)(a_1x + b_1y + c_1)(a_1x_2 + b_1y_2 + c_1)}\\ &+ \frac{(x - x_2)(y - y_2)}{(a_1x + b_1y + c_1)(a_1x_2 + b_1y_2 + c_1)}\left(\mu c_1 + \mu b_1y_2 - \frac{a_1k_1x_2}{1 + k_1N} - \frac{a_1x_2}{1 + k_1N} - \frac{c_1k_1y_2}{1 + k_1N} - \frac{c_1}{1 + k_1N}\right)\end{aligned}$$

Now, if we consider $\mu = \dfrac{1}{c_1 + b_1y_2}\left(\dfrac{a_1k_1x_2}{1 + k_1N} + \dfrac{a_1x_2}{1 + k_1N} + \dfrac{c_1k_1y_2}{1 + k_1N} + \dfrac{c_1}{1 + k_1N}\right)$ then above relation reduces to

$$\begin{aligned}\frac{dV_2}{dt} \leq& -\frac{(x - x_2)^2}{1 + k_1y} + \frac{a_1k_1y_2^2(x - x_2)^2}{(1 + k_1y)(a_1x + b_1y + c_1)(a_1x_2 + b_1y_2 + c_1)} + \frac{a_1y_2(x - x_2)^2}{(1 + k_1y)(a_1x + b_1y + c_1)(a_1x_2 + b_1y_2 + c_1)}\\ \leq& -\frac{(x - x_2)^2}{1 + k_1y}\left(1 - \frac{a_1k_1y_2^2}{c_1(a_1x_2 + b_1y_2 + c_1)} - \frac{a_1y_2}{c_1(a_1x_2 + b_1y_2 + c_1)}\right)\\ \leq& -\frac{(x - x_2)^2}{1 + k_1N}\left(1 - \frac{a_1k_1y_2^2}{c_1(a_1x_2 + b_1y_2 + c_1)} - \frac{a_1y_2}{c_1(a_1x_2 + b_1y_2 + c_1)}\right)\end{aligned}$$

Therefore, $\dfrac{dV_2}{dt} \leq 0$ if $\left(\dfrac{a_1k_1y_2^2}{c_1(a_1x_2 + b_1y_2 + c_1)} + \dfrac{a_1y_2}{c_1(a_1x_2 + b_1y_2 + c_1)}\right) < 1$; i.e., if $a_1y_2(k_1y_2 + 1) < c_1(a_1x_2 + b_1y_2 + c_1)$ and $\dfrac{dV_2}{dt} = 0$ when $(x, y, z) = (x_2, y_2, 0)$.
Hence by using Lyapunov-Lasalle's invariance principle [51] we can say that the planer equilibria $E_2(x_2, y_2, 0)$ is globally asymptotically stable.

Theorem 11 *The coexistence equilibria $E^*(x^*, y^*, z^*)$ is globally asymptotically stable if*

$$N\left(x^* + y^* + \frac{1}{a_2}\right) + d_1y^* + d_2z^* + \left(\frac{1 + x^*}{2}\right)^2 < \frac{\mu_1y^*}{(1 + k_2N)(a_1N + b_1N + c_1)} + \frac{\mu_2z*}{a_2N + b_2N + c_2} + \frac{x^*}{1 + k_1N}$$

holds.

Proof To established the global stability of coexistence equilibria $E^*(x^*, y^*, z^*)$ we introduced the Lyapunov function L^* as follows :

$$V^* = (x - x^* - x^* \log \frac{x}{x^*}) + (y - y^* - y^* \log \frac{y}{y^*}) + (z - z^* - z^* \log \frac{z}{z^*})$$

Then, time derivative of above expression is

$$\frac{dL^*}{dt} = \frac{(x-x^*)}{x}\frac{dx}{dt} + \frac{(y-y^*)}{y}\frac{dy}{dt} + \frac{(z-z^*)}{z}\frac{dz}{dt} \tag{7}$$

Using the Theorem 1, we have considered that there exists a positive constant $N = \frac{M}{d}$ satisfying relations $x(t),\ y(t),\ z(t) < N$, where $0 < d \leq \min d_1, d_2$ and $M = \frac{(1+d)^2}{4}$.
Hence, after some algebraic calculation equation (7) reduces to

$$\begin{aligned}\frac{dL^*}{dt} &\leq \frac{x - x^2 - x^* - xx^*}{1+k_1y} + x^*N - \frac{s_1y^*}{(1+k_2N)(a_1N+b_1N+c_1)} + Ny^* + \frac{1}{a_2}N - \frac{s_2z*}{a_2N+b_2N+c_2} - d_1y + d_1y^* \\ &\quad - d_2z + d_2z^* \\ &\leq -\frac{1}{1+k_1N}\left(x - \frac{1+x^*}{2}\right)^2 + \left(\frac{1+x^*}{2}\right)^2 - \frac{x^*}{1+k_1N} + x^*N - \frac{s_1y^*}{(1+k_2N)(a_1N+b_1N+c_1)} + Ny^* + \frac{1}{a_2}N \\ &\quad - \frac{s_2z^*}{a_2N+b_2N+c_2} + d_1y^* + d_2z^*\end{aligned}$$

From the above expression we can easily observed that $\frac{dL^*}{dt} \leq 0$ if

$$\left(\frac{1+x^*}{2}\right)^2 - \frac{x^*}{1+k_1N} + x^*N - \frac{s_1y^*}{(1+k_2N)(a_1N+b_1N+c_1)} + Ny^* + \frac{1}{a_2}N - \frac{s_2z*}{a_2N+b_2N+c_2} + d_1y^* + d_2z^* \leq 0$$

$$i.e., N\left(x^* + y^* + \frac{1}{a_2}\right) + d_1y^* + d_2z^* + \left(\frac{1+x^*}{2}\right)^2 \leq \frac{s_1y^*}{(1+k_2N)(a_1N+b_1N+c_1)} + \frac{s_2z*}{a_2N+b_2N+c_2} + \frac{x^*}{1+k_1N}.$$

Also, we have $\frac{dL^*}{dt} = 0$ if $(x, y, z) = (x^*, y^*, z^*)$.
Hence by using Lyapunov-Lasalle's invariance principle [51] we can conclude that the coexistence equilibria (x^*, y^*, z^*) is globally asymptotically stable if

$$N\left(x^* + y^* + \frac{1}{a_2}\right) + d_1y^* + d_2z^* + \left(\frac{1+x^*}{2}\right)^2 < \frac{s_1y^*}{(1+k_2N)(a_1N+b_1N+c_1)} + \frac{s_2z*}{a_2N+b_2N+c_2} + \frac{x^*}{1+k_1N}$$

The above condition of global stability of coexistence equilibria is too complicated in the sense of inferring any ecological justification. So, we will verify the global behaviour of the interior equilibria numerically.

Considering values of system parameters $k_1 = 1$, $k_2 = 1$, $a_1 = 0.65$, $a_2 = 20$, $b_1 = 0.1$, $b_2 = 0.91$, $c_1 = 0.2$, $c_2 = 10$, $d_1 = 0.4$, $d_2 = 0.01$, we see that system consist of non-interior equilibria $E_0(0,0)$, $E_1(1,0,0)$, $E_2(0.11982, 0.21670, 0)$ and only one interior equilibria $E^*(0.78077, 0.13886, 1.21888)$. Trivial E_0, axial E_1 are saddle equilibria, planer E_2 is unstable spiral without any limit cycle and coexistence E^* is a stable spiral. Solution trajectories with various starting points converges asymptotically to the stable coexistence equilibria E^* (see Fig. 2). This implies the global asymptotic stability of coexistence equilibria E^*.

5 Local bifurcation analysis

In this segment, we shall now identify some changes in structural behaviour of the model system (4). Qualitative behaviour of system solutions depending upon a certain parameter change as the parameter goes through a certain critical value and for changes in the value of parameter the vector field changes its structural behaviour and hence the system goes through a bifurcation. A certain value of the significant parameter at which the qualitative change of dynamics of our considered prey-predator model occur is called bifurcation point. Now, we discuss the occurrence of transcritical bifurcation at the axial equilibria, saddle-node bifurcation at the interior equilibrium point, Hopf bifurcation and direction of Hopf bifurcation in vicinity of coexistence equilibria concerning some bifurcation parameter.

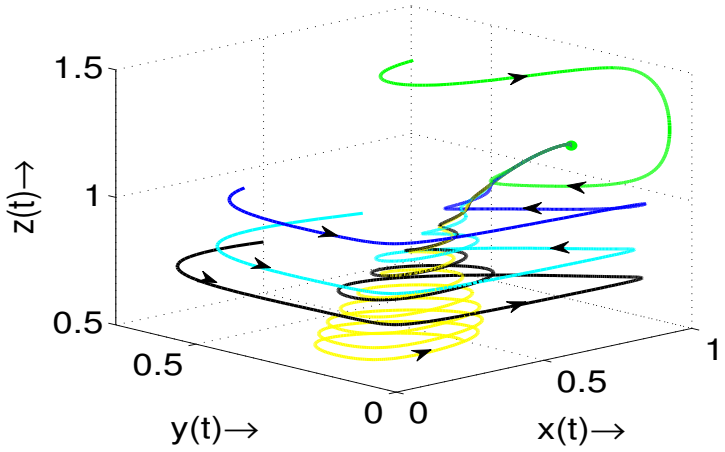

Fig. 2: Solution trajectories of model system (4) with various starting points considering $k_1 = 1$, $k_2 = 1$, $a_1 = 0.65$, $a_2 = 20$, $b_1 = 0.1$, $b_2 = 0.91$, $c_1 = 0.2$, $c_2 = 10$, $d_1 = 0.4$, $d_2 = 0.01$. Figure shows global asymptotic stability of interior equilibria $E^*(0.7807723516, 0.1388648586, 1.218888670)$.

5.1 **Transcritical bifurcation analysis**

We have seen that predator free axial equilibrium point $E_1(1, 0, 0)$ is stable if $d_1 > {d_1}^{[TC]}$ and no planer equilibrium point exists in this situation. The axial equilibria $E_1(1, 0, 0)$ becomes unstable and a stable planer equilibria E_2 creates as $d_1 < d_1^{[TC]}$. Thus axial and planer equilibrium points exchanges their stability as the parameter d_1 crosses threshold value $d_1 = {d_1}^{[TC]}$. The predator free axial equilibrium point E_1 becomes non-hyperbolic at $d_1 = {d_1}^{[TC]}$ as one eigenvalue of Jacobian matrix at that point becomes zero. Thus the system may goes through transcritical bifurcation at axial equilibria E_1 considering d_1 as bifurcation parameter if transversility conditions of Sotomayor's theorem are satisfied [52].

Theorem 12 *The system experiences transcritical bifurcation about axial equilibrium point E_1 at the critical value of $d_1 = d_1^{[TC]}$.*

Proof We shall verify transversality conditions of the considered model system (4) at axial equilibrium point E_1 for the occurrence of transcritical bifurcation considering d_1 as bifurcation parameter.
It is clear that Jacobian matrix $J(E_1)$ corresponding to axial equilibrium point E_1 has two negative eigenvalues and a zero eigenvalue at $d_1 = d_1^{[TC]}$.
Jacobian matrix $J(E_1)$ and its transpose $J(E_1)^T$ has eigenvector $V = (1, -(a_1+c_1), 0)^T$ and $W = (0, 1, 0)^T$ corresponding to zero eigenvalue respectively. Now

$$W^T F_{d_1}(E_1, d_1^{[TC]}) = 0$$
$$W^T [DF_{d_1}(E_1, d_1^{[TC]})V] = a_1 + c_1 \neq 0$$
$$W^T [D^2 F(E_1, d_1^{[TC]})(V, V)] = -2b_1 - \frac{2c_1}{a_1 + c_1} \neq 0$$

Hence all conditions of Sotomayer's theorem are satisfied and system experiences transcritical bifurcation as d_1 crosses the critical value $d_1 = d_1^{[TC]}$.

To present transcritical bifurcation graphically we consider $k_1 = 0.5$, $c_1 = 0.42$, $d_1 = 0.75$, $d_2 = 0.62$ and other parameters values as given in Table 2. The system contains one trivial, one axial and one planer equilibria. The planer equilibria is a stable spiral, while others are saddle. Then increasing the value of parameter d_1 to $d_1 = 0.95$, the planer equilibrium point loses its feasibility criterion and the axial equilibria becomes a stable node. Thus, axial equilibrium point exchanges its stability with planer equilibrium point through destruction of planer equilibrium point i.e., the system experiences transcritical bifurcation as the parameter d_1 goes through a critical value $d_1^{[TC]} = 0.92593$ (see Fig. 3).

Ecologically, the above result has high significance on system dynamics since there is a critical value of middle predator normal death rate d_1, above which it goes to extinction and as a result, the top predator also goes to extinction. Only the prey population survive in the system to its highest population density.

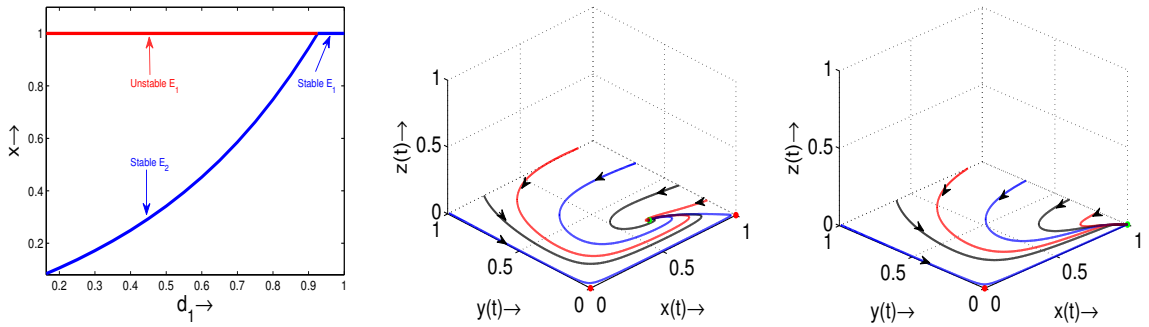

(a) One parameter bifurcation diagram (b) Phase diagram for $d_1 = 0.75$ (c) Phase diagram for $d_1 = 0.95$

Fig. 3: (a) One parametric bifurcation diagram with regard to the parameter d_1, blue & red lines represent the stable & unstable nature of the corresponding equilibria respectively and phase diagram of the model system (4) for: (a) $d_1 = 0.75$, (b) $d_1 = 0.95$ with $k_1 = 0.5$, $c_1 = 0.42$, $d_2 = 0.62$ considering other parameter values as given in Table 2.

5.2 **Saddle-node bifurcation analysis**

Suppose that for $k_1 = k_1^{[SN]}$ two interior equilibrium points of system (4) coincide. Now we investigate condition, under which there are two coexistence equilibria for $k_1 > k_1^{[SN]}$ (or $k_1 < k_1^{[SN]}$) and among them one is saddle point and other is a node. Also there is no interior equilibrium point for $k_1 < k_1^{[SN]}$ (or $k_1 > k_1^{[SN]}$). Thus two coexistence equilibria collide and then annihilated. At the coincident coexistence equilibria $\bar{E}^*(\bar{x}^*, \bar{y}^*, \bar{z}^*)$, Jacobian matrix has a zero eigenvalue and consequently the equilibrium point becomes non-hyperbolic. Thus the system can go through saddle-node bifurcation at interior equilibria E^* as the parameter k_1 passes through critical value $k_1 = k_1^{[SN]}$ if conditions of Sotomayor's theorem are satisfied [52].

Theorem 13 *If $\eta_2 < 0$, $\eta_3 = 0$ at $k_1 = k_1^{[SN]}$ and $\phi_1 p_1 + \phi_2 p_2 + \phi_3 p_3 \neq 0$, then the system (4) goes through saddle-node bifurcation at $k_1 = k_1^{[SN]}$ in vicinity of coincident coexistence equilibria $\bar{E}^*(\bar{x}^*, \bar{y}^*, z^*)$, where p_i, $i = 1, 2, 3$ are defined in the Appendix.*

Proof First we rewrite the consider model system (4) into the form

$$\dot{X} = F(X) \text{ where } X = (x, y, z)^T \text{ and } F = (F_1, F_2, F_3)$$

The Jacobian matrix of the system (4) at coincident coexistence equilibria $\bar{E}^*(\bar{x}^*, \bar{y}^*, z^*)$ has characteristic equation of the form

$$\lambda^3 + \eta_1 \lambda^2 + \eta_2 \lambda + \eta_3 = 0$$

where η_i is obtained from C_i $(i = 1, 2, 3)$ through replacing (x^*, y^*, z^*) by $(\bar{x}^*, \bar{y}^*, \bar{z}^*)$.
Here expressions of $\eta_i, i = 1, 2, 3$ depends on k_1. Hence, $det(J(\bar{E}^*)) = -\eta_3$ is a function of k_1 and we can control sign of $\eta_i, i = 1, 2, 3$. Changing value of parameter k_1, we can obtain critical value $k_1 = k_1^{[SN]}$ for which $\eta_2 < 0$, $\eta_3 = 0$ and consequently eigenvalues of Jacobian matrix $J(\bar{E}^*)$ will be zero, one positive, one negative in order to obtain saddle-node bifurcation at the equilibria $\bar{E}^*(\bar{x}^*, \bar{y}^*, \bar{z}^*)$.
Let θ and ϕ be eigenvectors of Jacobian matrix $J(E^*)$ and its transpose corresponding to eigenvalue zero respectively.
Then we obtain $\theta = (\theta_1, \theta_2, \theta_3)^T = \left(1, -\frac{b_{11}}{b_{12}}, \frac{b_{11} b_{32}}{b_{12} b_{33}}\right)^T$, $\phi = (\phi_1, \phi_2, \phi_3)^T = \left(1, -\frac{b_{11}}{b_{21}}, \frac{b_{11} b_{23}}{b_{21} b_{33}}\right)^T$.
Since

$$\phi^T [F_{k_1}(\bar{E}^*, k_1^{[SN]})] = -\frac{k_1^{[SN]} \bar{x}^* (1 - \bar{x}^*)}{(1 + k_1^{[SN]} \bar{y}^*)^2} \neq 0$$

$$\phi^T [D^2 F(\bar{E}^*, k_1^{[SN]})(\theta, \theta)] = \phi_1 p_1 + \phi_2 p_2 + \phi_3 p_3 \neq 0,$$

if $\phi_1 p_1 + \phi_2 p_2 + \phi_3 p_3 \neq 0$.
Hence the system undergoes through saddle-node bifurcation about coincident interior equilibria $\bar{E}^*(\bar{x}^*, \bar{y}^*, \bar{z}^*)$ at $k_1 = k_1^{[SN]}$.

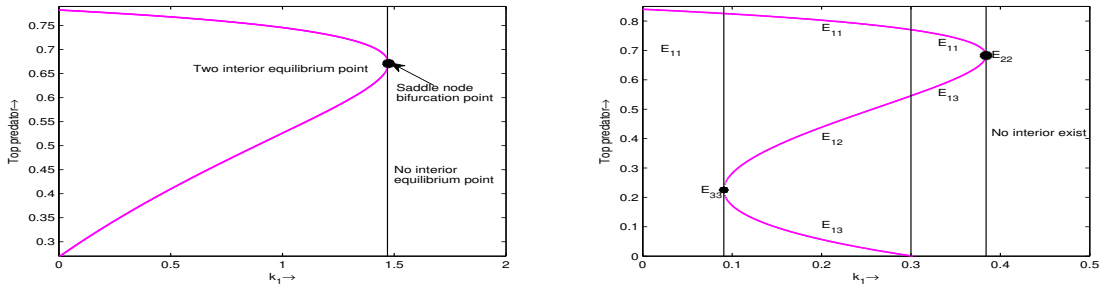

(a) (b)

Fig. 4: One parametric bifurcation diagram with regard to bifurcation parameter k_1 of top predator population considering (a) $a_1 = 0.7$, $b_2 = 0.4$, $c_2 = 1.2$ and other parameters (b) values of system parameters as given in Table 2. Black dot represents the bifurcation point at $k_1 = 1.47433536957$.

In Fig. 4 we have presented the one parametric bifurcation diagram with regard to k_1 for (a) $a_1 = 0.7$, $b_2 = 0.4$, $c_2 = 1.2$ and (b) $a_1 = 0.66$, $b_2 = 0.91$, $c_2 = 1.02$ and other parameters are taken from Table 2. It is clear from the figures that the system shows more complex dynamics in second case that when the mutual interference among the top predators is higher, environmental protection to the intermediate predator and its prey handling times are comparatively lower. In the first figure one saddle-node bifurcation point and in the second figure two saddle-node bifurcation point arises.
Considering values of system parameters as given in Table 2 with $k_1 = 1.3$, $a_1 = 0.7$, $b_2 = 0.4$, $c_2 = 1.2$ we have drawn one parametric bifurcation diagram of top predator with regard to k_1 (see Fig. 4(a)). Then the system (4) contain two interior equilibrium points along with one trivial, one axial and one planer equilibrium point. Among the two coexistence equilibria, one is stable node and other is saddle. Then as we increase value of parameter k_1 to $k_1^{[SN]} = 1.4743353695$ both interior equilibrium points coincide into one and finally diminishes from the system if we again increase the parameter k_1.
It is observed from Fig. 4(b) that the system (4) contains one coexistence equilibria for $k_1 < 0.09078075523$, at $k_1 = 0.09078075523$ the system contains two coexistence equilibria among them one is coincident, three interior equilibrium points (among two new coexistence equilibria one is saddle and other is unstable spiral with stable limit cycle) for $0.09078075523 < k_1 < 0.3$, two coexistence equilibria (one is saddle and other is unstable spiral with stable limit cycle) for $0.3 \leq k_1 < 0.3840366382$ and both the interior equilibrium point coincide at $k_1 = 0.3840366382$ then it diminishes. Here all the non-interior equilibrium points are always exists. The system goes through saddle-node bifurcation two times with regard to bifurcation parameter k_1 at critical values $k_1 = 0.09078075523$, $k_1 = 0.3840366382$. Phase diagrams of model system (4) before and after bifurcations values are similar as in Fig. 10((d), (a)) and 11((a), (c)).

It is clear from Fig. 4(a) that with the increase of fear parameter k_1 the co-existence possibility of all species decreases. In Fig. 5, we have drawn a phase portrait of the model system (4) for different values of k_1 in the left, right and at the critical value of parameter k_1 with other parameters as considered above. From the ecological point of view, we can say that as fear of middle predator to prey increases then the prey population decreases as a result it creates food crisis for both the predators. Consequently, the growth of both predators decreases and finally top predator population goes to extinction and population density of prey and middle predator varies periodically with time.
It is clear from Fig. 4(b) that with the increase of b_2 the co-existence region of all species with respect to k_1 decreases. Since with the increase of mutual interference among top predators, it becomes more busy in their intra-specific competition and less fear of middle predator is sufficient for the decrease of population density in top predator.

5.3 **Hopf bifurcation analysis**

In Hopf bifurcation, a periodic oscillatory solution of the model system appear or disappear throughout a local change in stability of an equilibria. Now, we discuss the occurrence of Hopf bifurcation at coexistence equilibria E^* of model system (4) concerning some bifurcation parameter. We shall vary the parameter k_1,

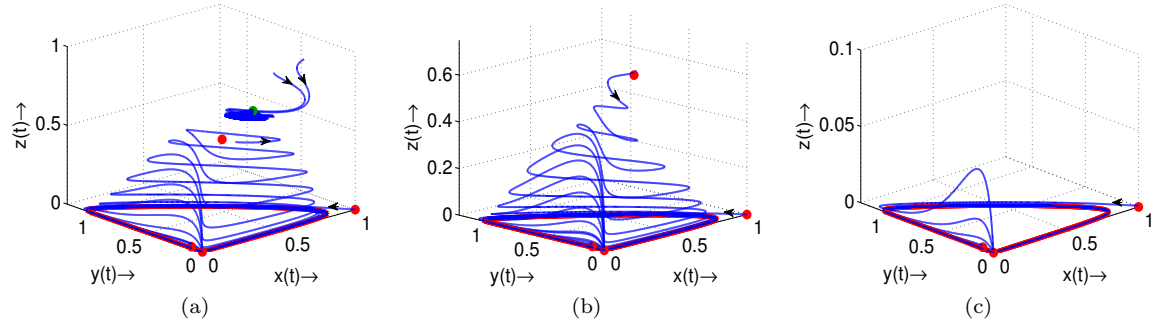

Fig. 5: Phase diagram of model system (4) for different values of the parameter k_1 like as : (a) $k_1 = 1.30$, (b) $k_1 = 1.47433536957$, (c) $k_1 = 1.55$ with $a_1 = 0.7$, $b_2 = 0.4$, $c_2 = 1.2$ and values of other system parameters as given in Table 2. Green dots represent the stable equilibria and red dots represent the unstable equilibria.

so as to obtain a Hopf bifurcation about coexistence equilibria $E^*(x^*, y^*, z^*)$.
The characteristic equation of Jacobian matrix of model system (4) at the coexistence equilibria $E^*(x^*, y^*, z^*)$ is given in (6). Expressions of $C_i; i = 1, 2, 3$ and $C_1C_2 - C_3$ are depends on k_1 if we fix other parameters at constants. Values as well as sign of $C_i; i = 1, 2, 3$ and $C_1C_2 - C_3$ can be controlled by changing values of parameter k_1. A Hopf bifurcation of the system (4) at coexistence equilibria $E^*(x^*, y^*, z^*)$ can be expected for a certain value $k_1 = k_1^*$, when $C_i > 0; i = 1, 2, 3$ and $C_1C_2 - C_3 = 0$. Then, from characteristic equation (6), we have

$$(\lambda^2 + C_2)(\lambda + C_1) = 0.$$

Solving above equation, we have roots as $\lambda_{1,2} = \pm i\sqrt{C_2}$, and $\lambda_3 = -C_1$.
Thus for any $k_1 \in (k_1^* - \epsilon, k_1^* + \epsilon)$, where ϵ is a pre assign positive number, roots of above equation are in general of the form : $\lambda_{1,2}(k_1) = \alpha_0(k_1) + \pm i\beta_0(k_1)$ and $\lambda_3(k_1) = -C_1(k_1)$. To occur Hopf bifurcation the transversality condition $\frac{d}{dk_1}(Re\lambda_i(k_1))|_{k_1=k_1^*} \neq 0, i = 1, 2$ must be satisfied.
Since λ_1 is a root of equation (6), hence

$$\lambda_1^3(k_1) + C_1\lambda_1^2(k_1) + C_2\lambda_1(k_1) + C_3 = 0.$$

Comparing real and imaginary parts, we have

$$\alpha_0^3(k_1) - 3\alpha_0(k_1)\beta_0^2(k_1) + C_1(k_1)\alpha_0^2(k_1) - C_1(k_1)\beta_0^2(k_1) + C_2(k_1)\alpha_0(k_1) + C_3(k_1) = 0,$$
$$-\beta_0^3(k_1) + 3\alpha_0^2(k_1)\beta_0(k_1) + 2C_1(k_1)\alpha_0(k_1)\beta_0(k_1) + C_2(k_1)\beta_0(k_1) = 0.$$

Taking derivative of above equations with respect to k_1, we get

$$A(k_1)\alpha_0'(k_1) - B(k_1)\beta_0'(k_1) + C(k_1) = 0 \tag{8}$$
$$B(k_1)\alpha_0'(k_1) + A(k_1)\beta_0'(k_1) + D(k_1) = 0 \tag{9}$$

where $A(k_1) = 3\alpha_0^2(k_1) + 2C_1(k_1)\alpha_0(k_1) + C_2(k_1) - 3\beta_0^2(k_1)$, $B(k_1) = 6\alpha_0(k_1)\beta_0(k_1) + 2C_1(k_1)\beta_0(k_1)$, $C(k_1) = C_1'(k_1)\alpha_0^2(k_1) + C_2'(k_1)\alpha_0(k_1) + C_3'(k_1) - C_1'(k_1)\beta_0^2(k_1)$ and $D(k_1) = 2C_1'(k_1)\alpha_0(k_1)\beta_0(k_1) + C_2'(k_1)\beta_0(k_1)$.
From equation (8) and (9), we get $\alpha_0'(k_1) = -\dfrac{B(k_1)D(k_1) + A(k_1)C(k_1)}{A^2(k_1) + B^2(k_1)}$ and hence using results $\alpha_0(k_1^*) = 0$, $\beta_0(k_1^*) = \sqrt{C_2(k_1^*)}$, we have

$$\begin{aligned}\frac{d}{dk_1}(Re\lambda_i(k_1))|_{k_1=k_1^*} =& \frac{B(k_1^*)D(k_1^*) + A(k_1^*)C(k_1^*)}{A^2(k_1^*) + B^2(k_1^*)} \\ =& [2C_2(k_1^*)(C_1(k_1^*)C_2'(k_1^*) + C_1'(k_1^*)C_2(k_1^*) - C_3'(k_1^*))]_{k_1=k_1^*} \neq 0\end{aligned}$$

where C_i' denotes derivative of C_i with respect to k_1.
Now, we summarise the above discussion in the form of following theorem :

Theorem 14 *If $C_1, C_2, C_3 > 0$; and $C_1C_2 - C_3 = 0$ at $k_1 = k_1^*$ with $(C_1C_2' + C_1'C_2 - C_3')|_{k_1=k_1^*} \neq 0$, then the system (4) exhibit a Hopf bifurcation, leading to a family of periodic solutions that bifurcates from $E^*(x^*, y^*, z^*)$ in vicinity of $k_1 = k_1^*$, where C_1, C_2, C_3 are defined above.*

5.3.1 **Stability direction of Hopf bifurcating periodic solution**

We find the direction of Hopf bifurcation by using the theorem of normal form. We also derive the stability property of bifurcating periodic solutions of model system (4) as discuss in the literature [53].
We have, eigenvectors v_1, v_2 of Jacobian matrix $J(E^*)$ corresponding to eigenvalues $\lambda_1 = i\omega$, $\lambda_3 = -C_1$ respectively at $k_1 = k_1^*$ are given by

$$v_1 = \begin{bmatrix} p_{11} - ip_{12} \\ p_{21} - ip_{22} \\ p_{31} - ip_{32} \end{bmatrix} \text{ and } v_3 = \begin{bmatrix} p_{13} \\ p_{23} \\ p_{33} \end{bmatrix}$$

where $p_{11} = \dfrac{b_{22}b_{33} - b_{23}b_{32} - \omega^2}{b_{21}b_{32}}$, $p_{12} = -\dfrac{\omega(b_{22} + b_{33})}{b_{21}b_{32}}$, $p_{13} = \dfrac{b_{12}(b_{33} + C_1)}{b_{32}(b_{11} + C_1)}$, $p_{21} = -\dfrac{b_{33}}{b_{32}}$, $p_{22} = \dfrac{\omega}{b_{32}}$, $p_{23} = -\dfrac{b_{33} + C_1}{b_{32}}$, $p_{31} = 1$, $p_{32} = 0$, $p_{33} = 1$. Using transformation $x = x^* + p_{11}x_1 + p_{12}y_1 + p_{13}z_1, y = y^* + p_{21}x_1 + p_{22}y_1 + p_{23}z_1, z = z^* + p_{31}x_1 + p_{32}y_1 + p_{33}z_1$ the model system (4) reduces to

$$\frac{dx_1}{dt} = P_1 \tag{10a}$$
$$\frac{dy_1}{dt} = P_2 \tag{10b}$$
$$\frac{dz_1}{dt} = P_3 \tag{10c}$$

where, $P_1 = \dfrac{p_{22}L_1 - p_{12}L_2 + (p_{12}p_{23} - p_{22}p_{13})L_3}{D}$, $P_2 = \dfrac{p_{23}L_1 + (p_{11} - p_{13})L_2 - p_{11}p_{23}L_3}{D}$, $P_3 = \dfrac{-p_{22}L_1 + p_{12}L_2 + p_{11}p_{22}L_3}{D}$ with

$$D = (p_{11}p_{22} - p_{13}p_{22} + p_{23}p_{12}), L_1 = \frac{(x^* + p_{11}x_1 + p_{12}y_1 + p_{13}z_1)[1 - (x^* + p_{11}x_1 + p_{12}y_1 + p_{13}z_1)]}{1 + k_1(y^* + p_{21}x_1 + p_{22}y_1 + p_{23}z_1)}$$
$$- \frac{(x^* + p_{11}x_1 + p_{12}y_1 + p_{13}z_1)(y^* + p_{21}x_1 + p_{22}y_1 + p_{23}z_1)}{a_1(x^* + p_{11}x_1 + p_{12}y_1 + p_{13}z_1) + b_1(y^* + p_{21}x_1 + p_{22}y_1 + p_{23}z_1) + c_1}$$
$$L_2 = \frac{(x^* + p_{11}x_1 + p_{12}y_1 + p_{13}z_1)(y^* + p_{21}x_1 + p_{22}y_1 + p_{23}z_1)}{[1 + k_2(z^* + p_{31}x_1 + p_{32}y_1 + p_{33}z_1)][a_1(x^* + p_{11}x_1 + p_{12}y_1 + p_{13}z_1) + b_1(y^* + p_{21}x_1 + p_{22}y_1 + p_{23}z_1) + c_1]}$$
$$- d_1(y^* + p_{21}x_1 + p_{22}y_1 + p_{23}z_1) - \frac{(y^* + p_{21}x_1 + p_{22}y_1 + p_{23}z_1)(z^* + p_{31}x_1 + p_{32}y_1 + p_{33}z_1)}{a_2(y^* + p_{21}x_1 + p_{22}y_1 + p_{23}z_1) + b_2(z^* + p_{31}x_1 + p_{32}y_1 + p_{33}z_1) + c_2}$$
$$L_3 = \frac{(y^* + p_{21}x_1 + p_{22}y_1 + p_{23}z_1)z}{a_2(y^* + p_{21}x_1 + p_{22}y_1 + p_{23}z_1) + b_2(z^* + p_{31}x_1 + p_{32}y_1 + p_{33}z_1) + c_2} - d_2(z^* + p_{31}x_1 + p_{32}y_1 + p_{33}z_1).$$

Here it is clear that system (10) has an equilibria at $E(0, 0, 0)$. Jacobian matrix of system (10) at equilibria $E(0, 0, 0)$ is $J(E) = \begin{bmatrix} \frac{\partial P_1}{\partial x_1} & \frac{\partial P_1}{\partial y_1} & \frac{\partial P_1}{\partial z_1} \\ \frac{\partial P_2}{\partial x_1} & \frac{\partial P_2}{\partial y_1} & \frac{\partial P_2}{\partial z_1} \\ \frac{\partial P_3}{\partial x_1} & \frac{\partial P_3}{\partial y_1} & \frac{\partial P_3}{\partial z_1} \end{bmatrix}$ where $\dfrac{\partial P_1}{\partial x_1} = \dfrac{\partial P_2}{\partial y_1} = \dfrac{\partial P_1}{\partial z_1} = \dfrac{\partial P_2}{\partial z_1} = \dfrac{\partial P_3}{\partial x_1} = \dfrac{\partial P_3}{\partial y_1} = 0$, $-\dfrac{\partial P_1}{\partial y_1} = \dfrac{\partial P_2}{\partial x_1} = \omega$ and $\dfrac{\partial P_3}{\partial z_1} = C_1$.
We calculate values of h_{11}, h_{02}, h_{20}, H_{101}, H_{110}, H_{21}, g_{11}, g_{20}, ω, w_{20}, w_{11} and h_{21} by using following

relations :

$$
\begin{aligned}
h_{11} =& \frac{1}{4}\left[\left(\frac{\partial^2 P_1}{\partial x_1^2}+\frac{\partial^2 P_2}{\partial y_1^2}\right)+i\left(\frac{\partial^2 P_2}{\partial x_1^2}+\frac{\partial^2 P_1}{\partial y_1^2}\right)\right],\\
h_{02} =& \frac{1}{4}\left[\left(\frac{\partial^2 P_1}{\partial x_1^2}-\frac{\partial^2 P_1}{\partial y_1^2}-2\frac{\partial^2 P_2}{\partial x_1 \partial y_1}\right)+i\left(\frac{\partial^2 P_2}{\partial x_1^2}-\frac{\partial^2 P_2}{\partial y_1^2}+2\frac{\partial^2 P_1}{\partial x_1 \partial y_1}\right)\right],\\
h_{20} =& \frac{1}{4}\left[\left(\frac{\partial^2 P_1}{\partial x_1^2}-\frac{\partial^2 P_1}{\partial y_1^2}+2\frac{\partial^2 P_2}{\partial x_1 \partial y_1}\right)+i\left(\frac{\partial^2 P_2}{\partial x_1^2}-\frac{\partial^2 P_2}{\partial y_1^2}-2\frac{\partial^2 P_1}{\partial x_1 \partial y_1}\right)\right],\\
G_{21} =& \frac{1}{8}\left[\left(\frac{\partial^3 P_1}{\partial x_1^3}+\frac{\partial^3 P_1}{\partial x_1 \partial y_1^2}+\frac{\partial^3 P_2}{\partial x_1^2 \partial y_1}+\frac{\partial^3 P_2}{\partial y_1^3}\right)+i\left(\frac{\partial^3 P_2}{\partial x_1^3}+\frac{\partial^3 P_2}{\partial x_1 \partial y_1^2}-\frac{\partial^3 P_1}{\partial x_1^2 \partial y_1}+\frac{\partial^3 P_1}{\partial y_1^3}\right)\right],\\
\omega =& -\frac{\partial P_1}{\partial y_1}, g_{11}=\frac{1}{4}\left(\frac{\partial^2 P_3}{\partial x_1^2}+\frac{\partial^2 P_3}{\partial y_1^2}\right), g_{20}=\frac{1}{4}\left(\frac{\partial^2 P_3}{\partial x_1^2}-\frac{\partial^2 P_3}{\partial y_1^2}-2i\frac{\partial^2 P_3}{\partial x_1 \partial y_1}\right).
\end{aligned}
$$

We find out the constants w_{11} and w_{20} solving two equations : $C_1 w_{11} = -h_{11}, (D - 2i\omega)w_{20} = -h_{20}$. Also,

$$
\begin{aligned}
H_{110} =& \frac{1}{2}\left[\left(\frac{\partial^2 P_1}{\partial x_1 \partial z_1}+\frac{\partial^2 P_2}{\partial y_1 \partial z_1}\right)+i\left(\frac{\partial^2 P_2}{\partial x_1 \partial z_1}-\frac{\partial^2 P_1}{\partial y_1 \partial z_1}\right)\right],\\
H_{101} =& \frac{1}{2}\left[\left(\frac{\partial^2 P_1}{\partial x_1 \partial z_1}-\frac{\partial^2 P_2}{\partial y_1 \partial z_1}\right)+i\left(\frac{\partial^2 P_2}{\partial x_1 \partial z_1}+\frac{\partial^2 P_1}{\partial y_1 \partial z_1}\right)\right],\\
g_{21} =& G_{21} + 2H_{110}w_{11} + H_{101}w_{20}.
\end{aligned}
$$

Another discriminant quantities which will determine the direction of Hopf bifurcation are listed below :

$$
\begin{aligned}
D_1(0) =& \frac{i}{2\omega}\left(h_{20}h_{11} - 2|h_{11}|^2 - \frac{1}{3}|h_{02}|^2\right) + \frac{1}{2}g_{21},\\
\sigma =& -\frac{Re\left\{D_1(0)\right\}}{\alpha'(0)},\\
\delta =& 2Re\left\{D_1(0)\right\},\\
T =& -\frac{Im\left\{D_1(0)\right\} + \sigma\omega'(0)}{\omega}
\end{aligned}
$$

where $\alpha'(0) = \frac{d}{dk_1}(Re\left\{\lambda_1(k_1)\right\})|_{k_1=k_1^*}$ and $\omega'(0) = \frac{d}{dk_1}(Im\left\{\lambda_1(k_1)\right\})|_{k_1=k_1^*}$.
Here, the sign of σ determines the direction Hopf-bifurcation. The direction of Hopf-bifurcation is super-critical (or sub-critical) if $\sigma > 0$ (or $\sigma < 0$); δ determines stability of periodic solutions according as if $\delta < 0$ (or $\delta > 0$) then solutions are stable (or unstable); and the period of bifurcating periodic solutions is determined by T according as the period increases (or decreases) if $T > 0$ (or $T < 0$).
Considering values of system parameters as given in Table 2, the system contains three interior equilibrium point along with three unstable non-interior equilibria. Among three coexistence equilibria, one is a stable spiral and the others are unstable spiral. With the increase of parameter k_1, the stable coexistence equilibria looses its stability and becomes center for the critical value of parameter k_1 at $k_1^* = 0.30198352$. If we further increase the parameter k_1, then the equilibrium point becomes an unstable spiral and any solution trajectory starting in the vicinity of the equilibria goes to a stable limit cycle around it. Thus the system goes through Hopf bifurcation with respect bifurcation parameter k_1 at critical value $k_1 = k_1^*$. In Fig. 6, we have drawn phase portrait of the model system for $k_1 < k_1^*$ and $k_1 > k_1^*$ with other parameters as given in Table 2. We have evaluated the first Lyapunov number σ of Hopf bifurcation at Hopf bifurcation point and the value is $\sigma = 0.7349$. Thus the from above discussion, we can say that the system (4) goes through supercritical Hopf bifurcation concerning the parameter k_1.

Again the system goes through sub-critical Hopf bifurcation with respect to bifurcation parameter k_2 at critical value $k_2^* = 1.073028$. We have drawn phase portrait of model system (4) for $k_2 < k_2^*$ and $k_2 > k_2^*$ in Figure 7 with other parameters as given in Table 2.

From the ecological point of view, we can say that parameters k_1, k_2 play a key role in the existence of all system population. With an increase of middle predator fear to prey k_1, the density of prey decreases, consequently the system loses its stability and the top predator population goes to extinction while prey and

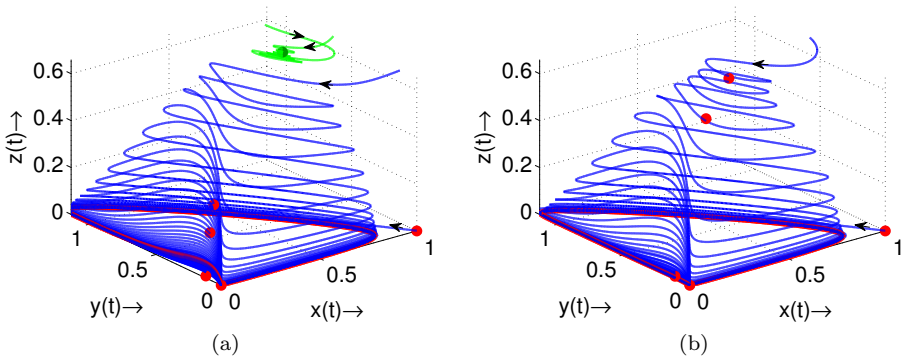

Fig. 6: Phase diagram of the model system (4) for different values of parameter k_1 like as : (a) $k_1 = 0.10$, (b) $k_1 = 0.35$ with values of other system parameters as given in Table 2. Green dot represents the stable equilibria and red dots represent unstable equilibria.

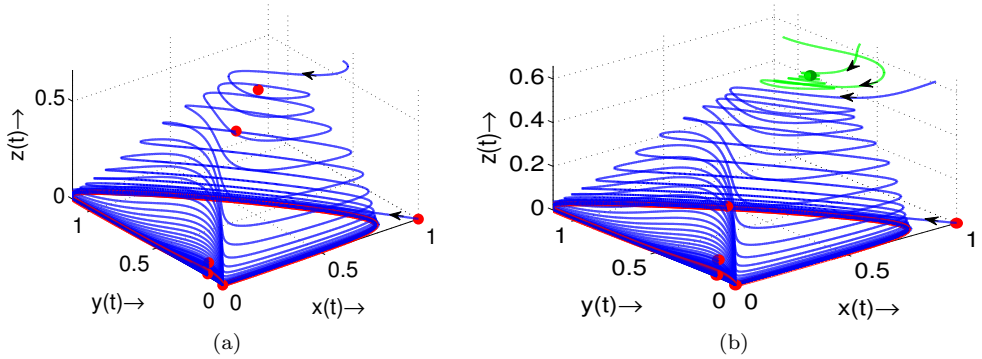

Fig. 7: Phase diagram of the model system (4) for different values of the parameter k_2 like as : (a) $k_2 = 1.0$, (b) $k_2 = 1.5$ with values of other system parameters as given in Table 2. Green dot represents the stable and red dots represent unstable equilibria.

middle predator population density vary periodically with time. Again with an increase of fear parameter k_2, a less number of middle predator are accessible in the system by a top predator. As a result, the consumption of prey by the middle predator will decrease and prey will be available for the top predators and the survival possibility of all three species in the system will increase.

6 Numerical illustration

In this segment of the paper using numerical simulations the theoretical finding of the previous sections will be justified. As the fear of top predator and intermediate predator reduces the growth rate of intermediate predator and prey population respectively, it will change the dynamics of the food chain model abruptly. We observed the significance of different system parameters through the graphical representation. For this purpose, we draw different bifurcation diagram and phase portrait of the system in the following figure.

(a) Dynamics of the system for different values of k_1 and k_2

To study the effect of fear of both the predators on the dynamics of the proposed food chain model different bifurcation curves in $k_1 - k_2$ parametric plane are drawn (see Fig. 8) with values of other parameters as given in Table 2. To discuss the existence and stability dynamics of different equilibria we have drawn saddle-node and Hopf bifurcation curve for coexistence equilibria in the $k_2 - k_1$ parametric plane considering values of other parameters as given Table 2 in Fig. 8.
In Fig. 8, the blue line is the creation or distraction of one interior equilibrium point and red, magenta lines

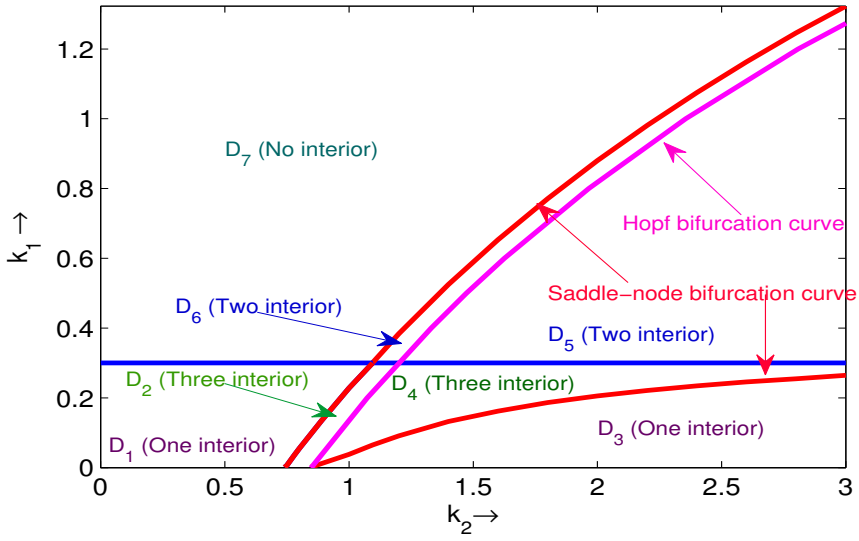

Fig. 8: Schematic bifurcation diagram of system (4) in $k_2 - k_1$ parametric plane considering values of other parameters as given in Table 2. Here blue, red and magenta lines are the creation or distraction of one interior equilibrium point, saddle-node and Hopf bifurcation curve for coexistence equilibria respectively.

are saddle-node, Hopf bifurcation curves for coexistence equilibria respectively. Thus $k_2 - k_1$ parametric plane divided into seven distinct subregion (D_1, D_2, D_3, D_4, D_5, D_6 and D_7) with different number or nature of equilibria. The trivial, axial and one planer equilibrium points always exist throughout the plane where the trivial, axial equilibrium points are saddle and the planer equilibrium point is an unstable spiral for the considered values of the parameters.

In the sub-region D_1 only one coexistence equilibria exists and it is an unstable spiral. A stable limit cycle arises in the phase space and all solution curve starting from anywhere in the phase space goes to the stable limit cycle (see Fig. 9((a), (b))). Then increasing k_2 enter in sub-region D_2, two new interior equilibria (one is saddle and other is unstable spiral) arise. All the three interior equilibrium points are unstable spiral here, a stable limit cycle arises around one of them (see Fig. 9((c), (d))). But if we increase k_1 instead of k_2 in the sub-region D_7, no coexistence equilibria exist i.e., the coexistence equilibria diminishes here and only the non-interior equilibrium points are exist here (see Fig. 11((c), (d))).

Then if we enter into the sub-region D_4 from D_2 crossing the Hopf bifurcation curve, the number of interior equilibria remain the same but the coexistence equilibria with the highest top predator population density becomes a stable spiral. Here the phase space divided into two distinct basin of attractor where solution curve starting from any basins either goes to the stable coexistence equilibria or goes to the stable limit cycle i.e., bi-stability occurs here (see Fig. 10((a), (b), (c))).
From sub-region D_4, if we decrease the parameter k_1 and enter into the subregion D_3, we observe that both the unstable interior equilibrium points are vanishes here but the bi-stability nature remains unaltered as previous. Thus one stable coexistence equilibria and a stable limit cycle exist here (see Fig. 10((d), (e), (f))). But if increase the parameter k_1 and enter into the subregion D_5, only one unstable interior equilibria vanishes and the remaining two coexistence equilibria has the same nature as in the sub-region D_4. Bi-stability also occurs here and the phase space divided into two distinct attractor (see Fig. 10((g), (h), (i))). The bi-stability has high significance from the biological point of view. Survival of populations not only depends on the parameter values but also on population density at the initial time. Next, if we decrease the parameter k_2 and enter into the subregion D_6 from D_5 crossing the Hopf bifurcation curve, we observe that the stable coexistence equilibria become an unstable spiral with a stable limit cycle and the other one remain same. Thus both interior equilibrium points are unstable and any solution curve goes to the stable limit cycle (see Fig. 11((a), (b))).
Thus from the above discussion one can conclude that both fear parameters (consequently fear effects) can regulate the co-existence of all three species for moderate values of system parameters. If the fear of top predator to intermediate predator increases the system goes to stable situation from periodic oscillatory

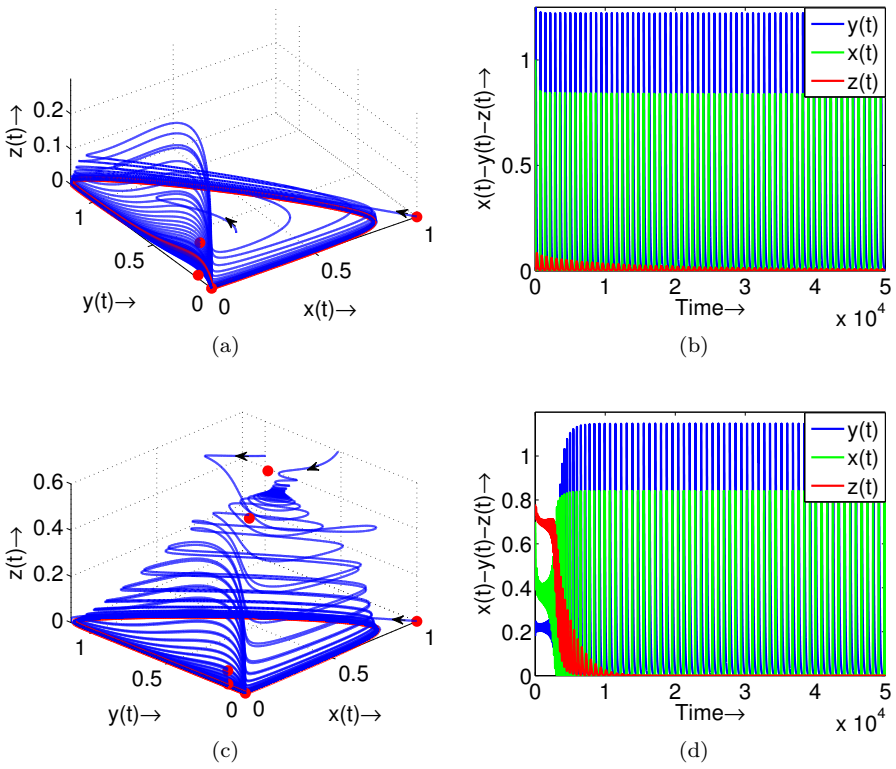

Fig. 9: Phase diagram and time series solution of different species of the model system (4) in different sub-region like as : (a), (b) in sub-region D_1, (c), (d) in sub-region D_2, with values of other system parameters as given in Table 2. Red dots represent the unstable equilibria.

behaviour. But if the fear of intermediate predator to prey increases the system enter into oscillatory behaviour from a stable situation.

(b) Chaotic dynamics of the system

In this segment we are interested to investigate the chaotic dynamics and its control strategies with respect to some important model parameters. For this purpose consider values of system parameters as $k_1 = 0.02$, $k_2 = 0.001$, $a_1 = 0.65$, $a_2 = 20$, $b_1 = 0.01$, $b_2 = 0.005$, $c_1 = 0.2$, $c_2 = 10$, $d_1 = 0.4$, $d_2 = 0.01$ taken from [47], the system consist of only one coexistence equilibrium point E^* $(0.830088, 0.125558, 8.922137)$ with one trivial, one axial, one planer equilibrium points and all equilibrium points are unstable here. With initial population density $(0.6, 0.52, 4.2)$, the solution trajectory shows higher periodic behaviour i.e., the model system (4) exhibits chaotic behaviour.

(I) Chaos control dynamics of the control parameter b_1

Now, we explore the impact of mutual interference among middle predator on controlling chaotic dynamics of model system (4). With the increase of parameter b_1, the system enters into stable situation from its chaotic state through the period-halving bifurcation (see Fig. 12 and Fig. 13). We show that system has chaotic, higher periodic oscillations in $b_1 < 0.0811$; then two periodic oscillations in the interval $(0.0811, 0.1703)$; limit cycle oscillations in the interval $(0.1703, 0.3867)$, and stable behaviour for $b_1 \geq 0.3867$. Therefore, for lower values of mutual interference among middle predator, the system shows chaotic behaviour. Then with the increase of values of mutual interference, the system becomes the stable focus from chaos.
In Fig. 12 and Fig. 13, we have drawn phase portrait and time series solution of the system (4) for different values of the parameter b_1. The first row of Fig. 12 shows the chaotic behaviour for $b_1 = 0.01$, second row of Fig. 12 exhibits the two periodic limit cycle oscillation for $b_1 = 0.08$. Then first row of Fig. 13

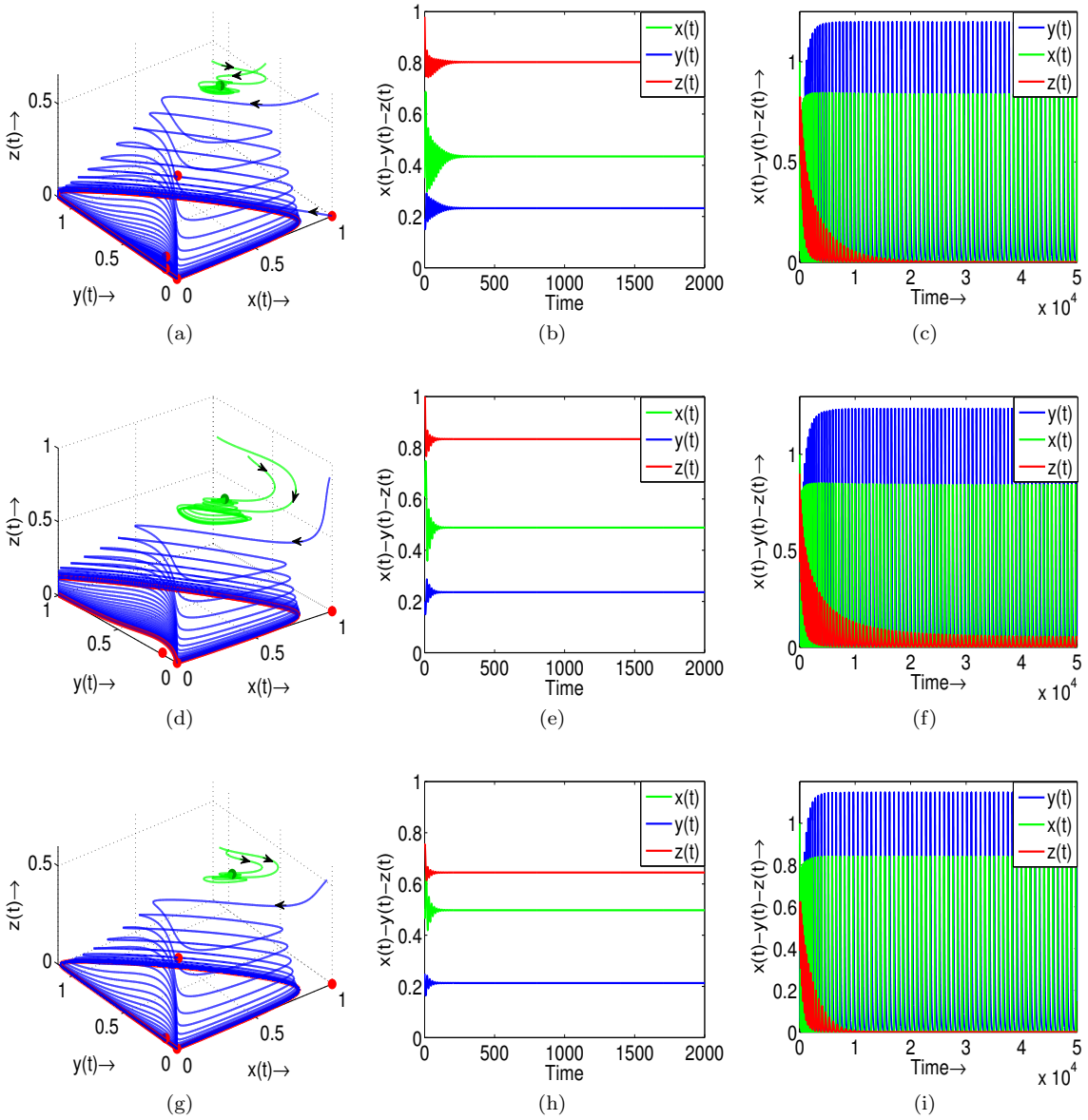

Fig. 10: Phase diagram and time series solution at stable and unstable equilibrium point respectively of different species of the model system (4) in different sub-region like as : (a), (b), (c) in sub-region D_4, (d), (e), (f) in sub-region D_3, and (g), (h), (i) in sub-region D_5 with values of other system parameters as given in Table 2. Green dot represents the stable equilibria and red dots represent the unstable equilibria.

shows one limit cycle oscillation for $b_1 = 0.20$ and second row of Fig. 13 shows stable behaviour for $b_1 = 0.41$.

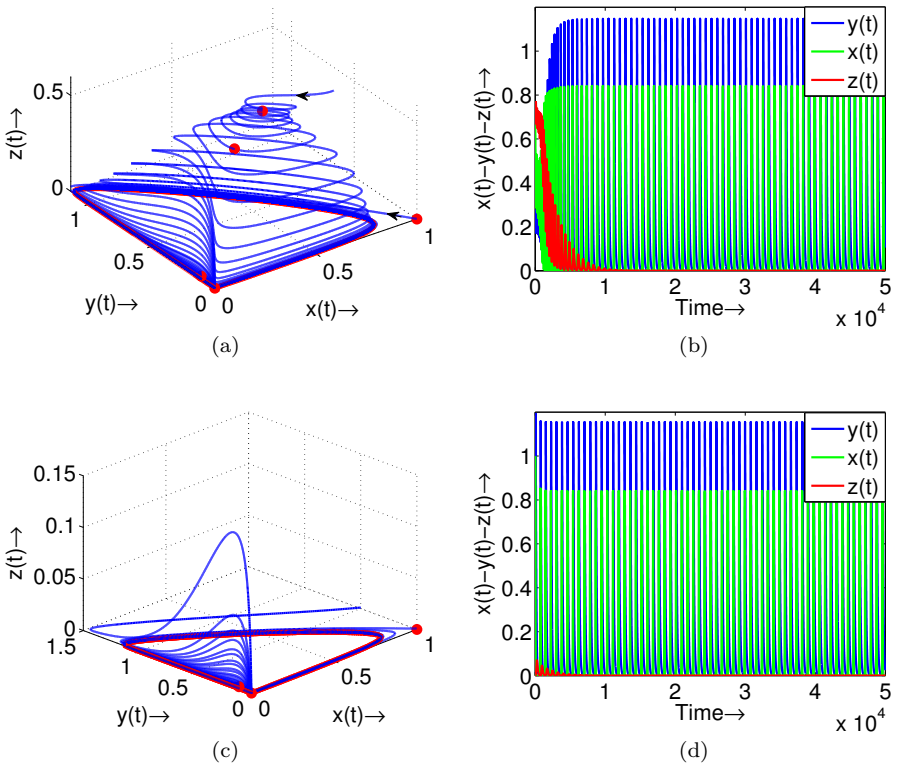

Fig. 11: Phase diagram and time series solution of different species of the model system (4) in different sub-region like as : (a), (b) in sub-region D_6, (c), (d) in sub-region D_7, with values of other system parameters as given in Table 2. Red dots represent the unstable equilibria.

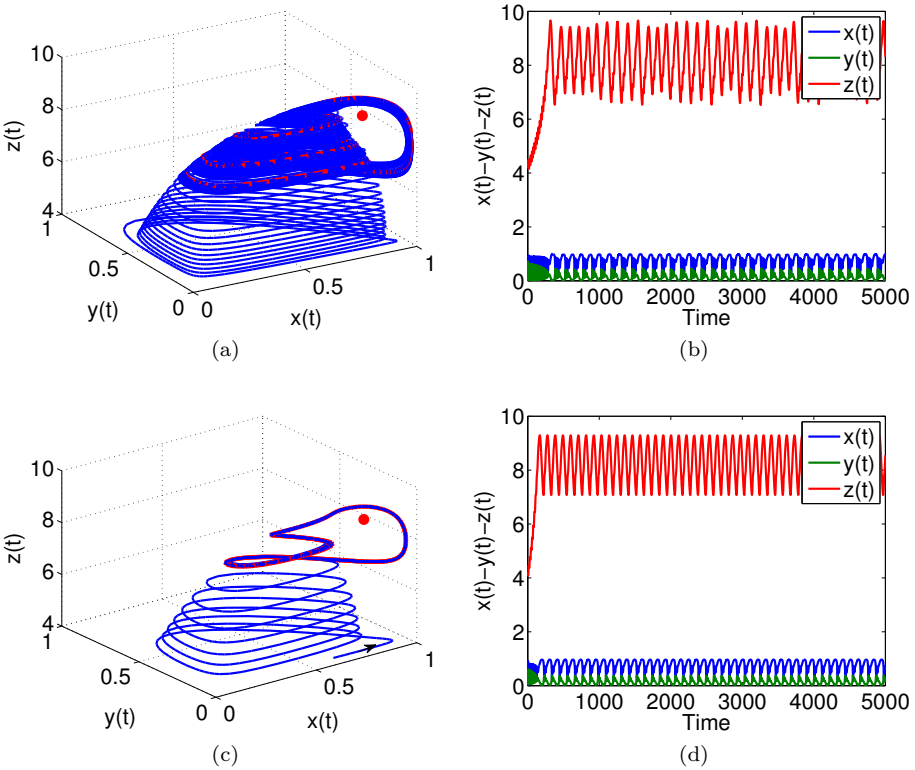

Fig. 12: Phase diagram and time series solution of all the three species of the system (4) for different values of b_1 like as : (a), (b) for $b_1 = 0.01$ and (c), (d) for $b_1 = 0.08$ with other parameters value as considered above. Red dot represent unstable equilibrium point.

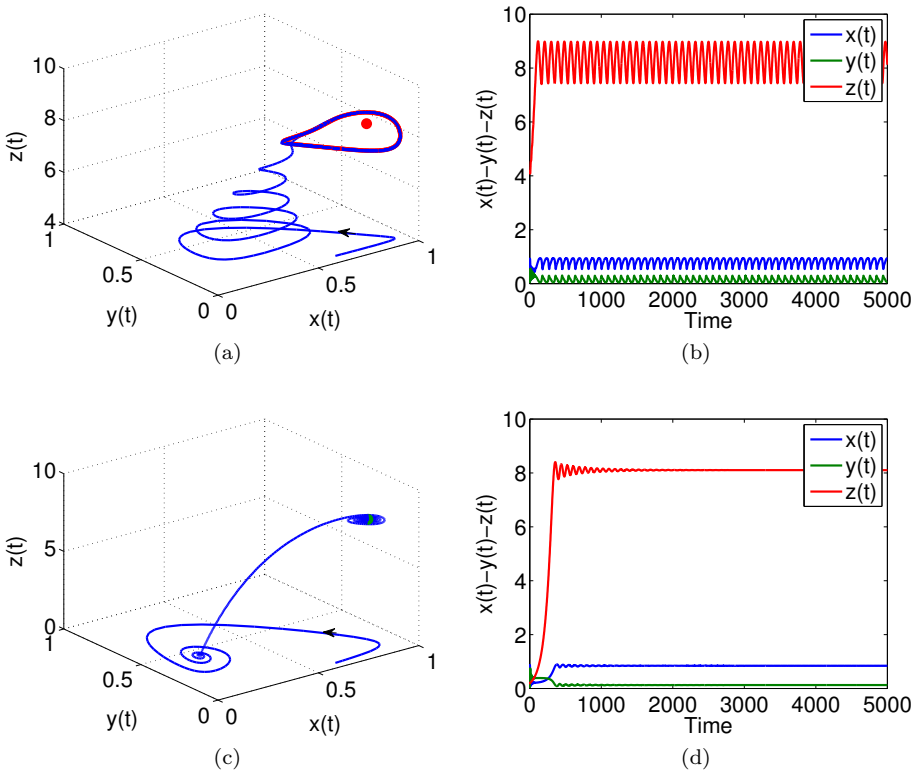

Fig. 13: Phase diagram and time series solution of all the three species of the system (4) for different values of b_1 like as : (a), (b) for $b_1 = 0.20$ and (c), (d) for $b_1 = 0.41$ with other parameters value as considered above. Green dot, red dot represent stable, unstable equilibrium points.

(II) Chaos control dynamics of the control parameter b_2

Similarly, the mutual interference among top predator b_2 can also control the chaotic dynamics of model system (4). With the increase of parameter b_2, the system enters into stable situation from its chaotic state through period-halving bifurcation (see Fig. 14 and Fig. 15). System shows chaotic, higher periodic oscillations in $b_2 < 0.1319$; then two periodic oscillations in the interval $(0.1319, 0.2213)$; limit cycle oscillations in the interval $(0.2213, 0.3119)$, and stable behaviour for $b_2 \geq 0.3119$.
In Fig. 14 and Fig. 15, we have drawn phase portrait and time series solution of the system (4) for different values of parameter b_2. The first row of Fig. 14 shows the chaotic behaviour for $b_2 = 0.005$, second row of Fig. 14 exhibits the two periodic limit cycle oscillation for $b_2 = 0.15$. Then first row of Fig. 15 shows one periodic limit cycle oscillation for $b_2 = 0.26$ and second row of Fig. 15 shows stable behaviour for $b_2 = 0.40$.

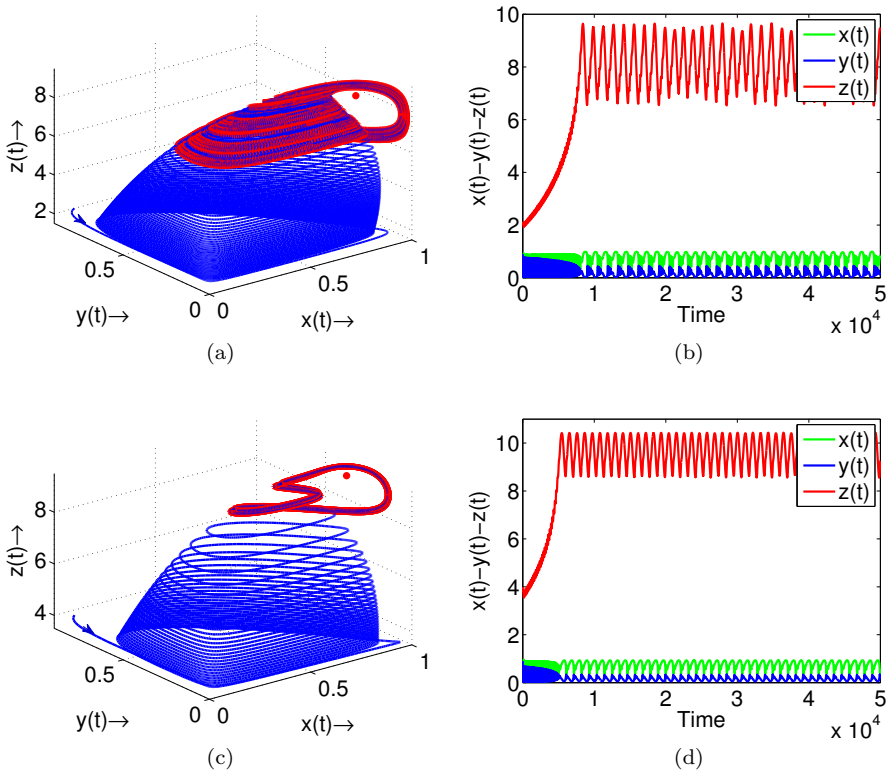

Fig. 14: Phase diagram and time series solution of all the three species of the system (4) for different values of b_2 like as : (a), (b) for $b_2 = b_2 = 0.005$ and (c), (d) for $b_2 = 0.15$ with other parameters value as considered above. Red dot represent unstable equilibrium point.

These phenomena of the system are significant from the ecological point of view. If the mutual interference among predator (middle or top) increase, predators become busy in their intra-specific collision and hence growth rate of predator decreases. As a result, less number of prey or middle predator are consumed by a middle predator or top predator. Consequently, the system becomes stable and all three populations can survive in the system with a positive density level. Mutual interference among middle predators and top predators both has a stabilizing effect on the system dynamics (see Fig. 20(a)).

(III) Chaos control dynamics of the control parameter k_1

Similarly, the fear of intermediate predator on prey k_1 can also control the chaotic dynamics of model system (4). With the increase of parameter k_1, the system enters into stable situation from its chaotic state through period-halving bifurcation (see Fig. 16 and Fig. 17). System shows chaotic, higher periodic oscillations in $k_1 < 0.8477$; then two periodic oscillations in the interval $(0.8477, 1.559)$; limit cycle oscillations in the interval $(1.559, 2.178)$, and stable behaviour for $k_1 \geq 2.178$.
In Fig. 16 and Fig. 17, we have drawn phase portrait and time series solution of the system (4) for different values of parameter k_1. The first row of Fig. 16 shows the chaotic behaviour for $k_1 = 0.02$, second row of Fig. 16 exhibits the two periodic limit cycle oscillation for $k_1 = 1.0$. Then first row of Fig. 17 shows one periodic limit cycle oscillation for $k_1 = 1.8$ and second row of Fig. 17 shows stable behaviour for $k_1 = 6.0$.

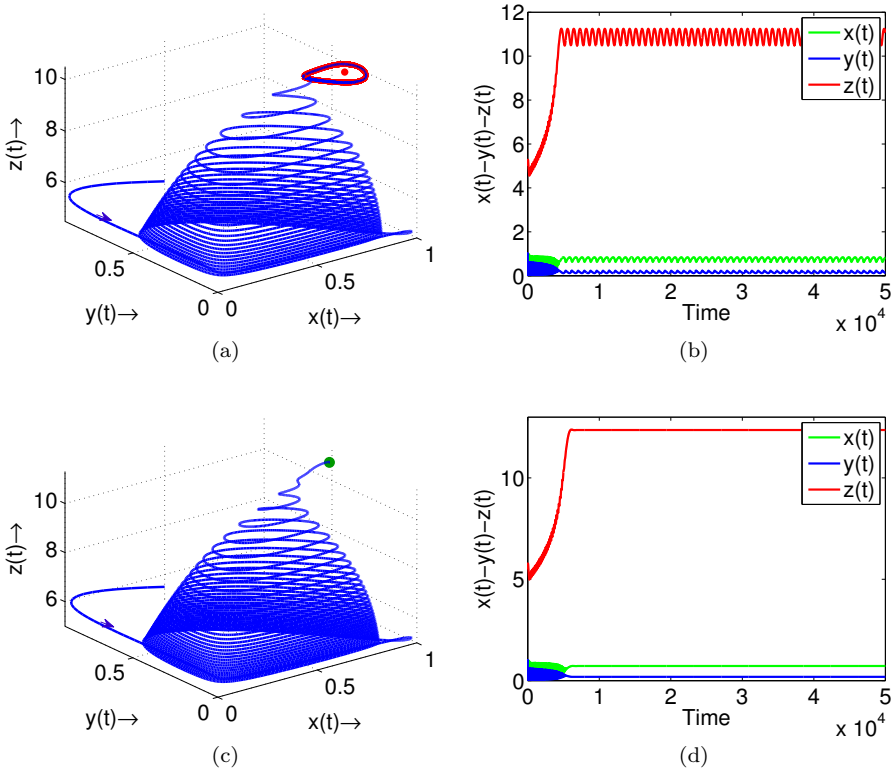

Fig. 15: Phase diagram and time series solution of all the three species of the system (4) for different values of b_2 like as : (a), (b) for $b_2 = 0.26$ and (c), (d) for $b_2 = 0.40$ with other parameters value as considered above. Green dot, red dot represent stable, unstable equilibrium points.

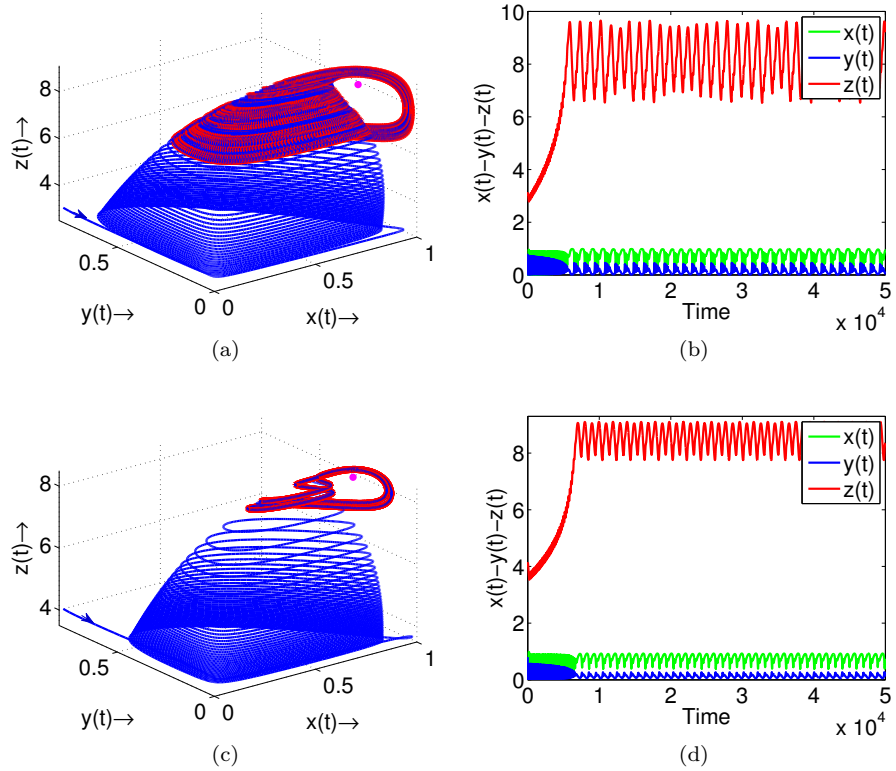

Fig. 16: Phase diagram and time series solution of all the three species of the system (4) for different values of k_1 like as : (a), (b) for $k_1 = 0.02$ and (c), (d) for $k_1 = 1.0$ with other parameters value as considered above. Red dot represent unstable equilibrium point.

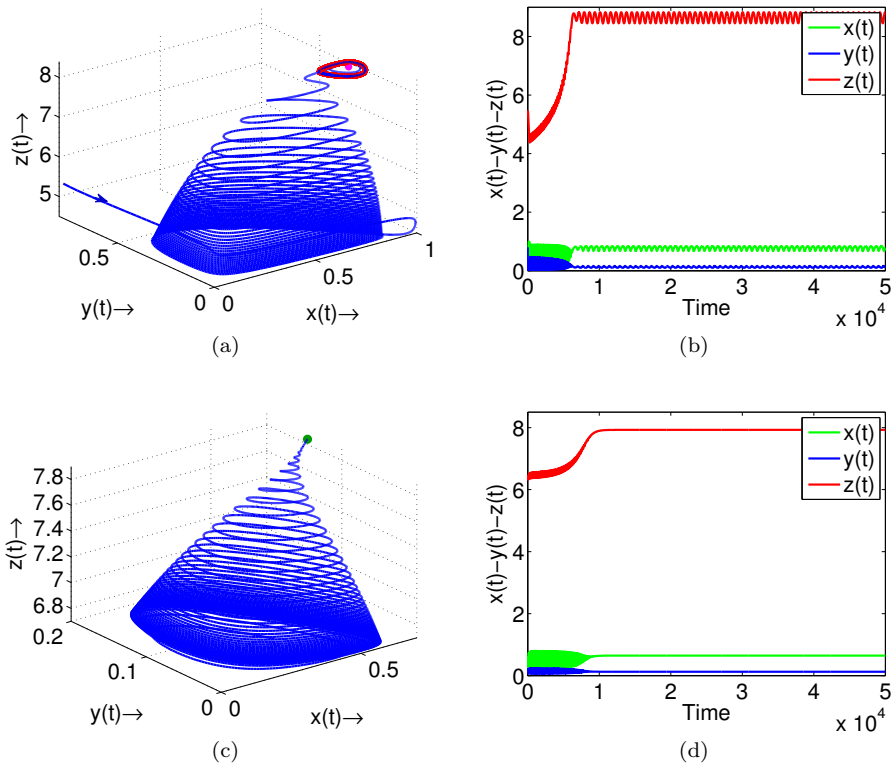

Fig. 17: Phase diagram and time series solution of all the three species of the system (4) for different values of k_1 like as : (a), (b) for $k_1 = 1.8$ and (c), (d) for $k_1 = 6.0$ with other parameters value as considered above. Green dot, red dot represent stable, unstable equilibrium points.

(IV) Chaos control dynamics of the control parameter k_2

Similarly, the middle predator on prey k_2 can also control the chaotic dynamics of model system (4). With the increase of parameter k_2, the system enters into stable situation from its chaotic dynamics through period-halving bifurcation (see Fig. 18 and Fig. 19). System shows chaotic, higher periodic oscillations in $k_2 < 0.0198$; then two periodic oscillations in the interval $(0.0198, 0.0593)$; limit cycle oscillations in the interval $(0.0593, 0.3931)$, and stable behaviour for $k_2 \geq 0.3931$.
In Fig. 18 and Fig. 19, we have drawn phase portrait and time series solution of the system (4) for different values of parameter k_2. The first row of Fig. 18 shows the chaotic behaviour for $k_2 = 0.001$, second row of Fig. 18 exhibits the two periodic limit cycle oscillation for $k_2 = 0.04$. Then first row of Fig. 19 shows one periodic limit cycle oscillation for $k_2 = 0.1$ and second row of Fig. 19 shows stable behaviour for $k_2 = 2.0$.

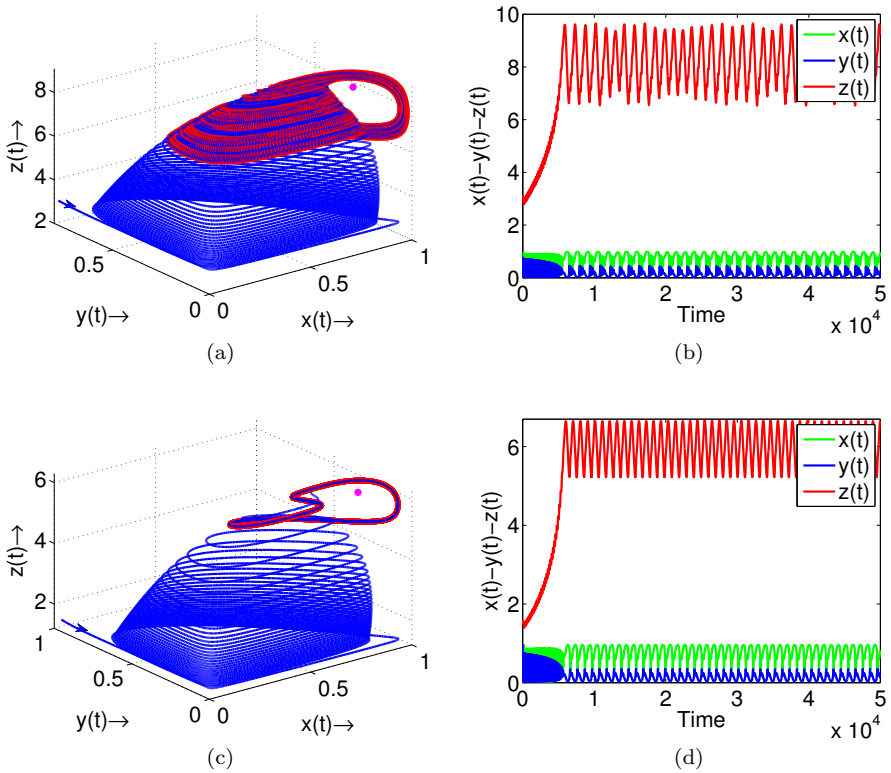

Fig. 18: Phase diagram and time series solution of all the three species of the system (4) for different values of k_2 like as : (a), (b) for $k_2 = 0.001$ and (c), (d) for $k_2 = 0.04$ with other parameters value as considered above. Red dot represent unstable equilibrium point.

Ecologically fear parameters k_1, k_2 are highly significant since these two parameters can control the chaotic dynamics of the system and turn into a stable one. With the increase of fear parameter k_1, k_2, growth rate of prey, intermediate predator decrease respectively and less number of prey, middle predators are captured by middle, top predator respectively in the system. Thus all three species survive in the system a with positive density level. Also, fear of intermediate predator on prey and fear of top predator on intermediate predator both has stabilizing effect on the system dynamics (see Fig. 20(b)).

7 Conclusion

In this investigation we have explored the dynamics of a tri-topic Hasting-Powell food web model incorporating the fear effect of the intermediate predator on growth function of prey, fear the effect of top predator on growth function of intermediate predator and replacing the prey dependent type II functional response by the ratio-dependent Beddington-DeAngelis functional response. In previous sections, we have shown that cost of fear can influence local and global dynamics of the system. Positivity, boundedness and persistence of the system solution imply that any feasible solution is always away from zero and remains bounded. We find all possible feasible equilibria and their feasibility condition in expressions of system parameters. Local asymptotical stability of different equilibrium points are determined. We also discuss the global stability of non-trivial equilibria. Transcritical bifurcation at axial equilibria concerning the middle predator death rate as bifurcation parameter and saddle-node, Hopf bifurcation at coexistence equilibria concerning the fear effect of the intermediate predator on prey population as bifurcation parameter are investigated. We also find the stability direction of Hopf bifurcating periodic solution concerning the fear effect of the middle predator as the bifurcation parameter. Finally, we justify theoretical findings and the significance of different system parameters numerically considering hypothetical values of system parameters.
Considering moderate values (see Table 2) of system parameters, we see that the system has three coexistence equilibria. With the increase of fear parameter k_1, the system becomes unstable from the stable

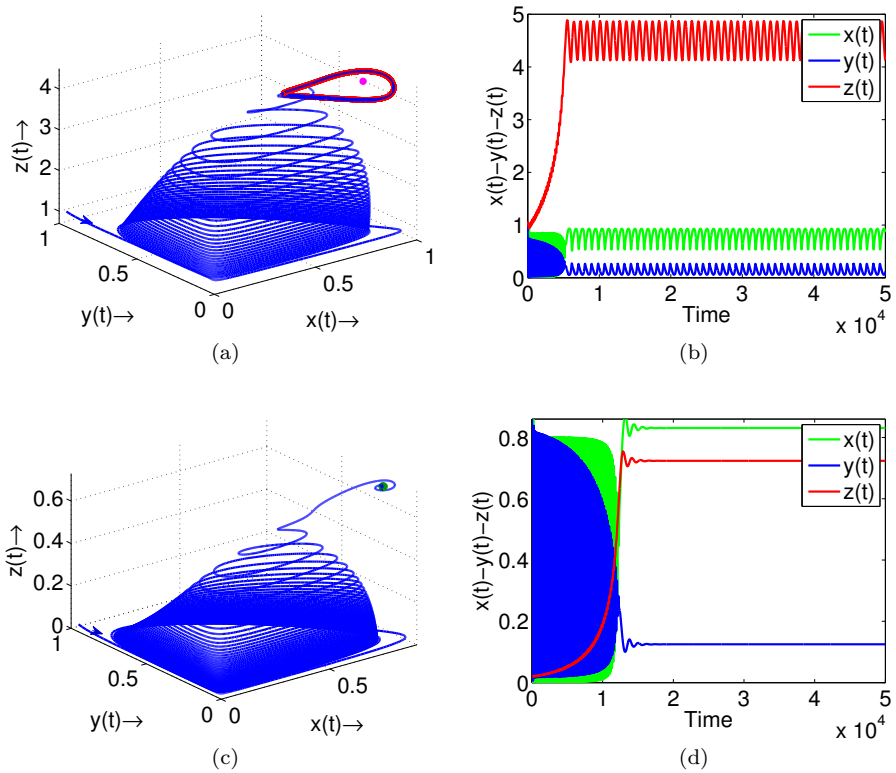

Fig. 19: Phase diagram and time series solution of all the three species of the system (4) for different values of k_2 like as : (a), (b) for $k_2 = 0.1$ and (c), (d) for $k_2 = 2.0$ with other parameters value as considered above. Green dot, red dot represent stable, unstable equilibrium points.

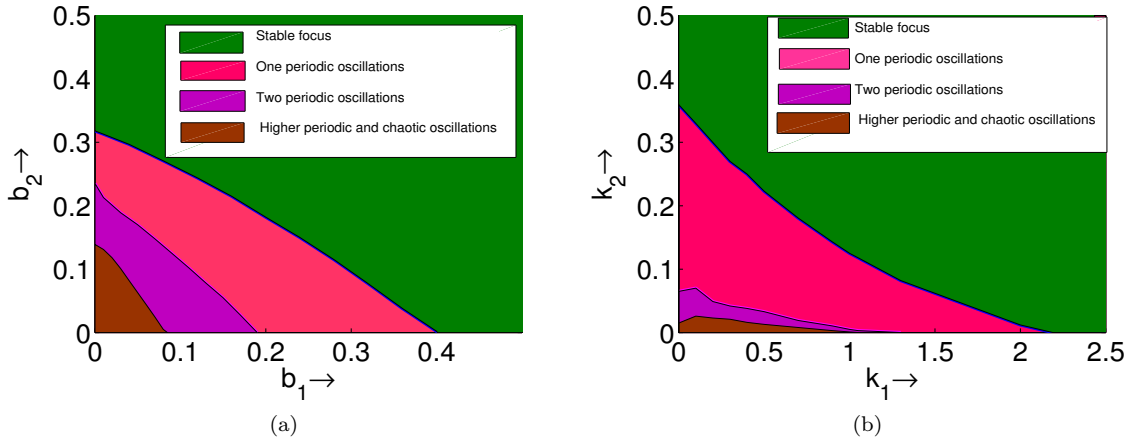

Fig. 20: Stability region in (a) $b_1 - b_2$, (b) $k_1 - k_2$ parametric plane of the system (4). The system exhibits chaotic or higher periodic, two periodic, one periodic oscillation and stable spiral in red, violet, magenta, green regions respectively. Both parameters have a stabilizing effect on the system dynamics.

situation but with the increase of fear parameter k_2 the system enters into a stable situation from unstable. There exists a set of values of the parameters k_1, k_2 for which bi-stability arises with one stable interior equilibria and another stable limit cycle around the top predator-free planer equilibria. Thus co-existence of all species or extinction of top predator depends not only on parametric restriction but also on initial population density size.

Again if the handling time of top predator, environmental protection for intermediate predator are high and mutual interference among intermediate, top predators are low, then the system shows highly complex dynamics like chaotic or higher periodic state, two periodic, one periodic and stable spiral situation.

Panday et al. [47] modified the three species Hasting-Powell food web model considering fear effect in growth function of prey and intermediate predator. They show that the cost of fear can stabilize the system from a chaotic situation through the period halving bifurcation. They also show that if the cost of fear increases top predator population goes to extinction. They claimed that the fear effect can regulate the stability of the system. The existence of prey and predator species depends on the cost of fear.

But we observe that not only fear parameters, mutual interference among middle and top predators can also regulate the system dynamics. Mutual interference among predator can also reduce the chaotic behaviour of the system through a period of halving bifurcation and the system becomes stable. Thus along with the increase of fear parameter and mutual interference among predator the system goes to the stable situation from chaotic one. Hence we have more options to reduce the chaotic situation of the modified Hasting-Powell food chain model and we will feel more relax to consider values of system parameters for a stable solution of the system.

It is important to note that most of the research work considering the fear effect are two species prey-predator model and there are only a nominal number of work considering three species prey-predator model. Middle predator foraging behaviour suppressed by the top predator and the impacts of overconsumption of intermediate predator by prey is thereby investigated. We showed this scenario by considering tri-topic food web model. We observe that fear and mutual interference among predators can make the system stable from the chaotic situation. Thus fear and mutual interference among predators enhances the persistence and stability of the tri-topic food web model. Therefore to conserve biodiversity and maintaining the ecosystems we can manipulate fear and mutual interference by artificial vocalization.

Compliance with ethical standards

Conflict of Interest : On behalf of all authors, the corresponding author states that there is no conflict of interest.

Data Availability : Data of this study will be made available from the corresponding author on reasonable request.

References

1. Shigesada, N., Kawasaki, K. and Teramoto, E., 1979. Spatial segregation of interacting species. *Journal of theoretical biology*, 79(1), pp.83-99.
2. Meng, X., Liu, R. and Zhang, T., 2014. Adaptive dynamics for a non-autonomous Lotka–Volterra model with size-selective disturbance. *Nonlinear Analysis: Real World Applications*, 16, pp.202-213.
3. Murray, J., 2003. Mathematical Biology II : Spatial Models and Biomedical Applications, 3rd edition (*Springer-Verlag, NY*).
4. Holmes, E.E., Lewis, M.A., Banks, J.E. and Veit, R.R., 1994. Partial differential equations in ecology: spatial interactions and population dynamics. *Ecology*, 75(1), pp.17-29.
5. Morozov, A., Petrovskii, S. and Li, B.L., 2004. Bifurcations and chaos in a predator-prey system with the Allee effect. *Proceedings of the Royal Society of London. Series B: Biological Sciences*, 271(1546), pp.1407-1414.
6. Ghosh, U., Pal, S. and Banerjee, M., 2021. Memory effect on Bazykin's prey-predator model: Stability and bifurcation analysis. *Chaos, Solitons and Fractals*, 143, p.110531.
7. Yin, C., Chen, Y. and Zhong, S.M., 2014. Fractional-order sliding mode based extremum seeking control of a class of nonlinear systems. *Automatica*, 50(12), pp.3173-3181.
8. Wang, X. and Zhao, M., 2011. Complex Dynamics in a Ratio-dependent Food-chain Model with Beddington-DeAngelis Functional Response. Procedia Environmental Sciences, 10, pp.135-140.
9. Perc, M. and Szolnoki, A., 2007. Noise-guided evolution within cyclical interactions. *New Journal of Physics*, 9(8), p.267.
10. Zhang, T. and Zang, H., 2014. Delay-induced Turing instability in reaction-diffusion equations. *Physical Review E*, 90(5), p.052908.
11. Malthus, T. R., 1798. An Essay on the Principle of Population, as it Affects the Future Improvement of Society, with Remarks on the Speculations of Mr. Godwin, M. Condorcet, and Other Writers (*The Lawbook Exchange, Ltd.*).
12. Kot, M., 2001 Elements of mathematical ecology. Cambridge University Press, Cambridge.
13. Lotka AJ. : "Elements of physical biology", Baltimore: *Williams and Wilkins*; 1925.
14. Volterra V. : "Variazioni e fluttuazioni del numero dindividui in specie animali conviventi", *Mem R Accad Naz Lincei Ser VI*; 2 : 31–113; 1926.

15. Holling, C.S., 1959. The components of predation as revealed by a study of small-mammal predation of the European Pine Sawfly1. The Canadian Entomologist, 91(5), pp.293-320.
16. Holling, C.S.: The functional response of predators to prey density and its role in mimicry and population regulation. Mem . Entomol. Soc.Can.45, 50-60(1965)
17. Debnath S, Ghosh U, Sarkar S. : Global dynamics of a tritrophic food chain model subject to the Allee effects in the prey population with sexually reproductive generalized-type top predator. Computational and Mathematical Methods 2. 2019; 2:e1079.
18. Wang, X., Zanette, L. and Zou, X. : "Modelling the fear effect in predator–prey interactions," *J. Math. Biol.*, **73**, 1179–1204 (2016).
19. Holling, C.S., 1966. The functional response of invertebrate predators to prey density. The Memoirs of the Entomological Society of Canada, 98(S48), pp.5-86.
20. Xiao, D. and Ruan, S., 2001. Global analysis in a predator-prey system with nonmonotonic functional response. SIAM Journal on Applied Mathematics, 61(4), pp.1445-1472.
21. Aguirre, P., González-Olivares, E. and Saez, E., 2009. Three limit cycles in a Leslie–Gower predator-prey model with additive Allee effect. SIAM Journal on Applied Mathematics, 69(5), pp.1244-1262.
22. Gonzalez-Olivares, E., Meneses-Alcay, H., Gonzalez-Yanez, B., Mena-Lorca, J., Rojas-Palma, A. and Ramos-Jiliberto, R., 2011. Multiple stability and uniqueness of the limit cycle in a Gause-type predator–prey model considering the Allee effect on prey. Nonlinear Analysis: Real World Applications, 12(6), pp.2931-2942.
23. Majumdar, P., Debnath, S., Sarkar, S. and Ghosh, U. : "The Complex Dynamical Behavior of a Prey-Predator Model with Holling Type-III Functional Response and Non-Linear Predator Harvesting", *International Journal of Modelling and Simulation*, pp.1-18. (2021).
24. May, R.M., 1972. Limit cycles in predator-prey communities. Science, 177(4052), pp.900-902.
25. Freedman, H.I. and Wolkowicz, G.S., 1986. Predator-prey systems with group defence: the paradox of enrichment revisited. Bulletin of Mathematical Biology, 48(5-6), pp.493-508.
26. Beddington, J.R., 1975. Mutual interference between parasites or predators and its effect on searching efficiency. The Journal of Animal Ecology, pp.331-340.
27. DeAngelis, D.L., Goldstein, R.A. and O'Neill, R.V., 1975. A model for tropic interaction. Ecology, 56(4), pp.881-892.
28. Chinnathambi, R. and Rihan, F.A., 2018. Stability of fractional-order prey–predator system with time-delay and Monod–Haldane functional response. Nonlinear Dynamics, 92(4), pp.1637-1648.
29. Kuang, Y. and Freedman, H.I., 1988. Uniqueness of limit cycles in Gause-type models of predator-prey systems. Mathematical Biosciences, 88(1), pp.67-84.
30. Takeuchi, Y., Wang, W., Nakaoka, S. and Iwami, S., 2009. Dynamical adaptation of parental care. Bulletin of mathematical biology, 71(4), pp.931-951.
31. Krivan, V., 2007. The Lotka-Volterra predator-prey model with foraging–predation risk trade-offs. The American Naturalist, 170(5), pp.771-782.
32. Creel, S. and Christianson, D., 2008. Relationships between direct predation and risk effects. Trends in ecology and evolution, 23(4), pp.194-201.
33. Hua, F., Sieving, K.E., Fletcher Jr, R.J. and Wright, C.A., 2014. Increased perception of predation risk to adults and offspring alters avian reproductive strategy and performance. Behavioral Ecology, 25(3), pp.509-519.
34. Lima, S.L. and Dill, L.M., 1990. Behavioral decisions made under the risk of predation: a review and prospectus. Canadian journal of zoology, 68(4), pp.619-640.
35. Cresswell, W., 2011. Predation in bird populations. Journal of Ornithology, 152(1), pp.251-263.
36. Zanette, L.Y., White, A.F., Allen, M.C. and Clinchy, M., 2011. Perceived predation risk reduces the number of offspring songbirds produce per year. Science, 334(6061), pp.1398-1401.
37. Wang, X. and Zou, X., 2017. Modeling the fear effect in predator–prey interactions with adaptive avoidance of predators. Bulletin of mathematical biology, 79(6), pp.1325-1359.
38. Preisser, E.L. and Bolnick, D.I., 2008. The many faces of fear: comparing the pathways and impacts of nonconsumptive predator effects on prey populations. PloS one, 3(6), p.e2465.
39. Creel, S., Christianson, D., Liley, S. and Winnie, J.A., 2007. Predation risk affects reproductive physiology and demography of elk. Science, 315(5814), pp.960-960.
40. Eggers, S., Griesser, M., Nystrand, M. and Ekman, J., 2006. Predation risk induces changes in nest-site selection and clutch size in the Siberian jay. Proceedings of the Royal Society B: Biological Sciences, 273(1587), pp.701-706.
41. Fontaine, J.J. and Martin, T.E., 2006. Parent birds assess nest predation risk and adjust their reproductive strategies. Ecology letters, 9(4), pp.428-434.
42. Ghalambor, C.K., Peluc, S.I. and Martin, T.E., 2013. Plasticity of parental care under the risk of predation: how much should parents reduce care?. Biology Letters, 9(4), p.20130154.
43. Sheriff, M.J., Krebs, C.J. and Boonstra, R., 2009. The sensitive hare: sublethal effects of predator stress on reproduction in snowshoe hares. Journal of Animal Ecology, 78(6), pp.1249-1258.
44. Wirsing, A.J. and Ripple, W.J., 2011. A comparison of shark and wolf research reveals similar behavioral responses by prey. Frontiers in Ecology and the Environment, 9(6), pp.335-341.
45. Elliott, K.H., Betini, G.S. and Norris, D.R., 2017. Fear creates an Allee effect: Experimental evidence from seasonal populations. Proceedings of the Royal Society B: Biological Sciences, 284(1857), p.20170878.
46. Das, A. and Samanta, G.P., 2018. Modeling the fear effect on a stochastic prey–predator system with additional food for the predator. Journal of Physics A: Mathematical and Theoretical, 51(46), p.465601.
47. Panday P., Pal N., Samanta S. and Chattopadhyay, J. : "Stability and bifurcation analysis of a three-species food chain model with fear", *Int. J. Bifurc. Chaos*, 28, 1850009; 2018.
48. Hastings A., Powell T. : "Chaos in three-species food chain", *Ecology*, 72 : 896–903; 1991.
49. Alonso D., Bartumeus F. and Catalan J. : "Mutual interference between predators can give rise to Turing spatial patterns", *Ecology*; 83, 28; 2002.
50. Wiggins S. : "Introduction to Applied Nonlinear Dynamical Systems and Chaos", *Springer*, New York, Vol. 2; 1990.
51. La Salle, J. : "The Stability of Dynamical Systems", *SIAM*, 1976
52. Perko L. : "Differential Equations and Dynamical Systems", *Springer*, New York, Volume 7; 1996.

53. Hassard B., Kazarinoff N. and Wan Y. : "Theory and Applications of Hopf Bifurcation", *CUP Archive, Cambridge*, vol. 41.; 1981.

Appendix

$$l_{11} = -\frac{2}{1+k_1^{[SN]}\bar{y}^*} + \frac{2a_1\bar{y}^*}{\left(a_1\bar{x}^*+b_2\bar{y}^*+c_1\right)^2} - \frac{2a_1^2\bar{x}^*\bar{y}^*}{\left(a_1\bar{x}^*+b_2\bar{y}^*+c_1\right)^3},$$

$$l_{22} = \frac{2{k_1^{[SN]}}^2\bar{x}^*(1-\bar{x}^*)}{\left(1+k_1^{[SN]}\bar{y}^*\right)^3} + \frac{2b_1\bar{x}^*}{\left(a_1\bar{x}^*+b_2\bar{y}^*+c_1\right)^2} - \frac{2b_1^2\bar{x}^*\bar{y}^*}{\left(a_1\bar{x}^*+b_2\bar{y}^*+c_1\right)^3},$$

$$l_{33} = 0,$$

$$l_{12} = -\frac{k_1^{[SN]}(1-\bar{x}^*)}{\left(1+k_1^{[SN]}\bar{y}^*\right)^2} + \frac{k_1^{[SN]}\bar{x}^*}{\left(1+k_1^{[SN]}\bar{y}^*\right)^2} - \frac{1}{a_1\bar{x}^*+b_2\bar{y}^*+c_1} + \frac{a_1\bar{x}^*}{\left(a_1\bar{x}^*+b_2\bar{y}^*+c_1\right)^2} + \frac{b_1\bar{y}^*}{\left(a_1\bar{x}^*+b_2\bar{y}^*+c_1\right)^2}$$
$$- \frac{2a_1b_1\bar{x}^*\bar{y}^*}{\left(a_1\bar{x}^*+b_2\bar{y}^*+c_1\right)^3},$$

$$l_{23} = 0,$$

$$l_{31} = 0,$$

$$m_{11} = -\frac{2a_1\bar{y}^*}{\left(1+k_2\bar{z}^*\right)\left(a_1\bar{x}^*+b_1\bar{y}^*+c_1\right)^2} + \frac{2a_1^2\bar{x}^*\bar{y}^*}{\left(1+k_2\bar{z}^*\right)\left(a_1\bar{x}^*+b_1\bar{y}^*+c_1\right)^3},$$

$$m_{22} = -\frac{2b_1\bar{x}^*}{\left(1+k_2\bar{z}^*\right)\left(a_1\bar{x}^*+b_1\bar{y}^*+c_1\right)^2} + \frac{2b_1^2\bar{x}^*\bar{y}^*}{\left(1+k_2\bar{z}^*\right)\left(a_1\bar{x}^*+b_2\bar{y}^*+c_1\right)^3} + \frac{2a_2\bar{z}^*}{\left(a_2\bar{y}^*+b_2\bar{z}^*+c_2\right)^2}$$
$$- \frac{2a_2^2\bar{y}^*z^*}{\left(a_2\bar{y}^*+b_2\bar{z}^*+c_2\right)^3},$$

$$m_{33} = \frac{2k_2^2\bar{x}^*\bar{y}^*}{\left(1+k_2\bar{z}^*\right)^3\left(a_1\bar{x}^*+b_1\bar{y}^*+c_1\right)} + \frac{2b_2\bar{y}^*}{\left(a_2\bar{y}^*+b_2\bar{z}^*+c_2\right)^2} - \frac{2b_2^2\bar{y}^*\bar{z}^*}{\left(a_2\bar{y}^*+b_2\bar{z}^*+c_2\right)^3},$$

$$m_{12} = \frac{1}{\left(1+k_2\bar{z}^*\right)\left(a_1\bar{x}^*+b_1\bar{y}^*+c_1\right)} - \frac{b_1\bar{y}^*}{\left(1+k_2\bar{z}^*\right)\left(a_1\bar{x}^*+b_1\bar{y}^*+c_1\right)^2} - \frac{a_1\bar{x}^*}{\left(1+k_2\bar{z}^*\right)\left(a_1\bar{x}^*+b_1\bar{y}^*+c_1\right)^2}$$
$$+ \frac{2a_1b_1\bar{x}^*\bar{y}^*}{\left(1+k_2\bar{z}^*\right)\left(a_1\bar{x}^*+b_1\bar{y}^*+c_1\right)^3},$$

$$m_{23} = -\frac{k_2\bar{x}^*}{\left(1+k_2\bar{z}^*\right)^2\left(a_1\bar{x}^*+b_1\bar{y}^*+c_1\right)} + \frac{b_1k_2\bar{x}^*\bar{y}^*}{\left(1+k_2\bar{z}^*\right)^2\left(a_1\bar{x}^*+b_1\bar{y}^*+c_1\right)^2} - \frac{1}{a_2\bar{y}^*+b_2\bar{z}^*+c_2}$$
$$+ \frac{b_2\bar{z}^*}{\left(a_2\bar{y}^*+b_2\bar{z}^*+c_2\right)^2} + \frac{a_2\bar{y}^*}{\left(a_2\bar{y}^*+b_2\bar{z}^*+c_2\right)^2} - \frac{2a_2b_2\bar{y}^*\bar{z}^*}{\left(a_2\bar{y}^*+b_2\bar{z}^*+c_2\right)^3},$$

$$m_{31} = -\frac{k_2\bar{y}^*}{\left(1+k_2\bar{z}^*\right)^2\left(a_1\bar{x}^*+b_1\bar{y}^*+c_1\right)} + \frac{a_1k_2\bar{x}^*\bar{y}^*}{\left(1+k_2\bar{z}^*\right)^2\left(a_1\bar{x}^*+b_1\bar{y}^*+c_1\right)^2},$$

$$n_{11} = 0,$$

$$n_{22} = -\frac{2a_2\bar{z}^*}{\left(a_2\bar{y}^*+b_2\bar{z}^*+c_2\right)^2} + \frac{2a_2^2\bar{y}^*\bar{z}^*}{\left(a_2\bar{y}^*+b_2\bar{z}^*+c_2\right)^3},$$

$$n_{33} = -\frac{2b_2\bar{y}^*}{\left(a_2\bar{y}^*+b_2\bar{z}^*+c_2\right)^2} + \frac{2b_2^2\bar{y}^*\bar{z}^*}{\left(a_2\bar{y}^*+b_2\bar{z}^*+c_2\right)^3},$$

$$n_{12} = 0,$$

$$n_{23} = \frac{1}{a_2\bar{y}^*+b_2\bar{z}^*+c_2} - \frac{b_2\bar{z}^*}{\left(a_2\bar{y}^*+b_2\bar{z}^*+c_2\right)^2} - \frac{a_2\bar{y}^*}{\left(a_2\bar{y}^*+b_2\bar{z}^*+c_2\right)^2} + \frac{2a_2b_2\bar{y}^*\bar{z}^*}{\left(a_2\bar{y}^*+b_2\bar{z}^*+c_2\right)^3}$$

$$n_{31} = 0.$$

$$p_1 = l_{11}\theta_1^2 + l_{22}\theta_2^2 + 2l_{12}\theta_1\theta_2,$$

$$p_2 = m_{11}\theta_1^2 + m_{22}\theta_2^2 + m_{33}\theta_3^2 + 2m_{12}\theta_1\theta_2 + 2m_{23}\theta_2\theta_3 + 2m_{31}\theta_3\theta_1,$$

$$p_3 = n_{22}\theta_2^2 + n_{33}\theta_3^2 + 2n_{23}\theta_2\theta_3.$$

Figures

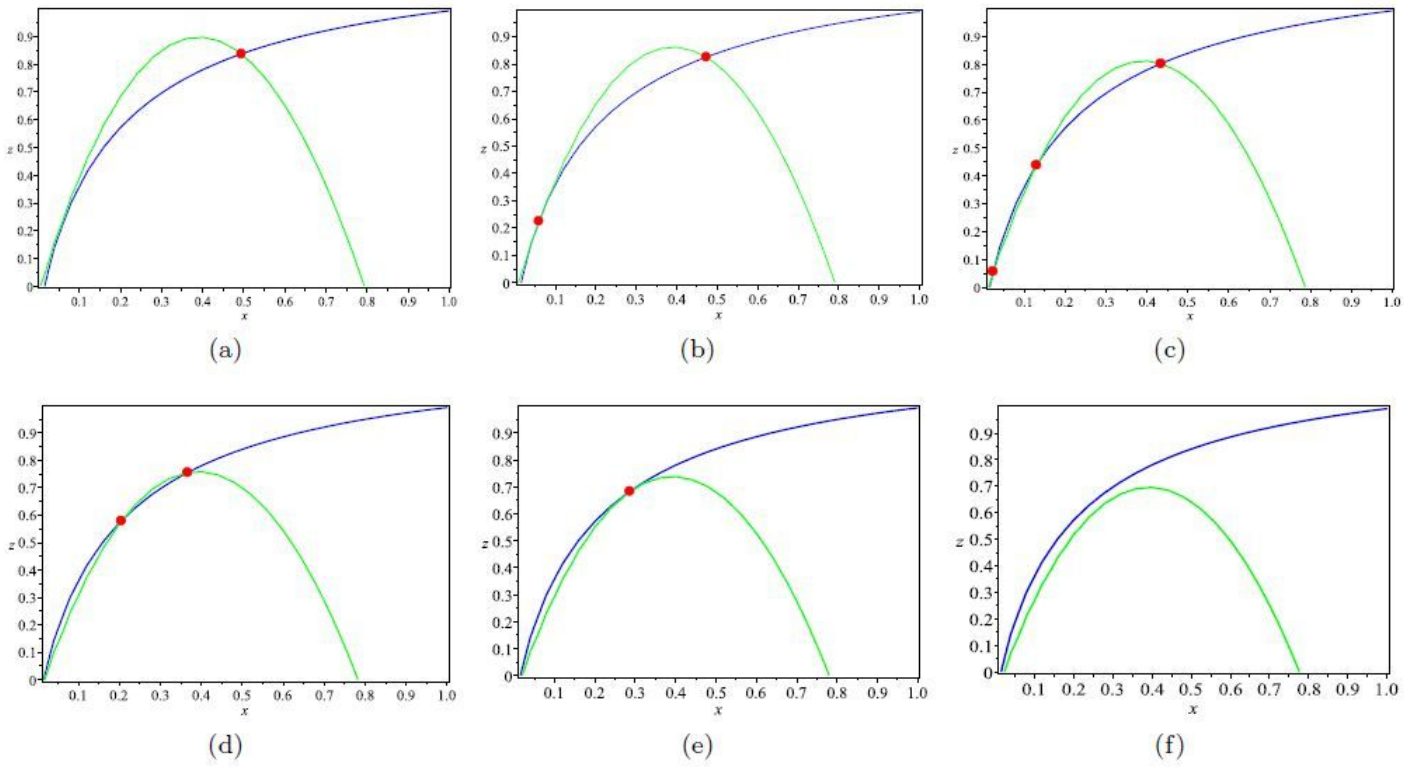

Figure 1

Projection of interior equilibrium points in the x-z plane for different values of parameter k1 of the system (4) as : (a) k1 = 0:02, (b) k1 = 0:09078075523, (c) k1 = 0:2, (d) k1 = 0:33, (e) k1 = 0:3840366382, (f) k1 = 0:5 and other system parameters are fixed in Table 2.

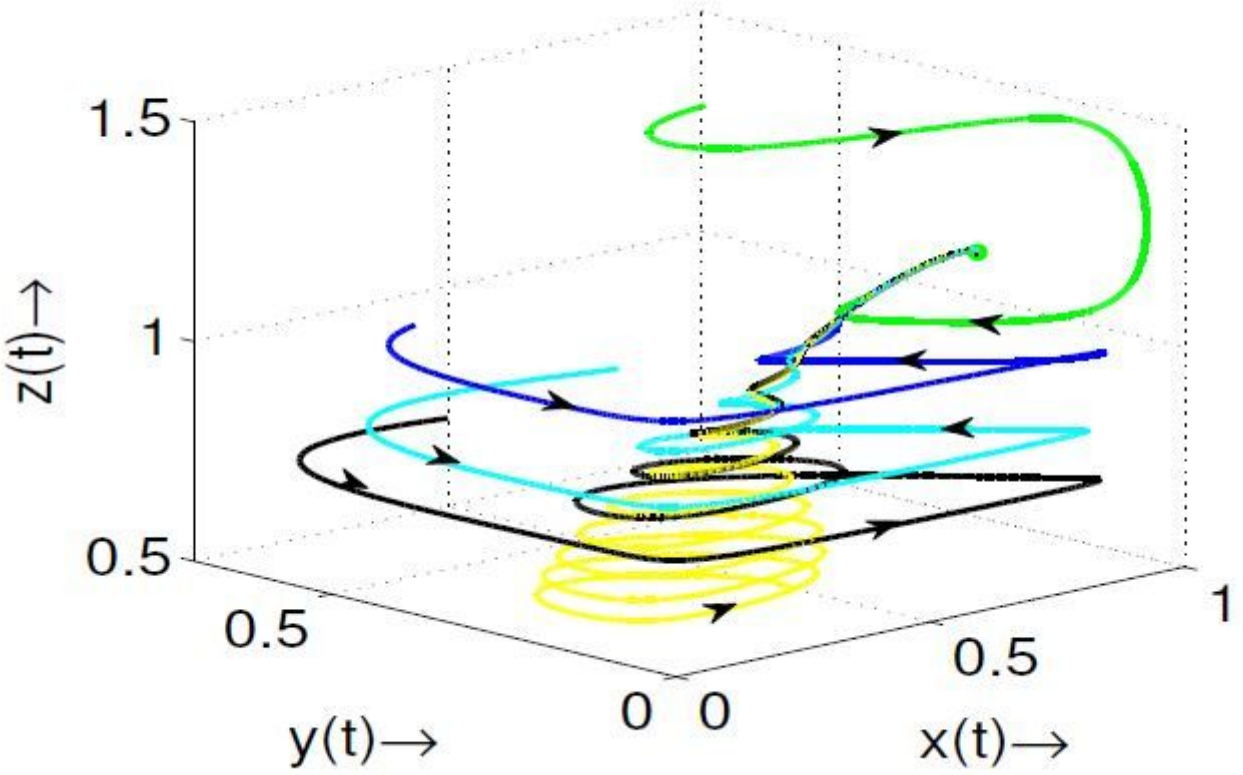

Figure 2

Solution trajectories of model system (4) with various starting points considering k1 = 1, k2 = 1, a1 = 0:65, a2 = 20, b1 = 0:1, b2 = 0:91, c1 = 0:2, c2 = 10, d1 = 0:4, d2 = 0:01. Figure shows global asymptotic stability of interior equilibria E*(0:7807723516; 0:1388648586; 1:218888670).

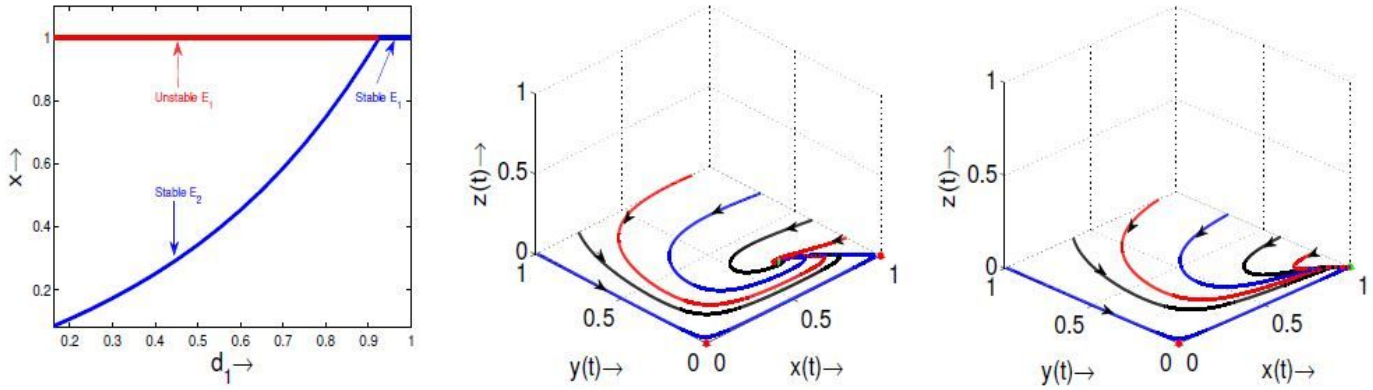

(a) One parameter bifurcation diagram (b) Phase diagram for $d_1 = 0.75$ (c) Phase diagram for $d_1 = 0.95$

Figure 3

(a) One parametric bifurcation diagram with regard to the parameter d1, blue & red lines represent the stable & unstable nature of the corresponding equilibria respectively and phase diagram of the model system (4) for: (a) d1 = 0:75, (b) d1 = 0:95 with k1 = 0:5, c1 = 0:42, d2 = 0:62 considering other parameter values as given in Table 2.

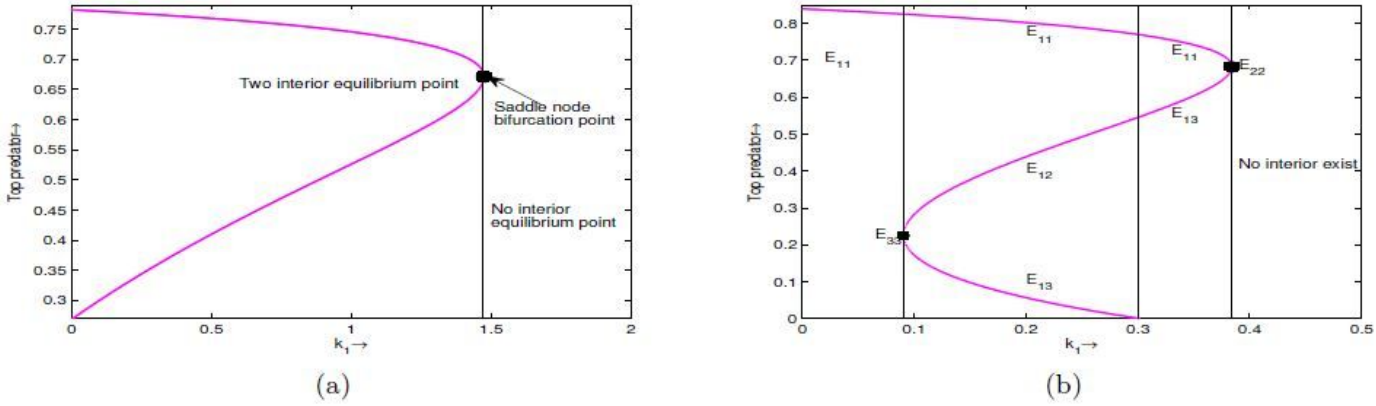

Figure 4

One parametric bifurcation diagram with regard to bifurcation parameter k1 of top predator population considering (a) a1 = 0:7, b2 = 0:4, c2 = 1:2 and other parameters (b) values of system parameters as given in Table 2. Black dot represents the bifurcation point at k1 = 1:47433536957.

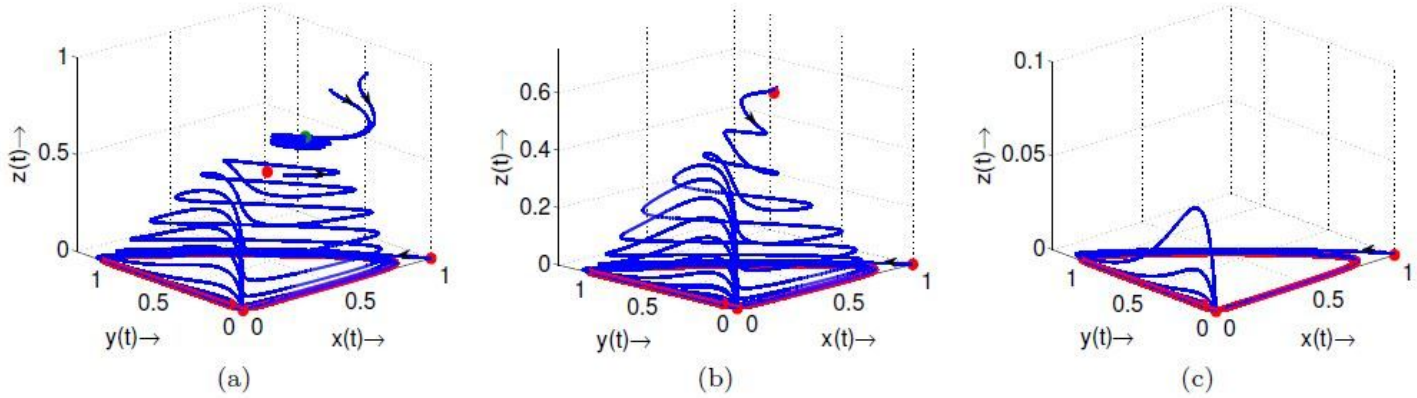

Figure 5

Phase diagram of model system (4) for different values of the parameter k1 like as : (a) k1 = 1:30, (b) k1 = 1:47433536957, (c) k1 = 1:55 with a1 = 0:7, b2 = 0:4, c2 = 1:2 and values of other system parameters as given in Table 2. Green dots represent the stable equilibria and red dots represent the unstable equilibria.

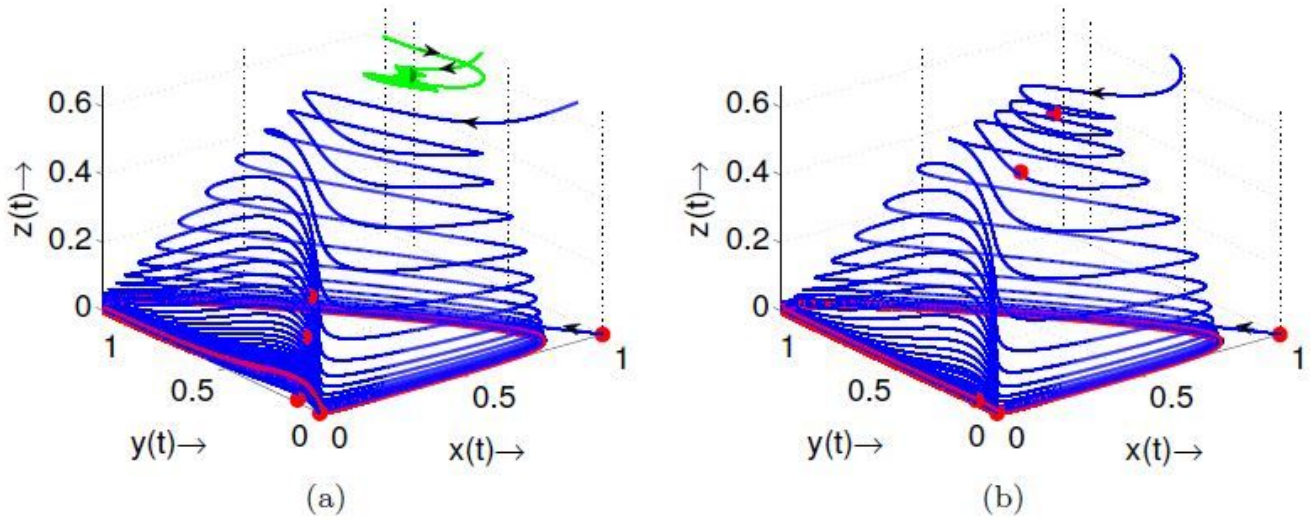

Figure 6

Phase diagram of the model system (4) for different values of parameter k1 like as : (a) k1 = 0:10, (b) k1 = 0:35 with values of other system parameters as given in Table 2. Green dot represents the stable equilibria and red dots represent unstable equilibria.

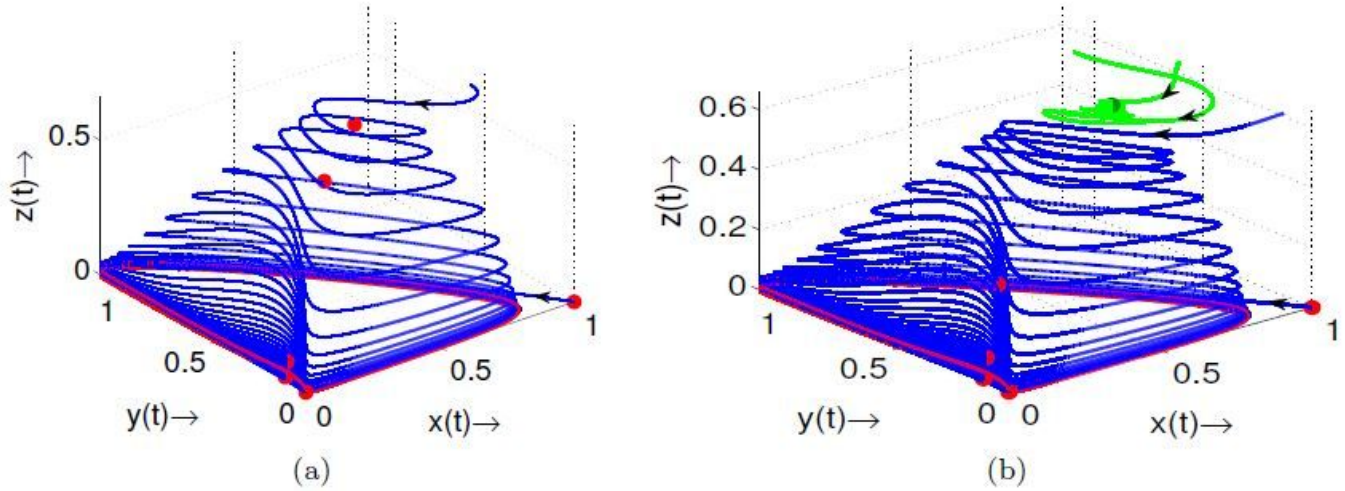

Figure 7

Phase diagram of the model system (4) for different values of the parameter k2 like as : (a) k2 = 1:0, (b) k2 = 1:5 with values of other system parameters as given in Table 2. Green dot represents the stable and red dots represent unstable equilibria.

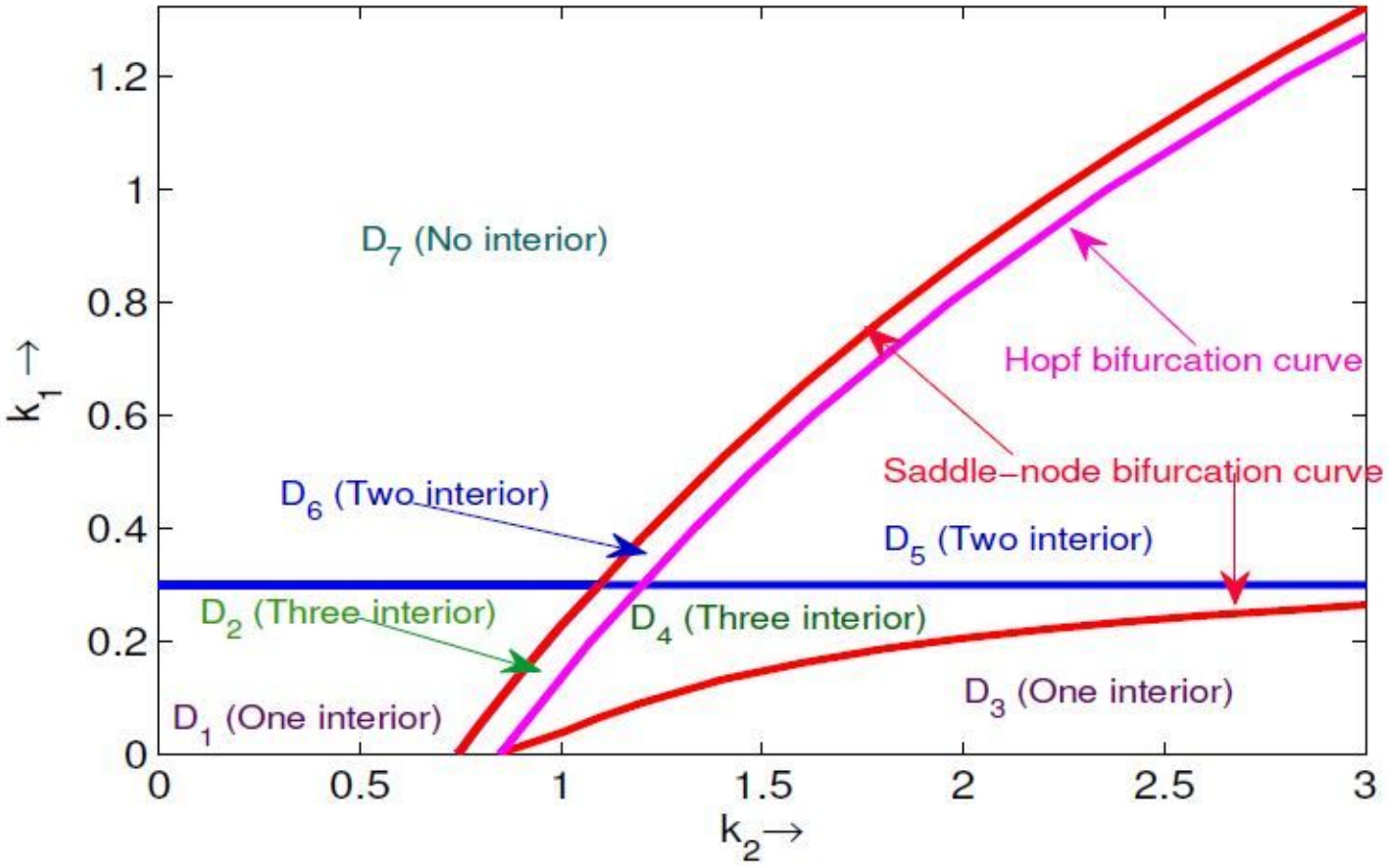

Figure 8

Schematic bifurcation diagram of system (4) in k2 - k1 parametric plane considering values of other parameters as given in Table 2. Here blue, red and magenta lines are the creation or distraction of one interior equilibrium point, saddle-node and Hopf bifurcation curve for coexistence equilibria respectively.

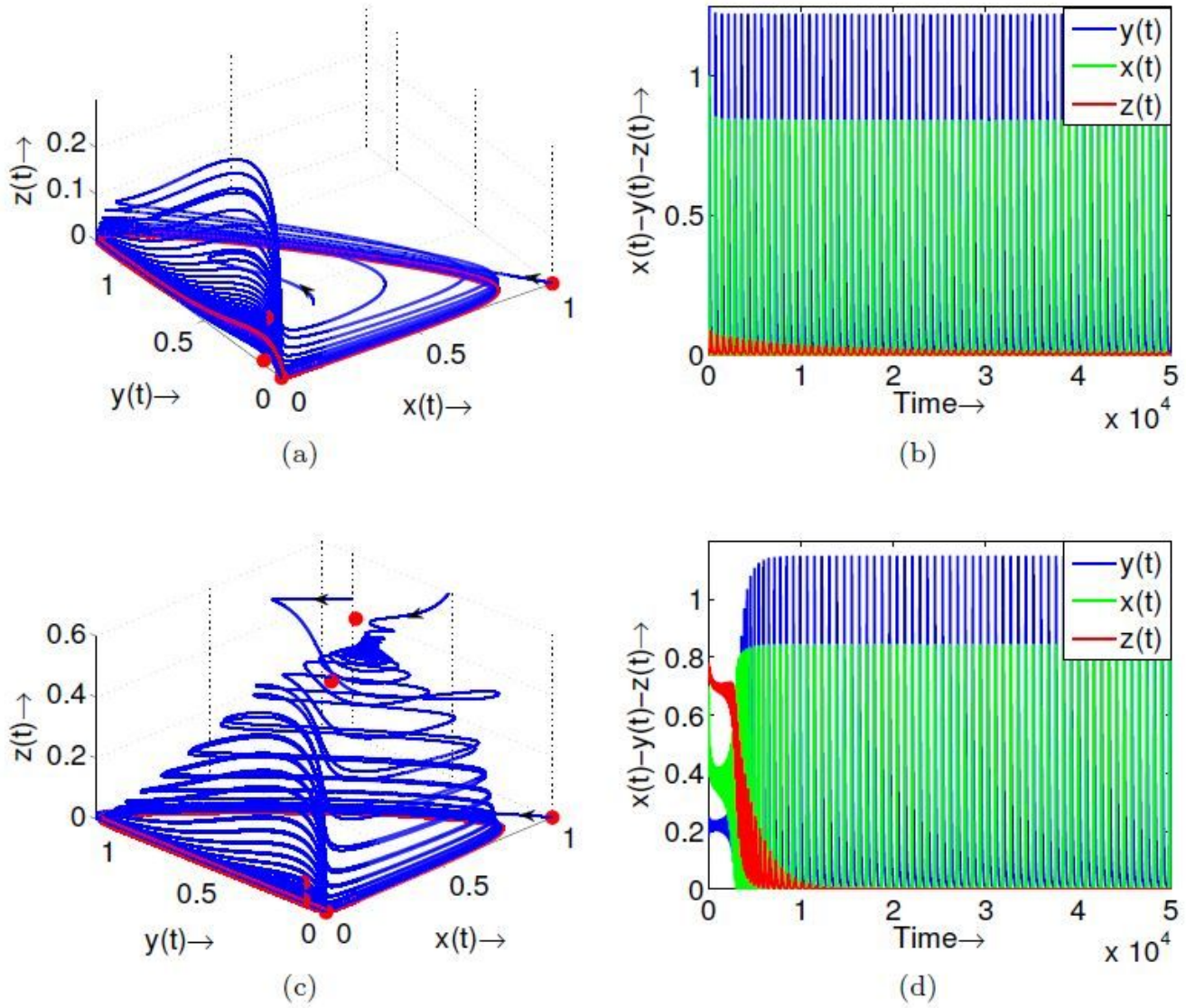

Figure 9

Phase diagram and time series solution of different species of the model system (4) in different sub-region like as : (a), (b) in sub-region D1, (c), (d) in sub-region D2, with values of other system parameters as given in Table 2. Red dots represent the unstable equilibria.

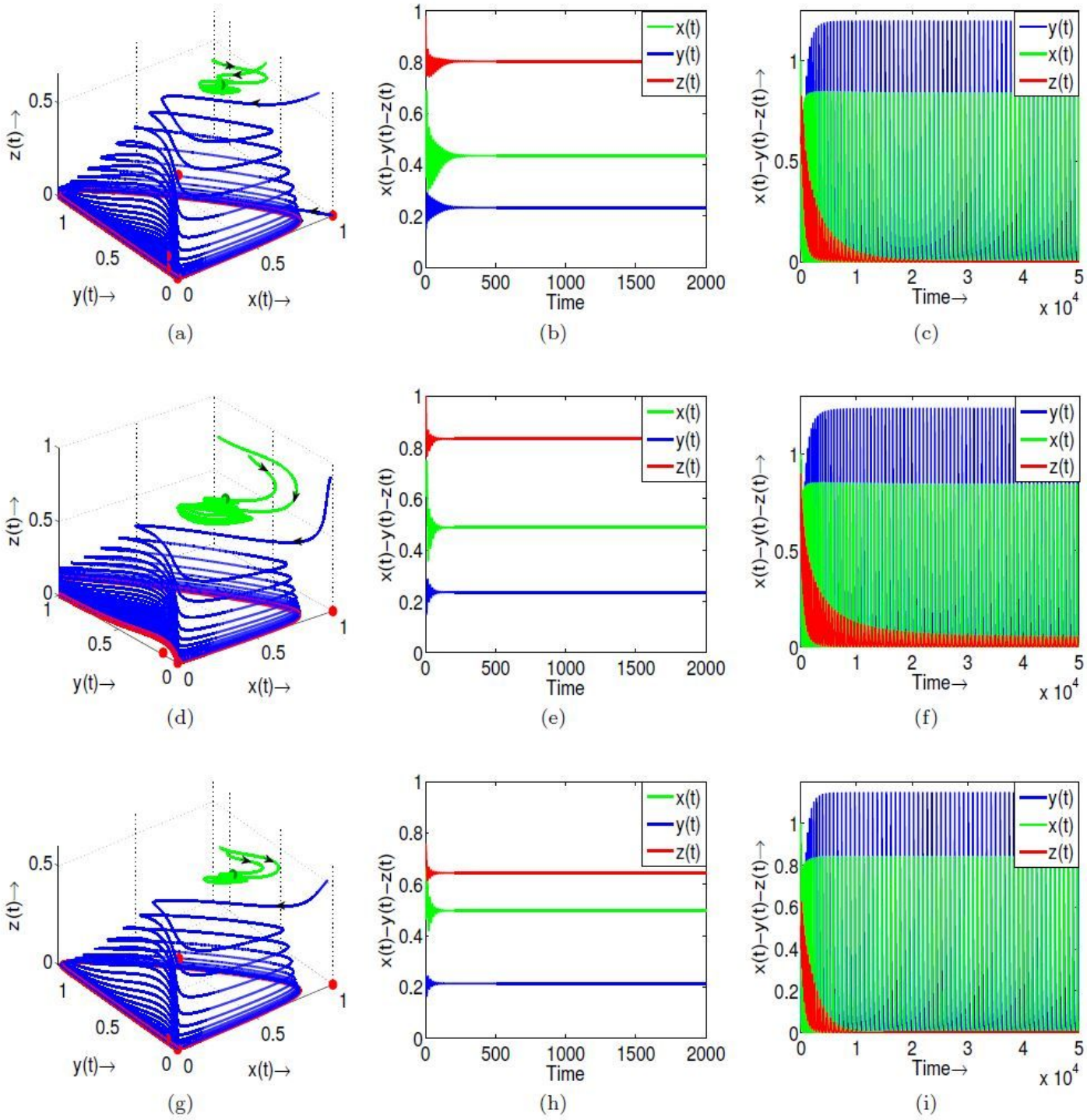

Figure 10

Phase diagram and time series solution at stable and unstable equilibrium point respectively of different species of the model system (4) in different sub-region like as : (a), (b), (c) in sub-region D4, (d), (e), (f) in sub-region D3, and (g), (h), (i) in sub-region D5 with values of other system parameters as given in Table 2. Green dot represents the stable equilibria and red dots represent the unstable equilibria.

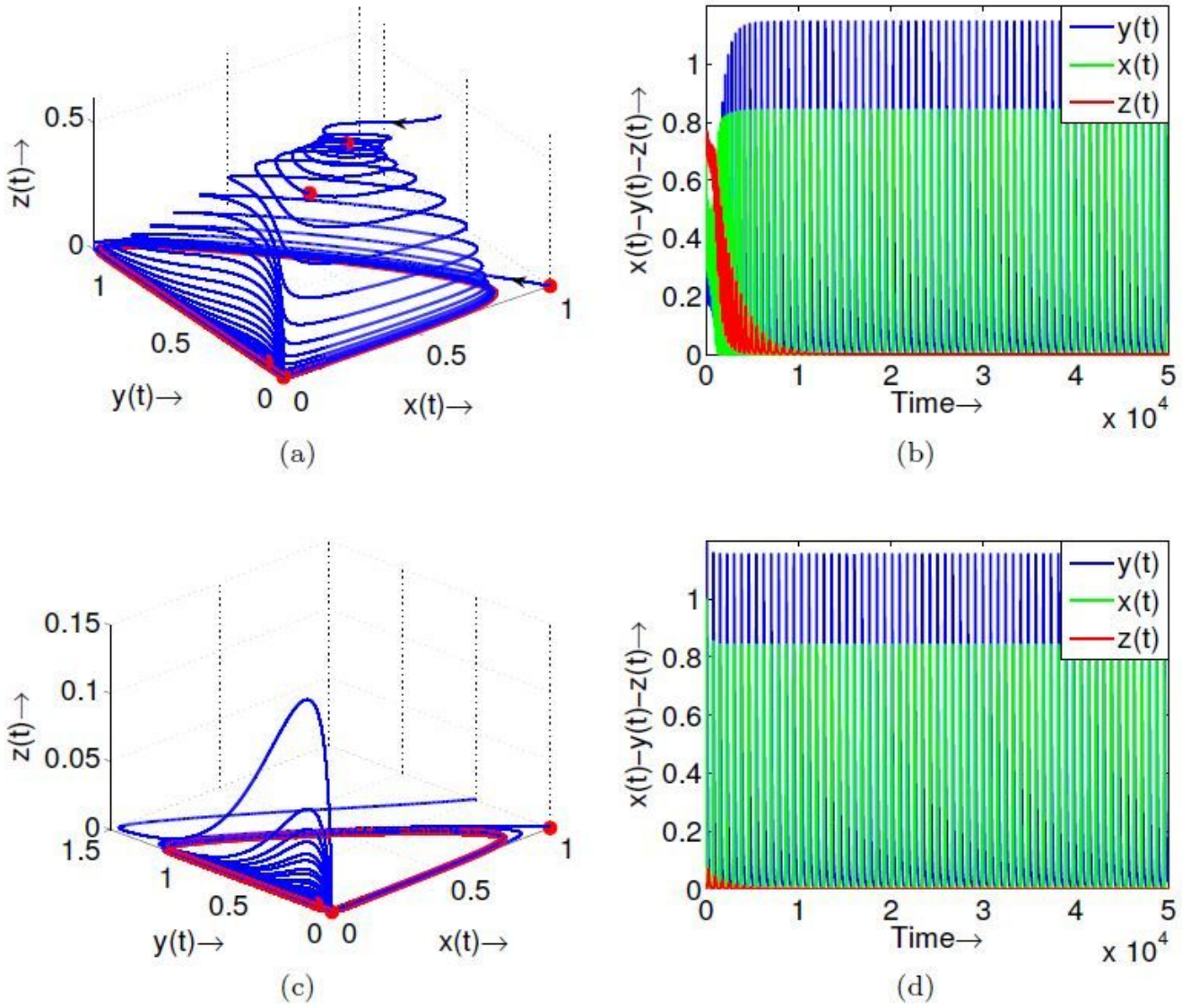

Figure 11

Phase diagram and time series solution of different species of the model system (4) in different sub-region like as : (a), (b) in sub-region D6, (c), (d) in sub-region D7, with values of other system parameters as given in Table 2. Red dots represent the unstable equilibria.

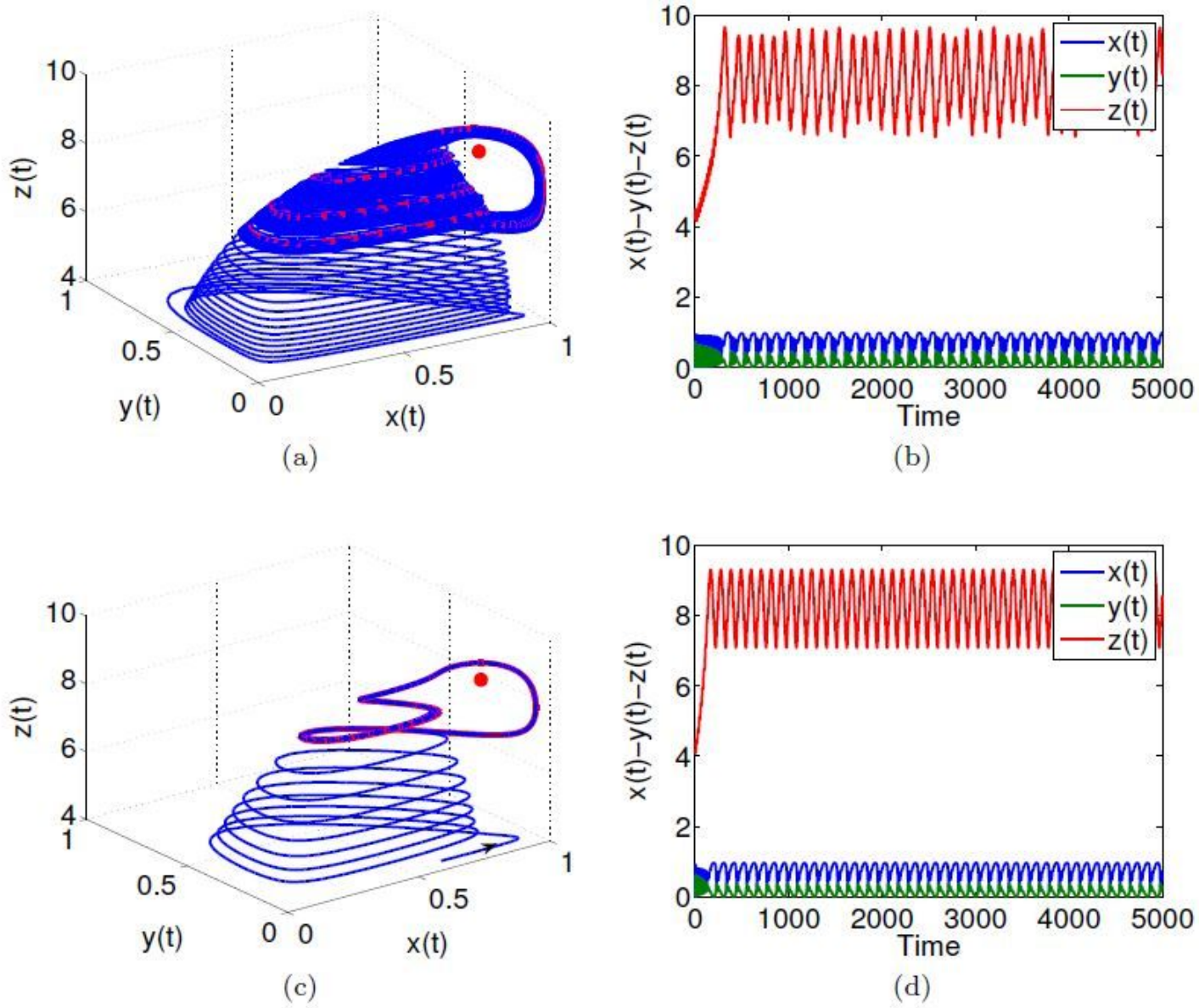

Figure 12

Phase diagram and time series solution of all the three species of the system (4) for different values of b1 like as : (a), (b) for b1 = 0:01 and (c), (d) for b1 = 0:08 with other parameters value as considered above. Red dot represent unstable equilibrium point.

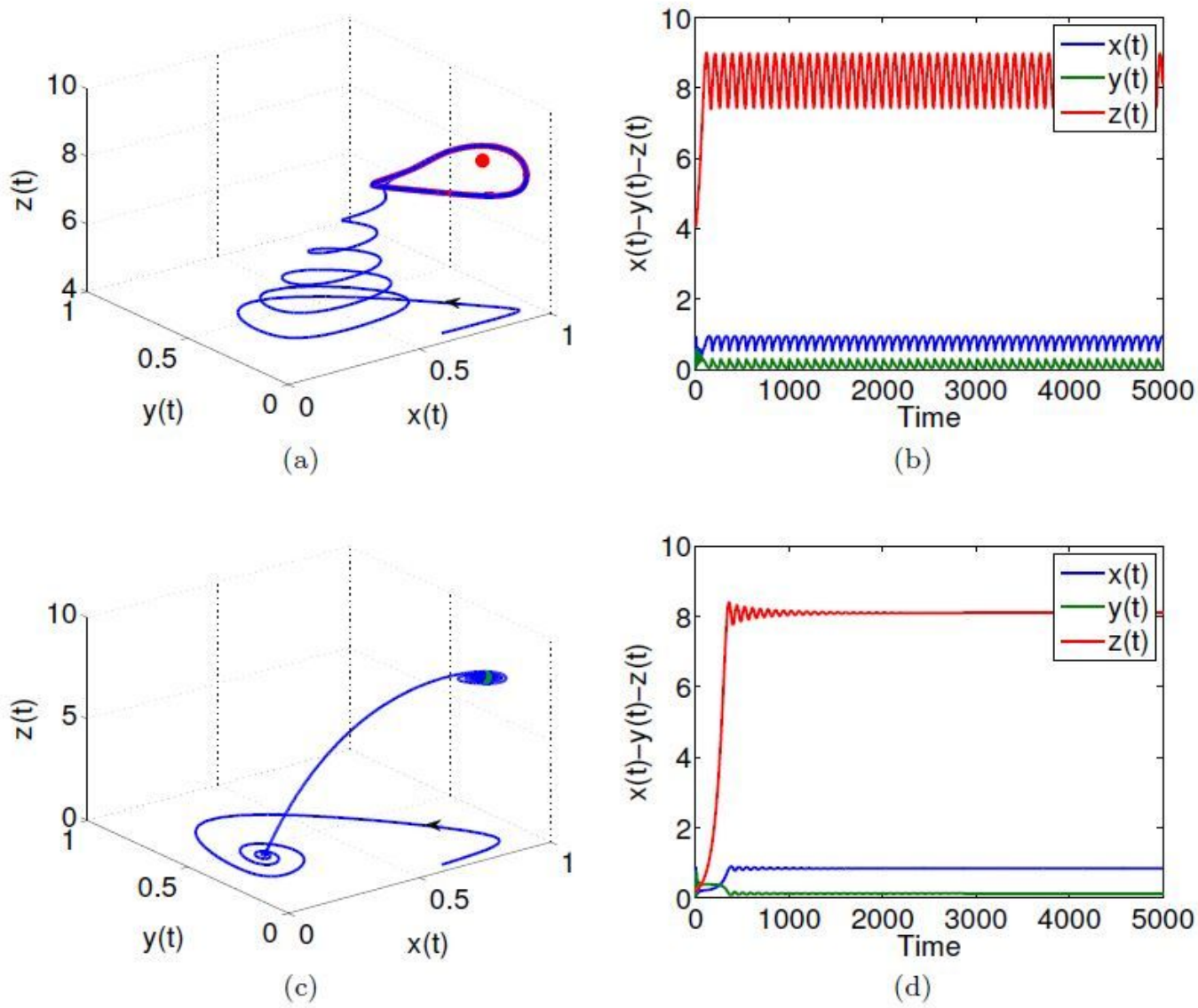

Figure 13

Phase diagram and time series solution of all the three species of the system (4) for different values of b1 like as : (a), (b) for b1 = 0:20 and (c), (d) for b1 = 0:41 with other parameters value as considered above. Green dot, red dot represent stable, unstable equilibrium points.

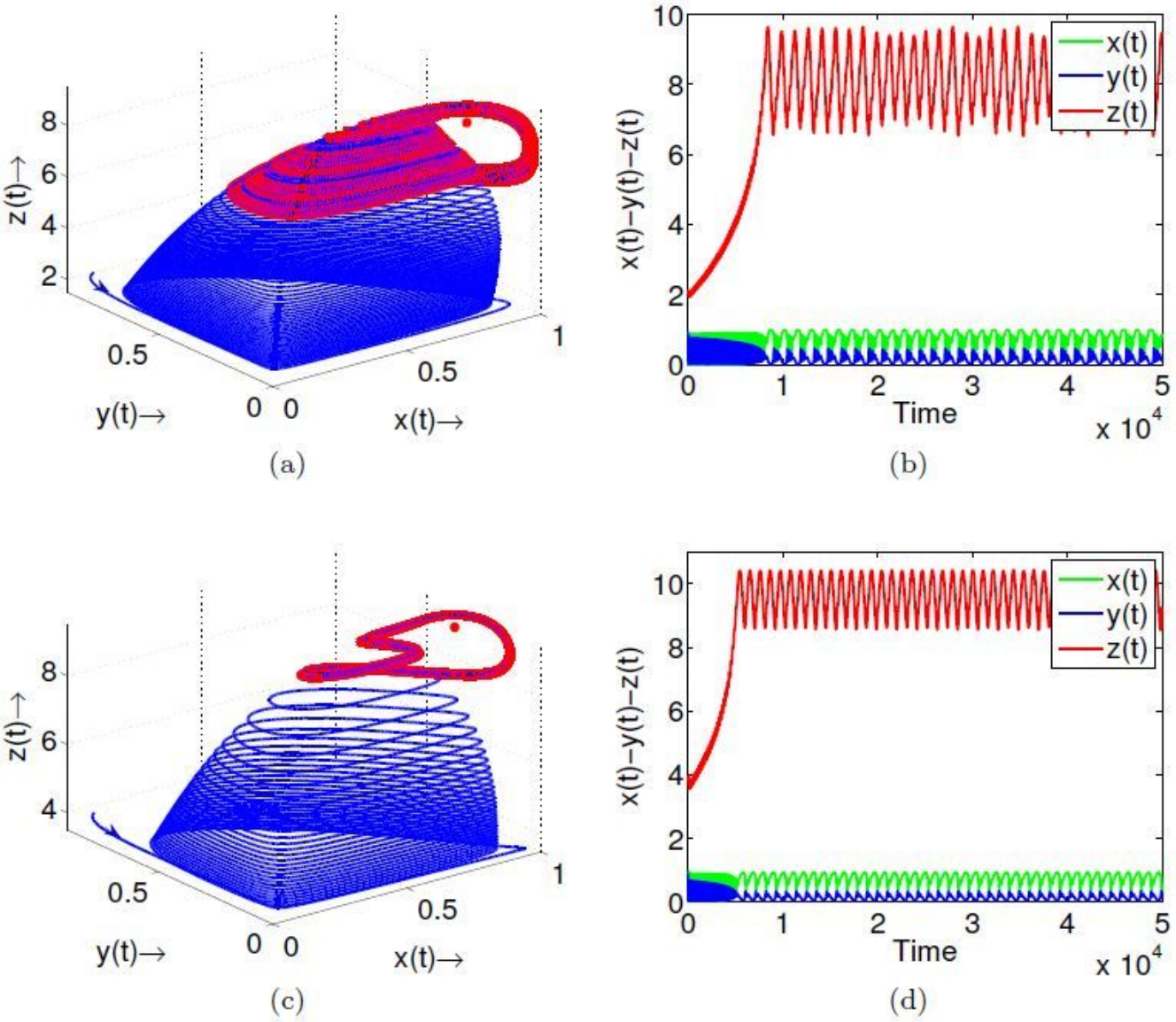

Figure 14

Phase diagram and time series solution of all the three species of the system (4) for different values of b2 like as : (a), (b) for b2 = b2 = 0:005 and (c), (d) for b2 = 0:15 with other parameters value as considered above. Red dot represent unstable equilibrium point.

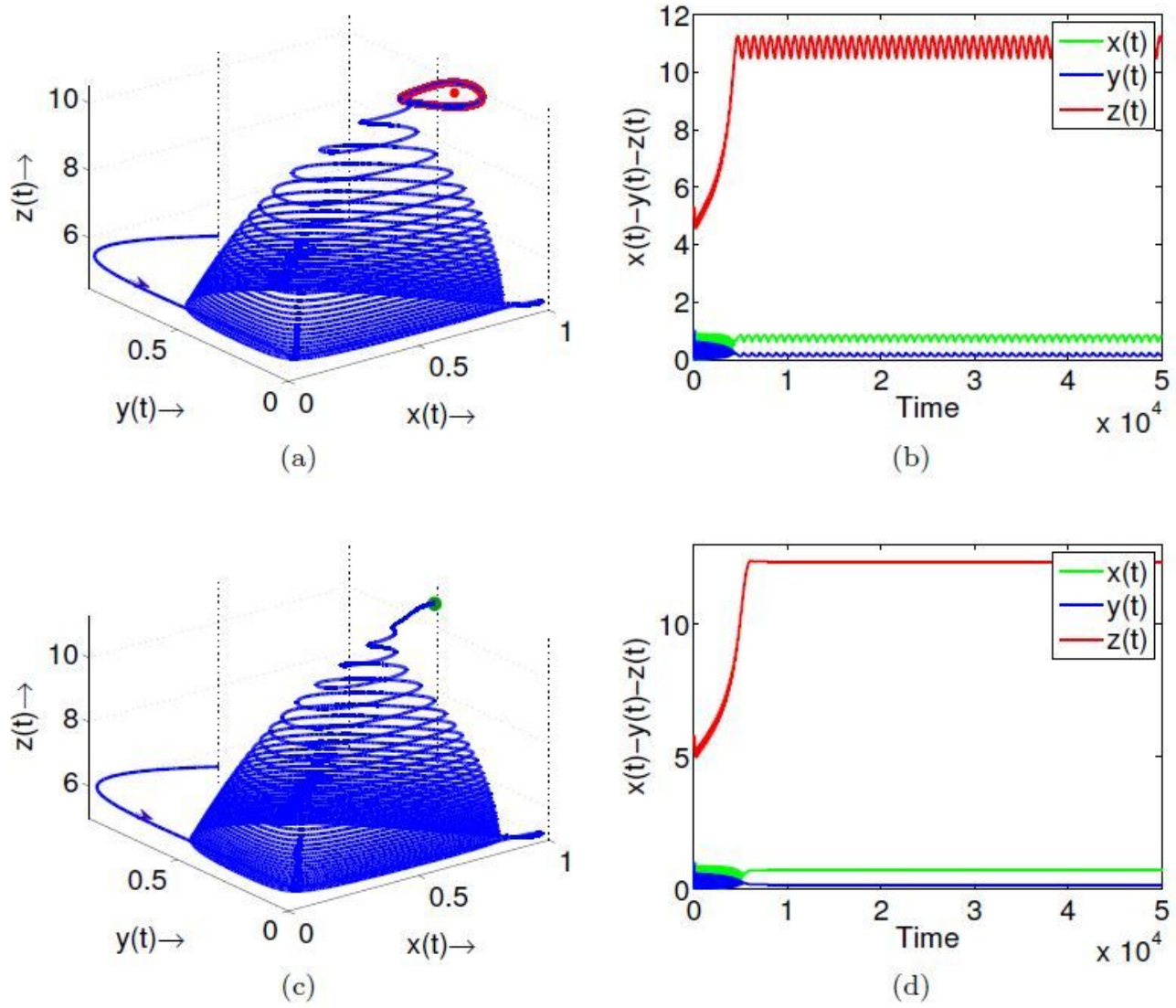

Figure 15

Phase diagram and time series solution of all the three species of the system (4) for different values of b2 like as : (a), (b) for b2 = 0:26 and (c), (d) for b2 = 0:40 with other parameters value as considered above. Green dot, red dot represent stable, unstable equilibrium points.

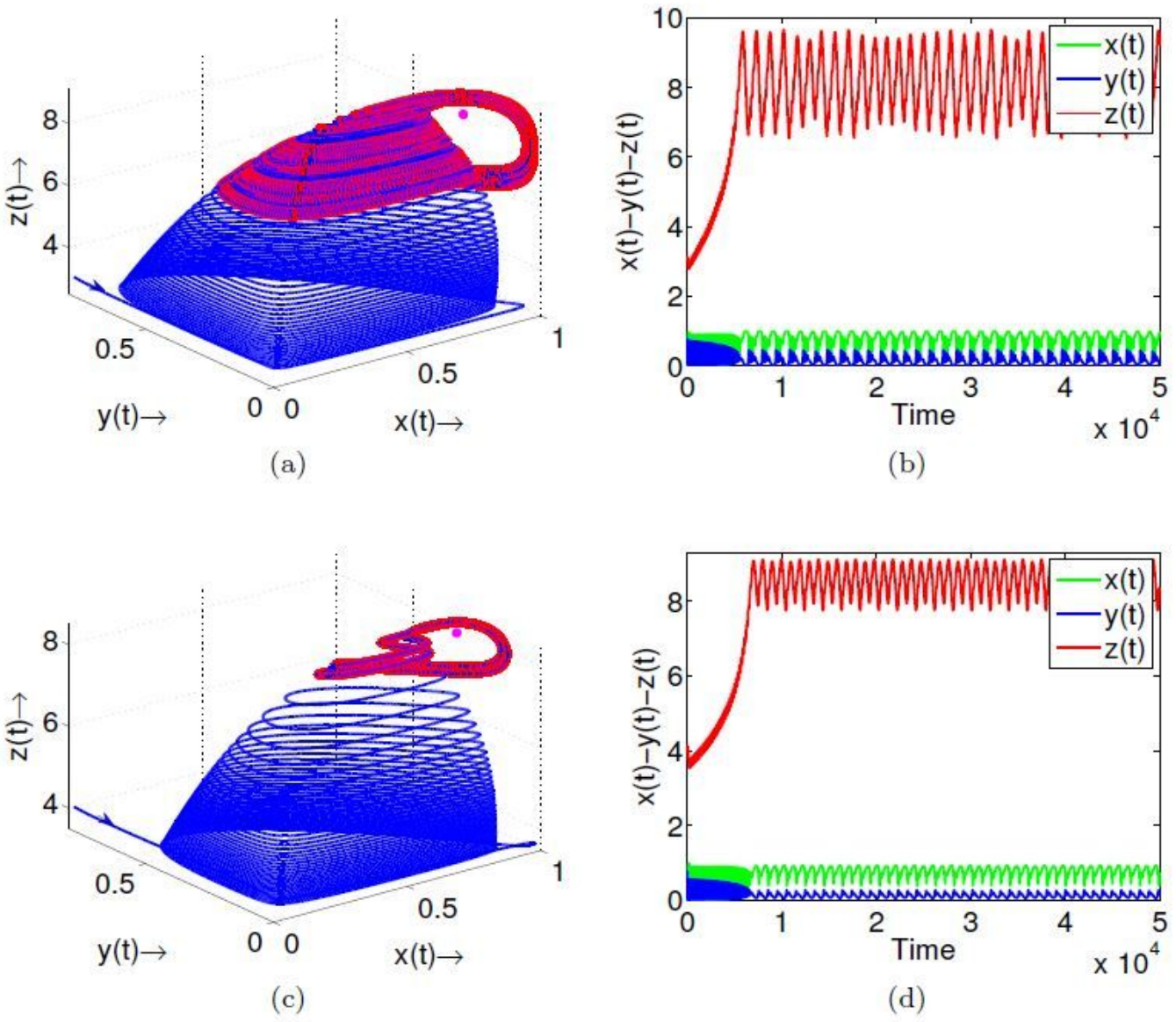

Figure 16

Phase diagram and time series solution of all the three species of the system (4) for different values of k1 like as : (a), (b) for k1 = 0:02 and (c), (d) for k1 = 1:0 with other parameters value as considered above. Red dot represent unstable equilibrium point.

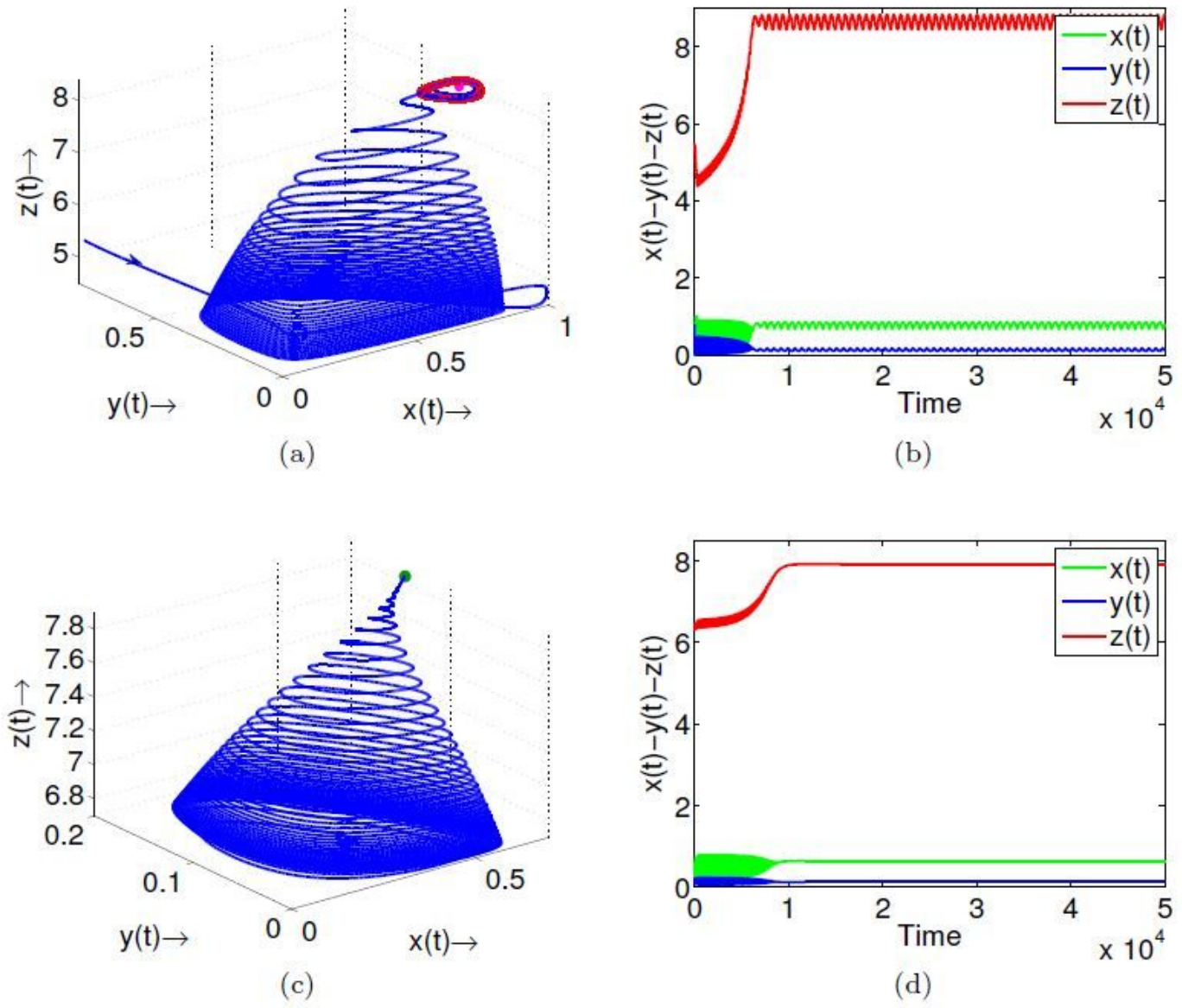

Figure 17

Phase diagram and time series solution of all the three species of the system (4) for different values of k1 like as : (a), (b) for k1 = 1:8 and (c), (d) for k1 = 6:0 with other parameters value as considered above. Green dot, red dot represent stable, unstable equilibrium points.

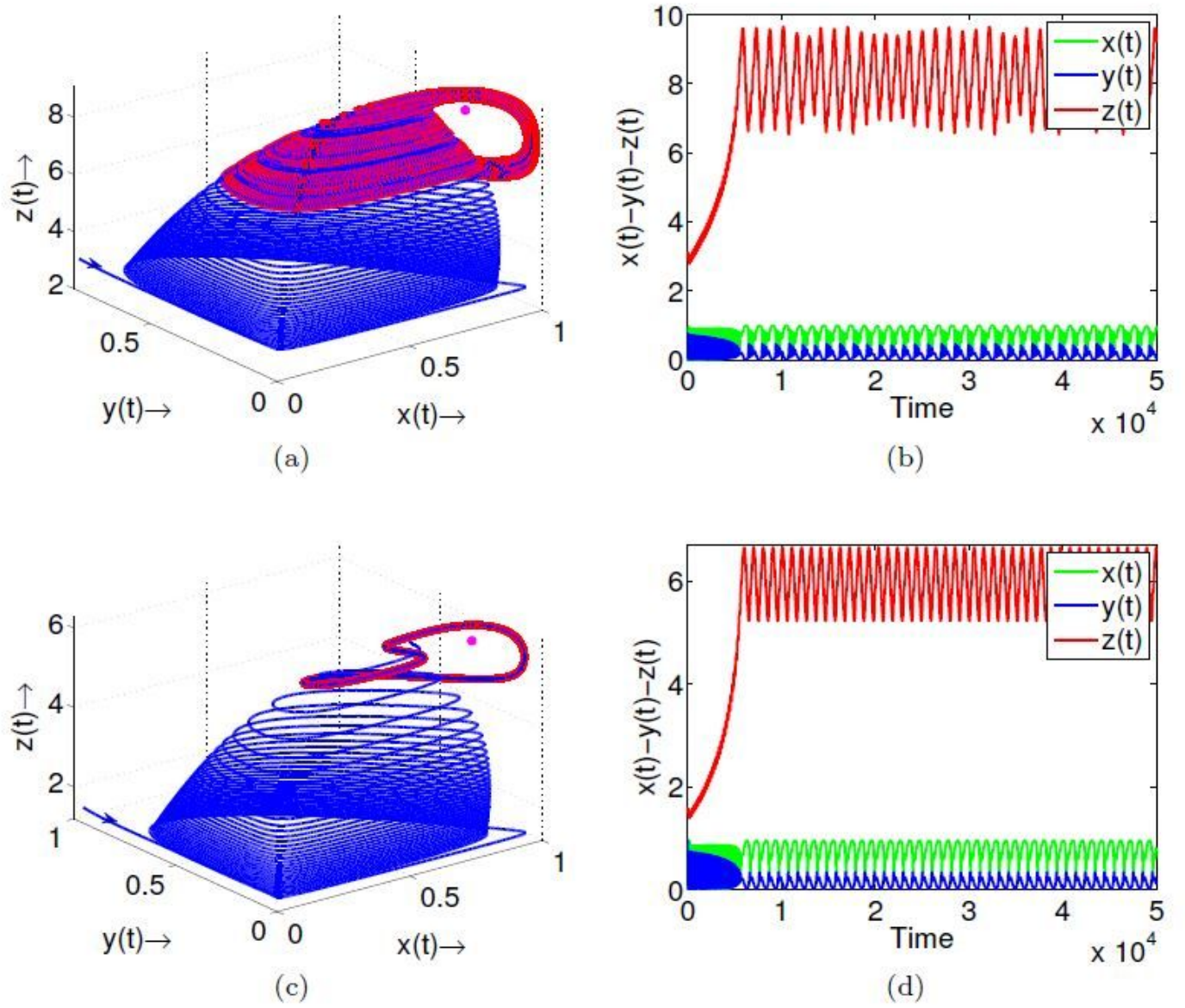

Figure 18

Phase diagram and time series solution of all the three species of the system (4) for different values of k2 like as : (a), (b) for k2 = 0:001 and (c), (d) for k2 = 0:04 with other parameters value as considered above. Red dot represent unstable equilibrium point.

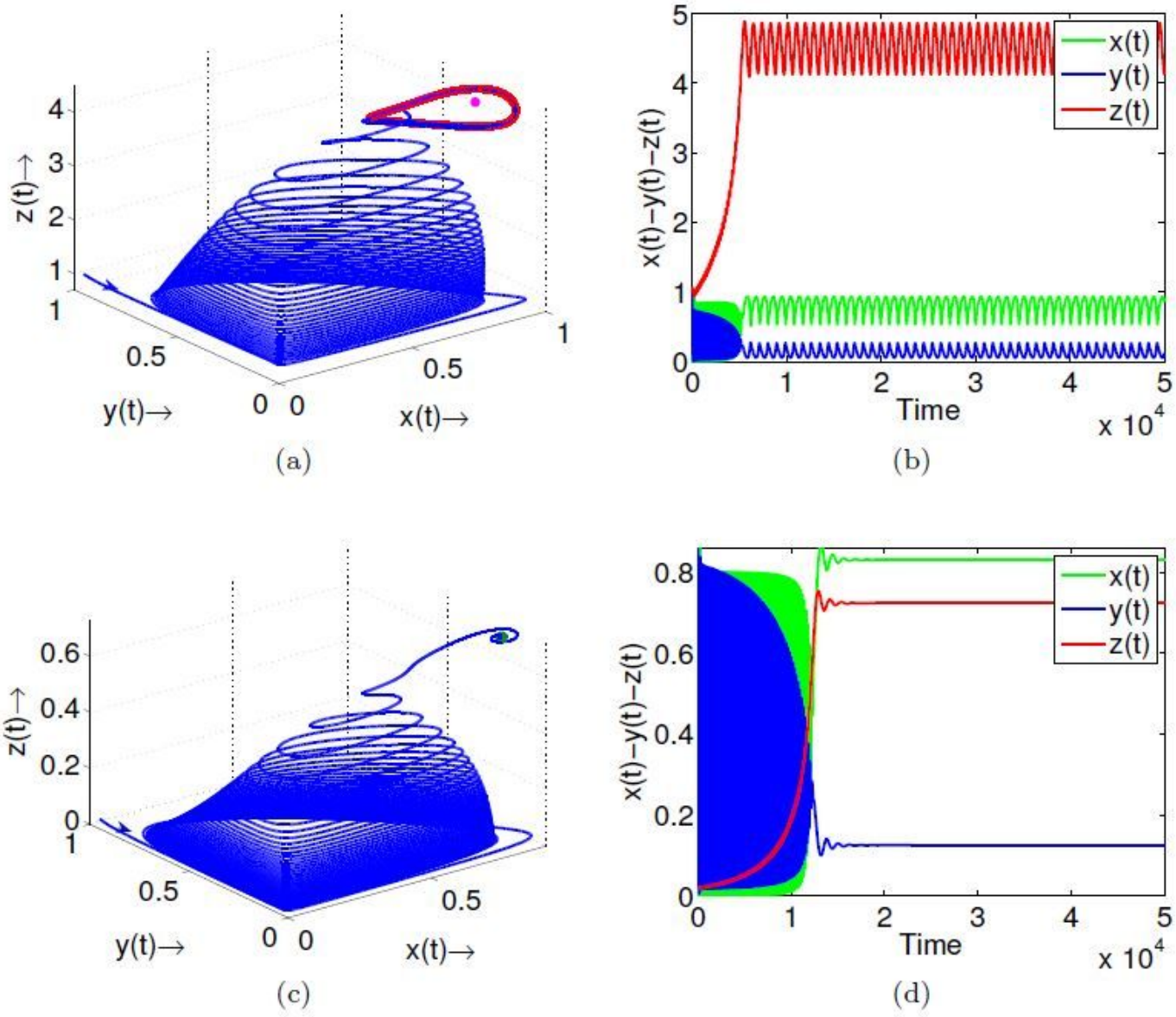

Figure 19

Phase diagram and time series solution of all the three species of the system (4) for different values of k2 like as : (a), (b) for k2 = 0:1 and (c), (d) for k2 = 2:0 with other parameters value as considered above. Green dot, red dot represent stable, unstable equilibrium points.

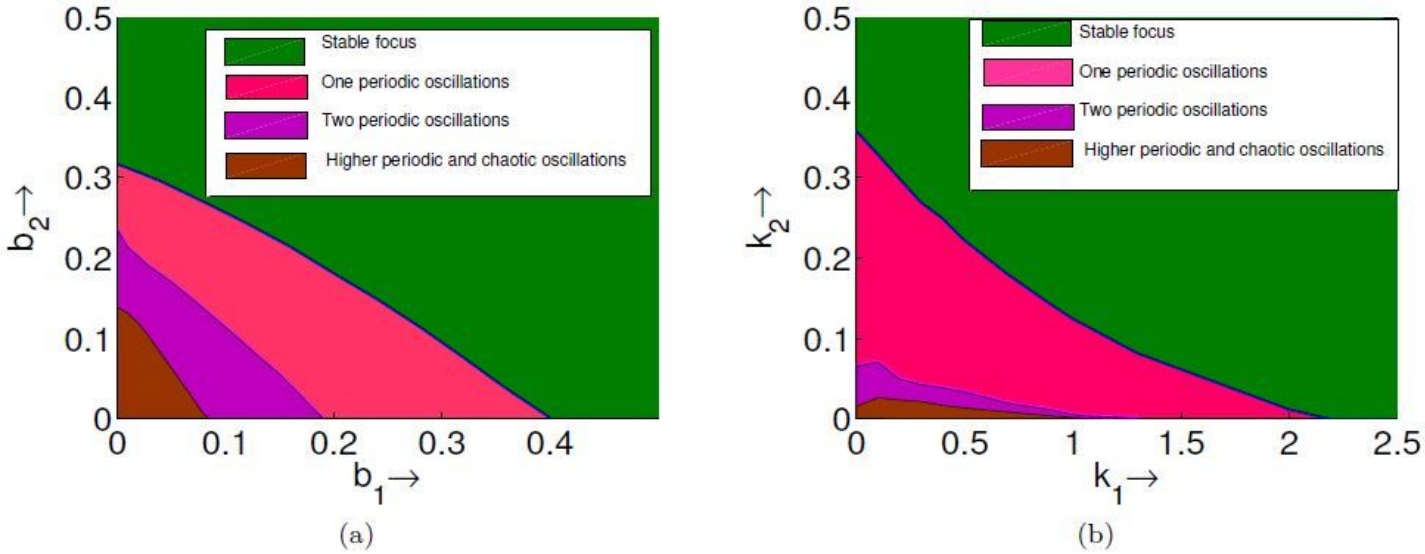

Figure 20

Stability region in (a) b1 - b2, (b) k1 - k2 parametric plane of the system (4). The system exhibits chaotic or higher periodic, two periodic, one periodic oscillation and stable spiral in red, violet, magenta, green regions respectively. Both parameters have a stabilizing effect on the system dynamics.